

Abstract

Title of dissertation: CHARACTERIZATION OF THE WEST NILE
 VIRUS PATHOGEN ASSOCIATED MOLECULAR
 PATTERNS

Jennifer German, Doctor of Philosophy, 2013

Dissertation directed by: Professor Brenda L. Fredericksen
 Department of Cell Biology and Molecular Genetics

The recent emergence of West Nile virus (WNV) in the western hemisphere has been marked by an increase in severe neurological disease. The factors that contribute to this increase in pathogenicity are poorly understood, however, there is evidence that the host antiviral response plays a significant role in controlling WNV mediated disease. The innate antiviral response is mediated by a variety of pathogen recognition receptors, including RIG-I. Here, we analyzed the RIG-I mediated antiviral response to WNV infection. We identified multiple regions of the pathogenic WNV-NY genome and antigenome that act as pathogen associated molecular patterns (PAMPs) capable of stimulating the RIG-I response. Additionally, preliminary examination of the related, non-pathogenic WNV-MAD78 genome has revealed stimulatory regions that differ from those found in the WNV-NY genome. One of PAMP

region, the 5'UTR, was analyzed further to elucidate the secondary structural elements present in the RNA, which may be contributing to the antiviral response. Similar, equally stimulatory structures were found in the 5'UTR of both the WNV-NY strain WNV-MAD78, indicating similar structures may be recognized for RIG-I activation. We also examined the role of DDX3, a DExD/H box helicase similar to RIG-I, in WNV infection. DDX3 appeared to co-localize with WNV protein and DDX3 expression was reduced at late points in infection, but DDX3 overexpression had no effect on viral replication or protein expression. Therefore, the exact role that DDX3 plays during the course of WNV infection remains unresolved. Taken together, our data suggests a specific structural requirement to activate the RIG-I mediated antiviral response.

**Characterization of the West Nile Virus Pathogen Associated Molecular
Patterns**

By

Jennifer German

Dissertation submitted to the Faculty of the Graduate School of the
University of Maryland, College Park, in partial fulfillment
of the requirements for the degree of
Doctor of Philosophy
2013

Advisory Committee:

Associate Professor Brenda L. Fredericksen, Chair

Professor Jonathan D. Dinman,

Professor Jeffery DeStefano

Associate Professor Louisa Wu

Associate Professor Daniel Perez, Dean's Representative

Acknowledgments

A number of people were instrumental in the completion of this dissertation, both directly and indirectly. I would like to thank them all sincerely and from the bottom of my heart.

I would first like to thank the many friends that I have made during the course of graduate school for providing emotional as well as academic and technical support during my work. In particular I would like to acknowledge the contributions of my fellow labmates Lisa Hoover and Dr. Rianna Vandergaast for performing the viral infections and plaque assays in Chapter 4, as well as Anna Pham for her tireless work contributing to the work detailed in both Chapter 2 and Appendix 1. I would also like to thank the other members of the Fredericksen lab, past and present, for their support, guidance, and endless good humor.

I would next like to acknowledge the support of my family, particularly my mom, dad, and brother for always believing in me and encouraging me to keep going. I would also especially like to thank my husband and son, who put up with my long hours and my frequently cranky mood while this work was being completed.

I would lastly like to acknowledge my committee members for their help, support, and suggestion in both the completion of my experiments as well as in writing this dissertation. In particular I would like to acknowledge and thank my mentor, Dr. Brenda Fredericksen, for her patience with me, her willingness to put up with me, and her support and motivation when I felt like I wanted to quit.

Table of Contents

Acknowledgements.....	ii
Table of Contents.....	iii
List of figures.....	vi
List of tables.....	viii
List of abbreviations.....	ix
Chapter 1: Introduction.....	1
West Nile virus.....	1
West Nile virus biology.....	1
Structure of the viral genome.....	2
Structure and function of the UTRs.....	3
Function of the WNV structural proteins.....	4
Function of the WNV nonstructural proteins.....	5
Strains and genetic diversity.....	8
The virus life cycle.....	9
The innate antiviral response.....	11
The TLRs.....	12
The RLRs.....	13
The IFN response.....	17
Viral PAMPs of RIG-I.....	19
RIG-I/RNA binding.....	24
Viral subversion of the antiviral response.....	25
The immune response to WNV.....	25
Chapter 2: Identification of multiple RIG-I-specific pathogen associated molecular patterns with the West Nile virus genome and antigenome.....	28

Introduction.....	28
Results.....	31
WNV protein is not capable of inducing an antiviral response.....	31
The 5' and 3' UTRs of WNV induce an antiviral response.....	32
Multiple regions of the WNV genome and antigenome induce a host antiviral response.....	34
The antiviral response to WNV PAMPs is RIG-I-dependent.....	35
Incorporation of WNV PAMPs into larger RNAs masks their stimulatory capacity.....	37
WNV genomic RNAs do not induce activation.....	39
Processing by the host contributes to the production of RIG-I PAMPs.....	40
Subgenomic flavivirus RNA does not induce RIG-I activation.....	42
Discussion.....	43
Chapter 3: Analysis of the WNV 5'UTR.....	47
Introduction.....	47
Results.....	50
The WNV 5'UTR is highly structured.....	51
The WNV-MAD78 5'UTR is capable of stimulating an antiviral response.....	55
Mutation of the WNV-NY 5'UTR to form a single stem loop reduces its stimulatory capacity.....	57
Truncation of the WNV-NY 5'UTR to fewer than 80 nucleotides abolishes RIG-I signaling capacity.....	60
Binding affinity of the WNV 5'UTR for RIG-I does not correlate with stimulatory capacity.....	63
The WNV-NY C(+) RNA does not bind to RIG-I.....	67
Discussion.....	68

Chapter 4: DDX3 as a potential antiviral protein during WNV.....	71
Introduction.....	71
Results.....	74
DDX3 co-localizes with WNV protein during infection.....	74
DDX3 does not have pro-viral affects during WNV infection.....	74
DDX3 expression is reduced at late times post WNV infection.....	77
Overexpression of DDX3 does not alter viral replication or the antiviral response.....	78
Discussion.....	79
Chapter 5: Discussion.....	85
Identification of WNV-NY PAMPs.....	85
Potential pathways involved in PAMP liberation.....	87
Examination of PAMPs during a native infection.....	91
Analysis of WNV PAMPs.....	92
Differences in WNV PAMPs between strains may account for differential activation of the antiviral response.....	92
ssRNA and tertiary interactions may influence RIG-I stimulation...	93
Steady state binding does not indicate RIG-I stimulatory capacity.....	94
The role of DDX3 during WNV infection.....	94
Chapter 6: Methods.....	95
Cells and viruses.....	97
Plasmids.....	97
Plasmid transfections.....	97
RNA fragments.....	98
Luciferase reporter assays.....	99

Trypsin digestion.....	99
SHAPE analysis.....	100
RIG-I binding.....	100
Radiolabeled primers and RNA.....	101
Immunofluorescence assay.....	101
Immunoblots.....	102
Virus infection.....	102
Plaque assays.....	103
Appendix 1: Preliminary WNV-MAD78 PAMP data.....	104
Appendix 2: Oligonucleotides.....	106
Appendix 3: Constructs used for protein expression.....	109
Appendix 4: Constructs used for <i>in vitro</i> transcription.....	111
Appendix 5: Structural predictions of WNV-NY PAMPs.....	113
Works cited.....	120

List of Figures

Figure 1: A schematic representation of the WNV genome.....	4
Figure 2: A simplified diagram of the WNV lifecycle.....	10
Figure 3: The innate antiviral signaling cascade.....	14
Figure 4: Structure of the RLR family members.....	16
Figure 5: Conformation of RIG-I with and without RNA bound.....	17
Figure 6: The IFN β receptor pathway.....	18
Figure 7: The 5'UTR (+) and 3'UTR (-) region of the WNV-NY genome induce and antiviral response.....	34
Figure 8: Multiple regions of the WNV genome and antigenome induce an antiviral response.....	35
Figure 9: WNV PAMPs induce a RIG-I specific antiviral response.....	36
Figure 10: Larger RNAs containing WNV PAMPs fail to activate an antiviral response.....	37
Figure 11: Larger RNAs containing WNV PAMPs fail to activate an antiviral response even with equivalent masses of RNA.....	38
Figure 12: WNV genomic RNAs do not induce an antiviral response.....	39
Figure 13: Larger RNAs containing WNV PAMPs induce an antiviral response over time.....	41
Figure 14: Stimulation of the antiviral response by larger WNV RNAs over time is RIG-I specific.....	42
Figure 15: WNV subgenomic RNAs do not induce an antiviral response.....	43
Figure 16: SHAPE analysis of the WNV 5'UTR.....	52
Figure 17: The WNV 5'UTR forms tertiary interaction and contains ssRNA regions.....	54
Figure 18: The WNV-MAD78 5'UTR forms tertiary interaction and contains ssRNA regions	56
Figure 19: RIG-I stimulation is similar between the WNV-NY and WNV-MAD78 5'UTRs.....	57
Figure 20: The WNV-NY-SL forms a complex structure.....	58

Figure 21: Stimulation by the WNV-NY-SL 5'UTR is reduced compared to WNV-NY.....	59
Figure 22: Truncation of the WNV-NY 5'UTR affects stimulation of RIG-I.....	61
Figure 23: Truncation of the WNV-NY 5'UTR is predicted to alter the secondary structures.....	62
Figure 24: Representative DRaCALA images used for Kd determination.....	65
Figure 25: Steady state binding of RIG-I to the WNV-NY 5'UTR to RIG-I is similar to WNV-MAD78 and WNV-NY-SL.....	66
Figure 26: Steady state binding of RIG-I to the full length WNV-NY 5'UTR is similar to the 1-90nt fragment but not the 1-80nt fragment.....	66
Figure 27: RIG-I binding of WNV-NY C(+) is non-specific.....	67
Figure 28: WNV protein co-localizes with DDX3 during infection in multiple cell types.....	75
Figure 29: DDX3 overexpression does not affect the viral replication or protein expression of a viral replicon.....	76
Figure 30: DDX3 expression is reduced by late points during WNV infection.....	77
Figure 31: DDX3 overexpression does not affect the antiviral response to WNV or viral replication	79
Figure 32: Stimulatory capacity of WNV-MAD78 RNAs.....	105
Figure 33: Predicted structures of the WNV-NY 5'UTR (+) and 3'UTR (-).....	113
Figure 34: Predicted structures of the WNV-NY NS2a(+).....	114
Figure 35: Predicted structures of the WNV-NY	115
Figure 36: Predicted structures of the WNV-NY	116
Figure 37: Predicted structures of the WNV-NY	117
Figure 38: Predicted structures of the WNV-NY	118
Figure 39: Comparison of the predicted structures of WNV-NY 5'UTR alone, within the 5'-prM and within the total genome.....	119

List of Tables

Table 1: Viruses identified by the RIG-I-like receptors.....	20
Table 2: Identified PAMP structures.....	22
Table 3: WNV protein expression does not induce a RIG-I response.....	23
Table 4: List of oligonucleotides used for various experiments.....	106
Table 5: Constructs used for protein expression studies.....	109
Table 6: Constructs used for <i>in vitro</i> transcription.....	111

List of Abbreviations

IM7	1-methyl-7-nitroisatoric anhydride
5'PPP	5' tri-phosphate
AP-1	Activator protein 1
CA	Core Anchor
CM	Convolute membranes
CS	Conserved sequence
CTD	C-terminal domain
DRaCALA	Differential radial capillary action of ligand assay
dsRNA	Double stranded RNA
E	Envelope
ER	Endoplasmic reticulum
FL-IT-WNV	Full length, <i>in vitro</i> transcribed West Nile virus
FL-WNV	Full length West Nile virus
HCV	Hepatitis C virus
HIV	Human immunodeficiency virus
Huh7	Human hepatoma 7
IFN β	Interferon beta
IFN	Interferon
IFNAR1	Interferon-alpha/beta receptor
I κ B α	Inhibitor of nuclear factor kappa-B alpha
I κ k ϵ	I κ β kinase epsilon
IPS-1	Interferon-beta promoter stimulator 1
IRF-3	Interferon response factor 3
IRAK	Interleukin-1 receptor-associated kinase

ISG	Interferon stimulated gene
ISGF3	Interferon stimulated gene factor 3
ISRE	Interferon-stimulated responsive elements
JAK	Janus kinase
JEV	Japanese encephalitis virus
LGP2	Laboratory of genetics and physiology 2
MAPK	Mitogen activated protein kinases
MDA5	Melanoma differentiation associated factor 5
MOI	Multiplicity of infection
NLRs	Nod-like receptors
NFκB	Nuclear factor kappa-light-chain-enhancer of activated B cells
NS	Nonstructural
PA	Paracrystalline arrays
PAGE	Polyacrylamide gel electrophoresis
PAMPs	Pathogen associated molecular patterns
prM/M	Pre-membrane/membrane
PRRs	Pattern recognition receptors
RD	Repressor domain
RIG-I	Retinoic acid inducible gene I
RLRs	RIG-I-like receptors
RSV	Respiratory syncytial virus
SenV	Sendai virus
sfRNA	Subgenomic flavivirus RNA
SHAPE	Selective 2'-hydroxyl acylation analysis by primer extension
SL	Stem loop
ssRNA	Single stranded RNA
STAT	Signal Transducer and Activator of Transcription

TAK-1	Transforming growth factor β -activated kinase 1
TBK1	Tank binding kinase 1
TIR	Toll/Interleukin-1 receptor
TLRs	Toll-like receptors
TRAF6	TNF receptor associated factor
Tyk2	Tyrosine kinase 2
TRIF	TIR-domain-containing adapter-inducing interferon- β
VP	Vesicle packets
VSV	Vesicular stomatis virus
WNV	West Nile virus
WNV-MAD78	West Nile virus Madagascar-78
WNV-NY	West Nile virus New York
UAR	Upstream AUG region
UTR	Untranslated region

Chapter 1 – Introduction

West Nile virus

The expansion of travel into new areas of the world and the subsequent increase in contact with members of the global community has meant that a growing number of pathogens, especially viruses, have emerged as threats to public health in the past few decades. One such virus, West Nile virus (WNV), is a pathogen that has only recently spread into the Western hemisphere, having been introduced to the United States in 1999 (111). WNV has been isolated throughout the continental United States as well as parts of Mexico, the Caribbean, and Canada.

West Nile virus biology

WNV is a positive sense, RNA virus belonging to the family *Flaviviridae*. This family contains a number of viruses, including hepatitis C virus (HCV), Japanese encephalitis virus (JEV), and Dengue virus, all of which contribute to significant morbidity and mortality worldwide and are therefore widely studied (98). WNV has been endemic to the Middle East and parts of Africa and Southeast Asia for many years, but the virus has spread in recent years to the United States, where it was first reported in New York (111, 137). The introduction of WNV to new areas of the world has increased the incidence of human infection. The traditional transmission cycle of the virus is from a

mosquito vector to birds, the natural host, with humans, horses and several other species serving as incidental, dead-end hosts (98, 174). The disease is generally asymptomatic in humans, or results in mild, flu-like symptoms with low-grade fever, referred to as a “West Nile fever.” In areas where WNV has been endemic, approximately 1% of cases present with severe symptoms, including high fever, paralysis, and encephalitis. Infection can even result in death in between 3-15% of these severe cases (67, 83, 111). In contrast, the outbreak in the western hemisphere is associated with a higher incidence of severe neurological disease, with an average of 30-50% of reported cases within the last decade in the United States being associated with neurological symptoms. WNV is now considered the leading cause of domestically-acquired arboviral disease and represents a serious public health risk (information found on the CDC website www.cdc.gov/ncidod/dvbid/westnile.idex.htm). Despite the increase in both case number and incidence of severe infection, the factors that contribute to pathogenicity and severe neurological symptoms in recently emerged strains are poorly understood.

The structure of the viral genome

The WNV genome is approximately 11 kb in length and encodes ten proteins: three structural proteins and seven non-structural proteins. The genome is translated as a single polyprotein and subsequently cleaved by both viral and host cell proteases to generate the individual proteins. The virus also contains two untranslated regions (UTRs) at the 5' and 3' ends of the genome (Figure 1). The virus is capped with a type 1 m⁷GPPPAm^pN₂ cap, but lacks a

poly-A tail (8, 11, 35,13). The 3' UTR also contains a secondary structure that results in the production of a single subgenomic RNA (sfRNA), which is common to all of the arthropod-borne flaviviruses (55, 164, 170).

Structure and Function of UTRs

The 5' and 3' UTRs of WNV are predicted to be highly structured regions and numerous studies have demonstrated they are required for both replication and translation of the viral genome (32, 54, 95, 103, 126). Despite the apparent importance of these structures, their secondary structures have not been confirmed by experimental structure probing. The 5'UTR is composed of the first 96 to 97 nucleotides (nt) of the genome, depending on strain, and is highly conserved between *flaviviradae* members (22, 98). There are two predicted structures present in the 5'UTR, identified as stem loops (SL) A and SLB (23, 95, 171). SLA consists of the first 70nt of the genome and similar SL structures in this position are found in most of the flaviviruses. SLB contains the 5' initiation element known as the upstream AUG region (UAR). The UAR base pairs with a complementary region in the 3'UTR to facilitate viral replication. Additionally, interactions between conserved sequence (CS) elements found within the core gene and the 3'UTR allow for cyclization of the genome, an important step in the synthesis of the minus strand RNA (11, 24, 54, 213). The 3'UTR also contain a SL structure responsible for the production of the sfRNA. The exact function of this sfRNA is unknown. However, recent studies indicate that it may play a role in disrupting the immune response, and mutation of the genome to abolish the

formation of this fragment resulted in reduced lethality in mice, suggesting that the sfRNA contributes to pathogenicity (94, 105, 108).

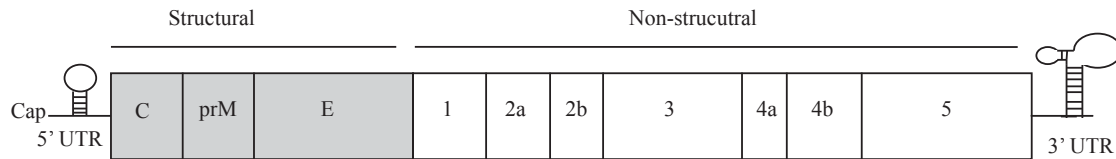


Figure 1: A schematic representation of the WNV genome.

Function of the WNV structural proteins

The first three genes of the viral genome, core (also referred to as capsid), pre-membrane/membrane (prM/M) and envelope (E), encode the structural proteins involved in viral particle formation. The virion is ~50 nm in diameter and is composed of an icosahedral protein shell composed of the E and M proteins incorporated into the viral envelope (22, 98). The outer surface of the virion is smooth, and contains 90 E dimers and 180 copies of M. The interior of the virion contains the nucleocapsid, which is comprised of core protein and viral genome. The E protein is a class-2 fusion protein and each monomer contains three domains. Upon acidification due to exposure to the low pH of the endosome, the dimers dissociate and rearrange into a trimeric arrangement, allowing for fusion with the endocytic membrane (49, 88, 118, 173, 215). The viral RNA and nucleocapsid then dissociate and translation of the genome can begin. The nucleocapsid is formed by dimers of Core. The proteins fold into a confirmation whereby positively charged residues cluster on the surface that interacts with the

RNA while the outer surface is composed of primarily hydrophobic residues. The core protein associates with cellular membranes during entry and egress, and therefore contains an internal hydrophobic region flanked by charged residues on the C and N terminus. The C terminal end of the protein also contains an anchor region, referred to as core anchor (CA). The CA acts as a signal peptide for translocation of the prM protein into the endoplasmic reticulum (ER) (98). The prM protein serves as a chaperone for proper folding of the E protein (88, 98, 214, 215). In its immature form, prM also prevents premature fusion during egress from the cell, as the pr portion of the protein covers the fusion peptide of E. PrM is cleaved by the host protease furin to form the M protein in the trans Golgi network during maturation, although cleavage is not always completely efficient and therefore prM can be found on the virion surface.

Functions of the WNV nonstructural proteins

The remaining seven genes of the viral genome encode the nonstructural (NS) proteins, identified as NS1, 2a, 2b, 3, 4a, 4b, and 5 (Figure 1). These proteins are involved in viral RNA replication, rearrangement of cellular membranes, evasion of the immune response and assembly of the virion (22). Most of the nonstructural proteins have been shown to co-localize within the replication complex, although in the case of NS1, NS2a, NS4a and NS4b, their exact roles within this complex remain to be defined.

NS1 is a glycoprotein with proposed roles in viral replication and as a pathogenicity factor. NS1 co-localizes with the double stranded replicative

intermediary form of the genome within replication complexes (200) . There has been some evidence to suggest that this association plays a role in the switch from viral replication to translation and that it acts to translocate the polyprotein during virion assembly (97, 130). NS1 can be secreted as a homodimer that associates with cellular membranes or as a soluble monomer or hexamer composed of three homodimers (2). Both the dimeric and monomeric form of the secreted NS1 protein can interact with glycoprotein factor H, an activator of the complement cascade, giving it a role in suppression of the host immune response (7, 8). In addition, the production of a frameshift alternative product, NS1', can increase neuroinvasiveness in mice (114).

NS2a, NS2b, NS4a and NS4b are all small, hydrophobic proteins with a variety of functions, although they are not fully characterized (22). Evidence suggests that NS2a is involved in the membrane rearrangement required for production of virus packets (VPs) and in virion assembly (101, 107, 124). It has also been shown to interfere with the antiviral response through interactions with the Janus kinase (Jak) protein, a critical kinase involved in the signaling cascade induced by IFN (102).

NS2b serves as a cofactor for the viral serine protease, NS3 (48, 50). Little is known about how the protein functions in its role as a cofactor, but crystal structure analysis of NS3 with and without the NS2b protein reveals that NS3 undergoes substantial structural rearrangement in the presence of NS2b. NS3 is a bi-functional protein, the function of which is dependent on the conformation adopted in relation to its cofactor proteins (60, 168, 169). The N-

terminal end of the protein contains the serine protease domain responsible for cleaving the polyprotein into the individual proteins. In order to be proteolytically active, NS2b must interact with NS3 to complete the active site of the protein. This conformation also provides a platform for the protease specificity site. The C-terminal region of the protein contains motifs that are homologous to an RNA helicase, NTPase and RTPase, suggesting a role in RNA replication. NS4a has been identified as the cofactor necessary for the helicase/ATPase activity of NS3 when it is in its alternate conformation. Indeed, initial studies demonstrated NS4a is required for replication as well as membrane rearrangement (3, 107, 149). The last small, hydrophobic protein is NS4b. In addition to a suggested role in replication, NS4b has been shown to block the IFN response, although the mechanism of disruption is not fully understood (119, 196, 199, 210).

The final protein is NS5 and is the best characterized of the NS proteins. Like NS3, NS5 is a bi-functional protein; the N-terminal end encodes the methyl transferase, which is required for capping of the genome, while the C-terminal end encodes the viral RNA dependent RNA polymerase. NS5 has also been shown to play a role in blocking the antiviral response by inhibiting the phosphorylation of or contributing to the degradation of proteins involved in the signaling cascade induced by IFN, thereby preventing the production of antiviral effector proteins (1, 86, 93, 108).

Strains and genetic diversity

One method for determining viral factors that influence pathogenicity is to analyze related strains of the virus that produce different disease outcomes. WNV has been divided into two primary lineages (92). The pathogenicity of the virus varies depending on the strain and is not lineage specific. WNV-NY, a lineage 1 strain, is a neuropathogenic virus that was isolated in the western hemisphere in 2000 from a crow. WNV-Madagascar (WNV-MAD78) is a lineage 2, non-neuropathogenic strain isolated in 1978 from a Greater Vassa Parrott. When injected directly into the brain of mice, both viruses are neurovirulent; however, WNV-MAD78 is considered to be non-neuroinvasive, as injection at a peripheral site does not result in neurological disease (92). Therefore, these strains make an excellent model system to define WNV virulence factors. The genomes are only 75% conserved at the nucleotide level. Direct sequence alignment does not reveal any specific region in which changes are clustered, although one primary difference that is readily apparent between these two strains is in their glycosylation sites. WNV-NY is glycosylated on both the E and prM protein, whereas WNV-MAD78 is glycosylated only on the prM protein. (16, 66, 127). Glycosylation of the E protein results in a more neuroinvasive virus in mice, increasing virion assembly in cells and viral infectivity (14, 66). The 3'UTR of WNV-MAD78 is also shorter than that of WNV-NY, potentially affecting viral replication, production or structure of the sfRNA, or recognition of the virus by the host. These differences may contribute to the variances in pathogenicity between these strains. Another possible explanation for the reduced

pathogenicity seen with WNV-MAD78 may lie in the host response. A differential innate immune response by the host to WNV-NY verses WNV-MAD78 may account for the difference in pathogenicity between the strains

The viral life cycle

Viral entry into the host cell begins with binding of the virus via a host-cell surface receptor. Several potential receptors have been proposed, including CD14, GRP78/BiP and $\alpha_v\beta_3$ integrin, and there is some evidence that different receptors are used in a cell-type specific manner (31, 35, 122). Binding can be enhanced by interaction with the attachment factor DC-SIGN/R (42). Following attachment, the virus is taken up by the cell through receptor-mediated endocytosis, possibly via clathrin-coated pits (34). The viral particle is uncoated and then released into the host cell cytoplasm. The positive sense genome is translated by host cell ribosomes into a single polyprotein, which is cleaved into the individual mature viral proteins by both cellular and viral proteases. The production of WNV proteins induces membrane reorganization within the cell, including the proliferation of ER membranes, resulting in the formation of VPs, randomly folded convoluted membranes (CM) adjacent to the ER, and highly structured paracrystalline arrays (PA) (71, 124, 200). The double-membrane VPs produced during membrane rearrangements provide a platform for viral genome replication. Protein translation and proteolytic cleavage are believed to take place within the CM and PA structures. Minus sense RNA (also referred to as antigenome or antigenomic RNA) is then produced by the viral polymerase, and can in turn serve as a template for further replication of positive sense

strands. Production of antigenomic RNA is asymmetric, with an approximate 1:10 ratio of antigenomic to genomic RNA being produced (197). When sufficient levels of the structural proteins and genome have accumulated, viral particle assembly takes place on the surface of the rough ER. Virus particles exit the cell by moving through the host secretory pathway and are released at the cell surface (Figure 2).

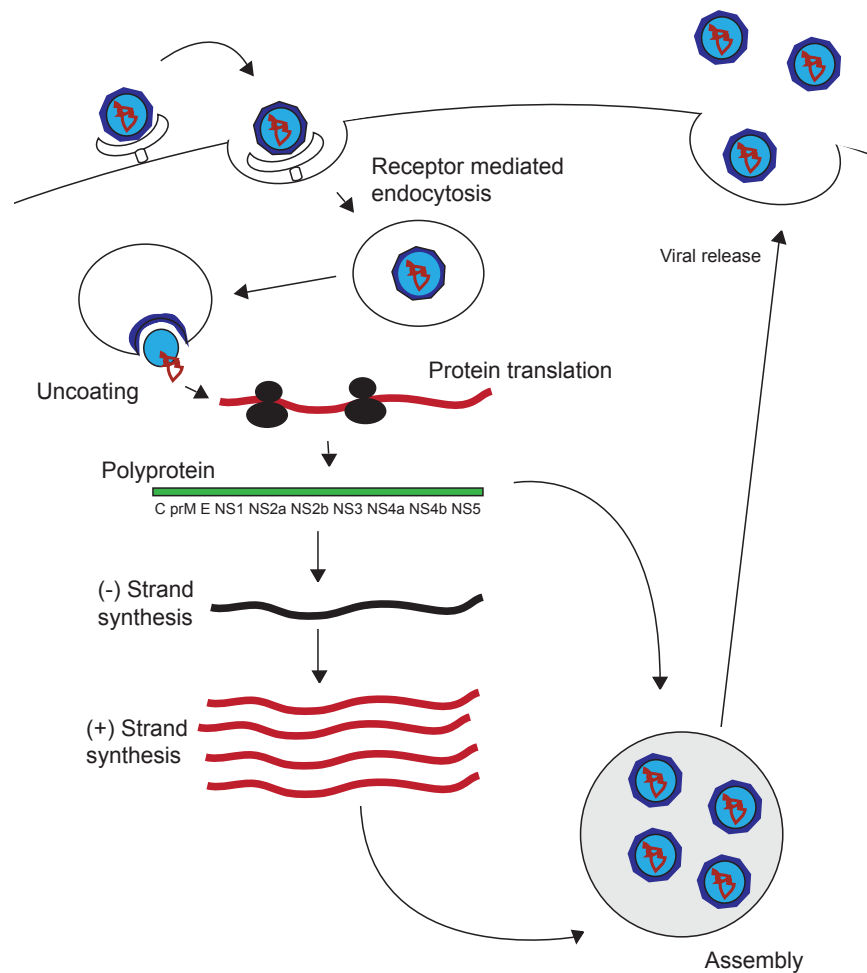


Figure 2: A Simplified diagram of the WNV lifecycle

The innate antiviral response

The ability of a host to detect and respond to invading pathogens is crucial in controlling infection. The host cell innate immune response serves as the first level of control against viral pathogens. The innate antiviral response results in the production of cytokines and chemokines that function to limit viral spread. This response has multiple consequences, including stimulating the adaptive immune response to target infected cells for destruction, and the induction of an antiviral state within infected cells. The innate immune response is mediated by a variety of pathogen recognition receptors (PRRs), including the Toll-like receptors (TLRs), the RIG-I-like receptors (RLRs), and the Nod-like receptors (NLRs). These PRRs are able to recognize pathogen associated molecular patterns (PAMPs) in order to initiate an antiviral response. Several other proteins have also been implicated as PRRs, including the cytoplasmic DExD/H box helicase DDX3, although this is not their primary function (162). Binding of PAMPs to these receptors results in the activation of signaling cascades. Activation of these signaling cascades results in subsequent activation of transcription factors capable of inducing the expression of a number of antiviral effector proteins, as well as cytokines such as type I IFN. IFN production in particular is an important step in establishing immunity, as this molecule is able to stimulate responses linking innate immunity to adaptive immunity, further enhancing the host response to infection.

The TLRs

The TLR family is comprised of a number of proteins, with 13 reported members, of which 10 are found in humans (6). They are numbered 1 through 13, and those responsible for recognition of viral PAMPs are TLR-3, -7/-8, and -9. These TLRs are able to recognize double stranded (ds) RNA, single stranded (ss) RNA and DNA, respectively, within the endosomal compartment and on the surface of cells. There has also been some recent evidence to suggest that TLR-2 and -4 can serve as antiviral PRRs, as they are capable of recognizing viral proteins (17, 26, 38, 89, 145, 179). During the course of West Nile virus infection, viral RNA has been shown to activate the antiviral response through both TLR-3 and TLR-7.

All members of the TLR family contain a Toll-IL-1 receptor (TIR), which serves as a signaling domain. However, the TLRs signal via one of two distinct pathways (Figure 3). Upon binding to their cognate ligands, TLR-7/8 recruits Myd88, an adaptor protein utilized by several of the TLRs. Myd88 engages the interleukin 1R-associated kinase (IRAK) complex, consisting of several IRAK proteins. These IRAKs in turn phosphorylate TNF receptor-associated factor 6 (TRAF6). Phosphorylation of TRAF6 can result in the activation of a number of transcription factors including nuclear factor kappa-light-chain-enhancer of activated B cells (NFkB) and activator protein (AP-1). NFkB is activated when phosphorylation of the inhibitor Ikb α results in its degradation. Removal of Ikb α reveals a nuclear localization signal on NFkB, allowing free NFkB to translocate into the nucleus. AP-1 phosphorylation is mediated by the activation of a series

of kinases, including transforming growth factor β -activated kinase 1 (TAK-1) and the mitogen activated protein kinases (MAPKs).

In contrast, TLR-3 recruits Toll-IL-1 receptor domain-containing adaptor inducing IFN- β (TRIF). While TRIF activation induces signaling through TRAF6, it can also signal through a separate cascade. It activates the protein kinases tank binding kinase 1 (TBK1) and inhibitor of kappaB kinase- ϵ (Ikk ϵ), forming a dimer of the two proteins. This hetero-dimer then in turn phosphorylates IRF-3, thus converting it to a transcriptionally active form. Activated IRF-3 forms a homodimer and is preferentially retained in the nucleus. In concert with several other transcription factors, IRF-3 functions to induce the transcription of interferon- β (IFN- β) as well as a number of interferon-stimulated genes (ISGs), such as ISG-56, also known as IFIT1, and ISG15 (61).

The RLRs

The RLRs are cytoplasmic DExD/H box helicases belonging to the superfamily 2 helicases (181). Activation of either RIG-I or MDA5 results in a signaling cascade with the eventual activation of transcription factors that induce IFN expression (Figure 2). In contrast to TLRs, the RLR proteins recognize viral RNA in the infected-cell cytoplasm. There are three members of the RLR family: Retinoic acid-inducible gene I (RIG-I), melanoma differentiation association gene 5 (MDA5) and laboratory of genetics and physiology 2 (LGP2) (Figure 4).

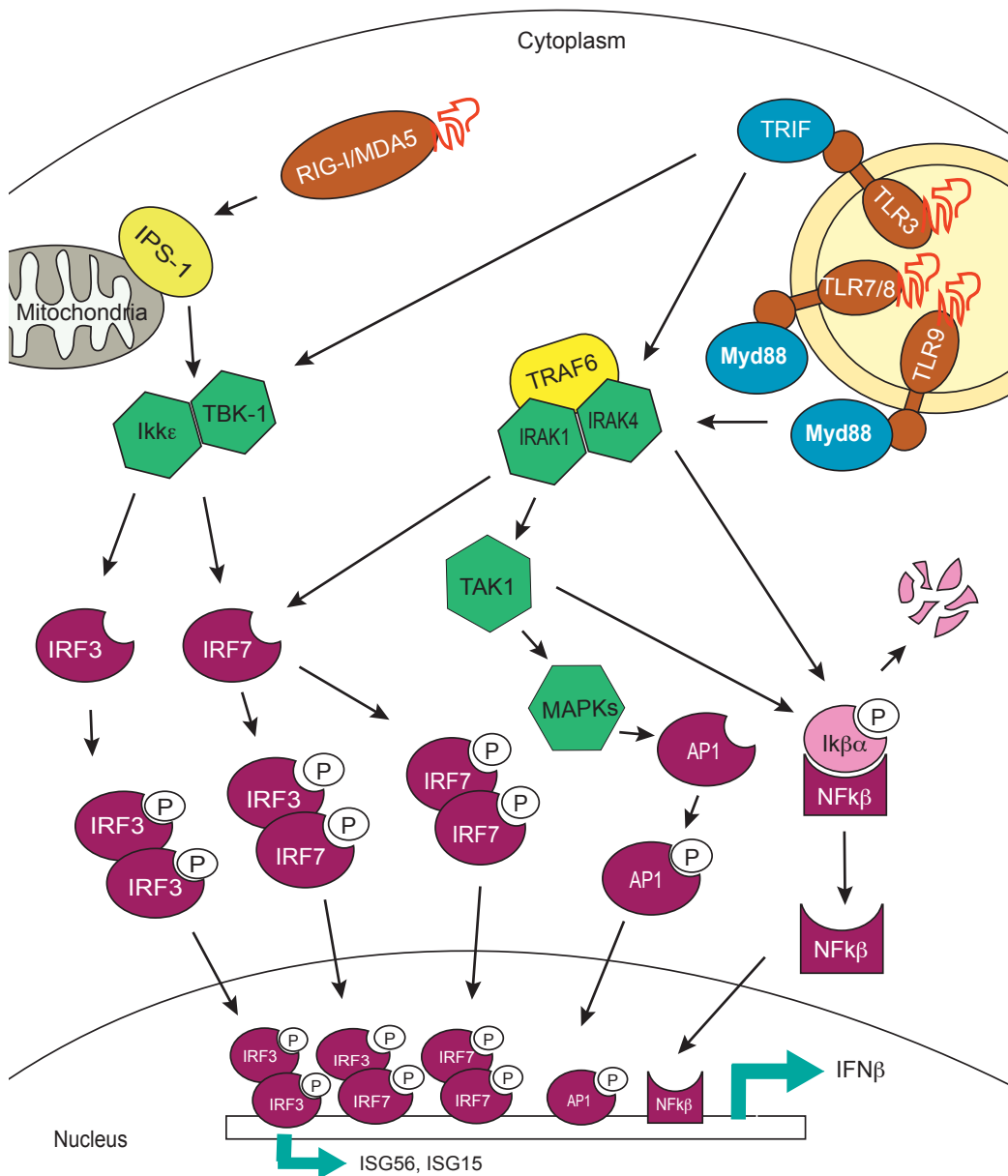


Figure 3: The innate antiviral signaling cascade. Several PRRs (orange) are able to recognize viral PAMPs in the host cell cytoplasm (the RLRs) or endocytic vesicles (the TLRs). Activation of these PRR proteins induces signaling cascades that mediate the activation of several different kinases (green), which are then able to phosphorylate and activate a number of transcription factors (red). These transcription factors are able to induce the expression of INF, as well as directly induce the expression of several ISGs, including ISG56 and ISG15.

RIG-I and MDA5 are involved in the recognition of viral RNA and the activation of the innate immune response, and both contain two tandem N-terminal caspase activation and recruitment domains (CARDs), a helicase domain, and a repressor domain (RD) found on the C-terminal end of the protein. Together, the helicase domain and RD constitute the C-terminal domain (CTD). LGP2 lacks the RNA recognition domain present in RIG-I and MDA5 and therefore does not serve as a PRR. LGP2 contains only the helicase and repressor domains. LGP2 has been shown, however, to regulate RIG-I and to mediate CD8+ T-cell expansion in response to infection (178). Mutation or elimination of the CARDs ablates the signaling capacity of RIG-I or MDA5, while overexpression of the tandem CARDs alone results in constitutive signaling, even in the absence of viral RNA (10). The RD, which contains the RNA binding domain, acts to repress signaling of the CARD by binding to both the CARD and helicase domains (39, 151). The helicase domain contains an ATP-binding domain and a helicase domain. In uninfected cells, the protein is thought to exist in a “closed” conformation in which the repressor sterically hinders access to the CARD and helicase domains, preventing signaling (Figure 5). This closed conformation is altered in the presence of viral RNA. RNA binds the RNA binding domain of the RD and ATP binds in the helicase domain. This results in a conformation in which the protein is “opened,” allowing the CARD to interact with downstream proteins (Figure 5) (10). The now accessible CARD domain of the activated RLR interacts with the IPS-1, also referred to as MAVS, VISA, and

Cardif (70, 81, 116, 165, 204), another CARD containing protein which is associated with the outer membrane of the mitochondria.

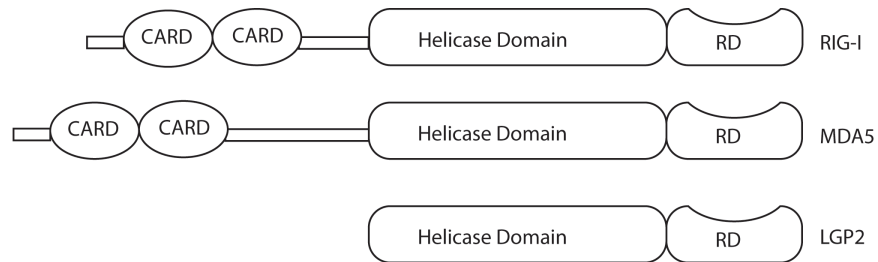


Figure 4: Structure of the RLR family members. The RLR family is composed of three members: RIG-I, MDA5 and LGP2. All three family members are comprised of a helicase domain, which contains an ATP binding domain and a Repressor domain (RD). RIG-I and MDA5 also contain two tandem CARDs, which serve as the signaling domain to downstream proteins.

Both RIG-I and MDA5 signal through this protein, and cells lacking a functional IPS-1 are unable to stimulate IFN expression through the RLR pathway, regardless of the presence of functional RIG-I or MDA5. Activated IPS-1 then signals the phosphorylation of many different proteins, including TBK1 and Ikk ϵ , which then in turn phosphorylates IRF-3. IPS-1 can also activate TRAF6 and subsequently other factors such as NF κ B. The activation of IRF-3, NF κ B results in the subsequent induction of IFN β expression (69). The RLR and TLR pathways are therefore somewhat redundant, activating the same subset of transcription factors in order to produce IFN β and result in an antiviral state.

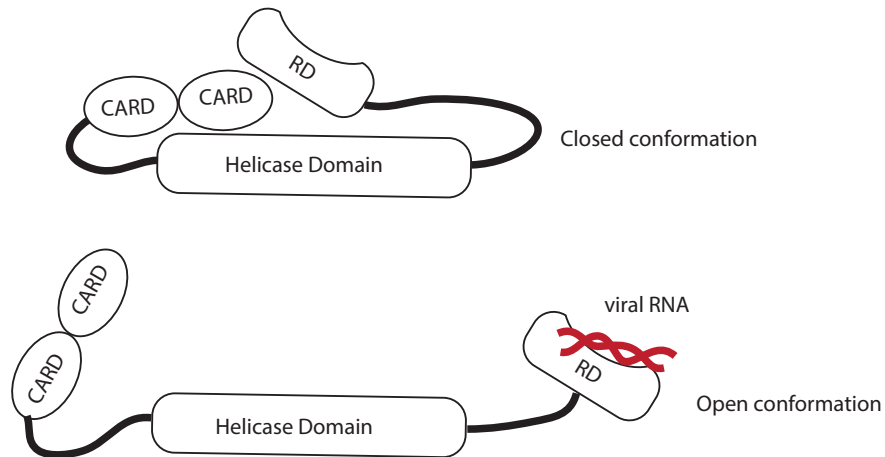


Figure 5: Conformation of the RIG-I protein both with and without a RNA bound. RIG-I is autoinhibited in the absence of an RNA PAMP. The flexible linker regions between the CARDs and Helicase domain and the helicase domain and RD allow for the RD to be folded over onto the CARDs, creating a “closed,” inactive conformation. When RNA binds the RD, the CARDs are released and are then free to participate in downstream signaling.

The IFN response

IFN- β acts in an autocrine or paracrine fashion, inducing the expression of effector proteins to promote an antiviral state (175). IFN- β is able to bind to the IFN receptor (IFNAR) and activate the receptor associated kinases Jak-1 and Tyrosine kinase-2 (Tyk-2). Jak-1 and Tyk-2 then phosphorylate and activate the signal transducers and activators of transcription (STAT) proteins, which are able to hetero- or homodimerize. The dimerized STAT proteins bind IRF-9, forming the transcription factor ISGF3. ISGF3 induces the expression of ISGs, including IRF-7, by binding to IFN-responsive sequence elements (ISREs) within the genome (Figure 6). In addition to establishing an antiviral state, thereby preventing viral infection of new cells, the production of IFN, ISGs, and other cytokines help to limit infection through a variety of mechanisms (30, 41, 110,

160, 175, 209). IFN stimulates expression of MHCII to target infected cells for killing by adaptive immune cells, as well as promoting apoptosis of infected cells, contributing to viral clearance. Additionally, recent work has demonstrated that type I IFNs can stimulate the maturation of dendritic cells, which can further enhance the adaptive immune response.

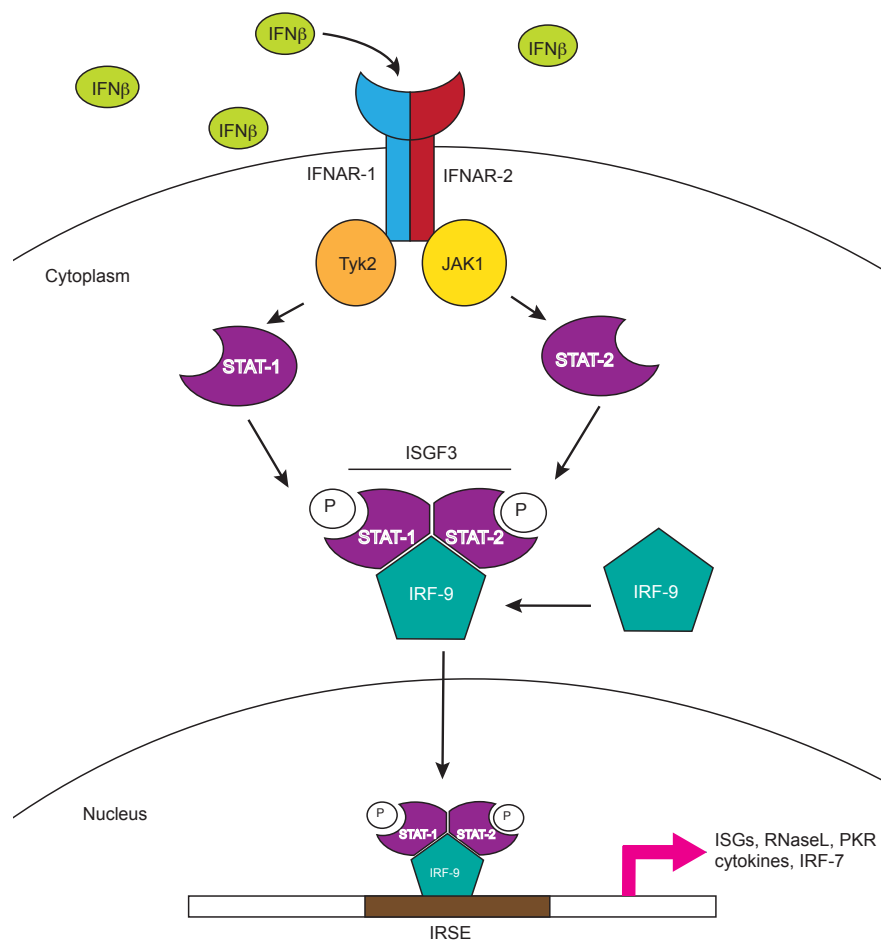


Figure 6: The IFNβ receptor pathway. IFN is able to act in a paracrine or autocrine fashion, binding to the IFNα/β receptor on the cell surface and activating the kinases JAK and Tyk, which phosphorylate STATs 1 and 2. Activated STATs 1 and 2 form a complex along with IRF-9, the ISGF3, which is able to translocate to the nucleus and bind ISRE in the genome to induce expression of effectors proteins, such as cytokines and other antiviral proteins.

IFN production has also been shown to act as a stimulator of antibody production. The varied responses induced by type I-IFN makes its production an important bridge between the innate intracellular antiviral response and the adaptive immune response

Viral PAMPs of RIG-I

Several viruses have been shown to be recognized by either RIG-I, MDA5 or both (Table 1) (41, 58, 100, 104, 107, 109, 113, 149, 75, 11). RIG-I recognizes RNA viruses with both positive and negative sense genomes. Positive sense viruses include human immunodeficiency virus (HIV), flaviviruses such as JEV and HCV, and several paramyxoviruses, including Sendai virus, Newcastle disease virus, and respiratory syncytial virus (RSV). Negative sense viruses recognized by RIG-I include vesicular stomatitis virus (VSV) and influenza A. MDA5 is activated by picornaviruses, such as encephalomyocarditis virus and Theiler's virus. RIG-I and MDA5 are both involved in signaling during dengue virus and WNV infection, as well as the dsRNA reoviruses. The wide variety of viruses that are recognized by RIG-I and/or MDA5 suggests these proteins are capable of recognizing general properties of viral RNA as opposed to motifs or sequences specific to individual viruses. In the case of WNV, RIG-I serves as the initial PAMP sensor. Both RIG-I and MDA5 are ISGs and are therefore simulated after IFN expression. MDA5 serves to expand and/or amplify the antiviral response late in infection (53).

Table 1: Viruses recognized by the RLRs





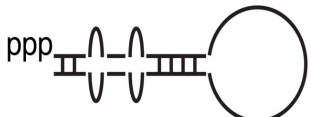
Virus/ligand	genome	RLR
<u><i>Flaviviridae</i></u> HCV JEV Dengue WNV	(+) ssRNA	RIG-I RIG-I RIG-I/MDA5 RIG-I/MDA5
<u><i>Picornaviridae</i></u> EMCV Theiler's virus Poliovirus	(+) ssRNA	MDA5 MDA5 MDA5
HIV	(+) ssRNA	RIG-I
<u><i>Paramyxoviridae</i></u> Sendai RSV Newcastle disease virus	(-) ssRNA	RIG-I RIG-I RIG-I
VSV	(-) ssRNA	RIG-I
influenza A	(-) ssRNA	RIG-I
ebola	(-) ssRNA	RIG-I
reoviruses	dsRNA	RIG-I/MDA5

It is important that the host is able to distinguish between viral and “self” RNAs, thus the viral PAMPs recognized by both RIG-I and MDA5 must be uniquely “viral” in structure. Viral genomes can be long, un-capped plus or minus sense RNAs. In addition, regions of dsRNA within the genome can form complex secondary and tertiary structures. Host cellular RNAs are typically capped, short, singled stranded RNAs with limited secondary structure. RIG-I and MDA5 may be able to recognize viral verses host RNAs due to these differences. Analysis of viral PAMPs has revealed a variety of features that serve to activate the RLRs (Table 2). It has been shown that dsRNA containing a 5’PPP serves as a potent

inducer of RIG-I signaling (74, 79, 140, 157, 158). Blunt-ended, dsRNA is also bound by RIG-I, although the affinity is weaker than for RNAs containing the triphosphate (94, 112). MDA5 has been shown to recognize long, dsRNA, at least 200nt in length (79).

Several studies have identified ligands of RIG-I that are virus specific, although these features are still structural in nature rather than related to viral sequence. The leader RNA of the measles and rabies viruses has both been shown to stimulate RIG-I. Additionally, a distinct polyU/C region in the 3'UTR of several viruses, including HCV, rabies and ebola virus are potent RIG-I activators. Products formed by the degradation of HCV RNA by the cellular antiviral effector, RNaseL, and panhandle structures found at the end of the influenza A genome, particularly those that are blunt ended and also contain a 5'PPP have also been shown to activate RIG-I (12, 143, 146, 152). RNAs lacking the 5'PPP have been shown to stimulate RIG-I, although this stimulation is generally much weaker than seen with RNA that does contain a 5'PPP (105, 192). Some non-viral RIG-I ligands include regions of dsRNA formed as result of copyback during *in vitro* transcription as well as poly(IC) (79, 157, 158).

Table 2: Structures capable of stimulating a RIG-I response. Adapted from Onoguchi, K. et al. 2010. Journal of Interferon and Cytokine Research.

RIG-I-stimulating RNA Structures	
Short (~300 bp) poly I:C Kato et al. 2008	pp  pp
In vitro T7 transcript with copyback Schlee et al. 2009, Schmidt et al. 2009	ppp  ppp
HCV RNA Saito et al. 2008	ppp  (polyU, UC) _n
RNaseL cleavage product (RNA of host/virus) Malathi et al. 2007	p  p
Viral genomic RNA (with panhandle structure) Rehwinkel et al. 2010	ppp  ppp

While RNAs containing 5'PPP have been identified as PAMPs, the experiments used to determine them do not take into consideration that viral RNAs are rarely found as “naked” RNA in the cell. RIG-I recognition of RNA containing a free 5'PPP fails account for the fact that some viruses are capped in order to mimic the host cell RNA; either stealing host caps or producing a cap-like structure. Thus, while RNA containing a 5'PPP is considered the most potent RIG-I activator, other PAMP structures are likely similarly stimulatory during a native infection.

Studies identifying viral PAMPs have also found that regions of dsRNA formed as the result of secondary and tertiary interactions can also serve as RIG-

I ligands. The regions of the HCV, ebola, measles and rabies virus that contain identified viral PAMPs are known to be highly structured. Additionally, several studies have found that the presence of a hairpin or panhandle structure at the 5' end of an RNA molecule is a strong stimulator of the RIG-I response (12, 146, 157, 176). This suggests that RIG-I recognition is related to a secondary structural motif found within these RNAs. This is not surprising, as RNA readily forms complex secondary and tertiary interactions and several secondary structures found in viral RNAs have been shown to be indispensable for viral replication and are therefore stably maintained within the genome.

In the case of WNV, the viral genome is capped at the 5' end and therefore lacks a free 5'PPP. Additionally, WNV RNA is contained within membrane structures formed in order to facilitate replication, and therefore would not necessarily be accessible. The virus does not encode a distinct polyU/UC region, nor does it synthesize a leader RNA during replication. This would suggest that another factor(s) is being recognized by RIG-I upon initial infection. Within the WNV genome, both 5'UTR and 3'UTR are reported to be highly structured, and there is also evidence for a strong stem loop structure within the viral genome at the junction between NS1 and NS2a (114). These structural elements may be contributing to the recognition of the viral genome by RIG-I.

RIG-I/RNA binding

Several studies have detailed the structure of RIG-I bound to a RNA ligand (36, 76, 84, 106). RIG-I bound to a dsRNA 10-mer shows that the CTD completely encases the RNA within a binding pocket. This pocket is lined with positively charged residues, which interact with the negatively charged RNA backbone to mediate binding. The bound RNA retains its conformation and does not show any signs of de-stabilization or unwinding, despite a reported helicase domain within RIG-I. The 2'-hydroxyl groups of the bound RNA interact with amide groups found in the binding cavity of the CTD, and these particular interactions explain the finding that modification of the 2' end of the RNA can inhibit RIG-I activation (106). RIG-I binding to RNA based on charge interactions further supports a structural component, such as the 5'PPP, being required for recognition by RIG-I, rather than a specific RNA sequence. Interactions within the binding pocket and the 5'PPP of the ligand RNA result in stronger binding than RNAs lacking a 5'PPP (76, 84, 87, 106). However, there is also evidence that RNA can bind, albeit more weakly, to the helicase domain of RIG-I. It is proposed that the weaker interaction between this domain and RNA allows RIG-I to constantly bind RNAs within the cell to "scan" for potential PAMPs; only upon binding an RNA that contains a 5'PPP or other structural element denoting it as "non-self" can it undergo the conformational change that allows CARD signaling (personal communication, Michael Gale). The "scanning model" is supported by work that demonstrates RIG-I can act as a translocase, moving along the RNA without inducing signaling (120).

Viral subversion of the antiviral response

A number of viruses have developed mechanisms to escape or actively interfere with the host innate antiviral response. For example, HCV inhibits the innate antiviral response by blocking signaling through the RIG-I pathway. The viral protease, NS3/4a cleaves the IPS-1 protein, thereby disrupting the signaling cascade and preventing RIG-I induced IFN expression (51, 96). WNV is able to similarly interfere with the innate immune response at later points in infection, after viral protein production has begun. The WNV NS2a, NS4b, and NS5 proteins have all been shown to interfere with or block IFN signaling and the antiviral response. However, at early points post infection, WNV evades detection by the host cell rather than actively impeding the RIG-I signaling pathway. This is evidenced by the fact that the appearance of antiviral effector proteins coincides with peak viral titers, between 16 and 24 hours post infections (hpi). This delay is beneficial for WNV, as the virus is able to establish a productive infection before the innate antiviral response is induced. The virus is thus able to replicate and spread before the induction of the IFN, as well as allow time for the accumulation of proteins that act to shut down antiviral signaling.

The immune response to WNV

The factors that contribute to the pathogenicity of WNV are not well understood. One factor may be the strength or kinetics of induction of the innate immune response. It is therefore important to understand the host innate intracellular immune response to infection. Several studies have analyzed the

immune responses, both innate and adaptive, to WNV and other *flaviviridae* family members, in an effort to characterize the factors that influence pathogenesis. During the innate response to WNV, TLR-3 and -7, as well as RIG-I and MDA5, can serve to induce the expression IFN and initiate an antiviral response. However, the precise role of TLR-3 in WNV infection remains controversial. TLR-3 has been reported as being important for stimulating an immune response to WNV. Abrogation TLR-3 resulted in enhanced lethality in infected mice (40). There has also been a report, however, that the knock down of TLR-3 increases the resistance to lethal WNV infection in mice (190).

In contrast to TLR-3, TLR-7 knock down in mice resulted in increased neuroinvasion as a result of the failure of macrophages to migrate to the sites of infection and prevent the spread of the virus (185). This suggests that TLR7 signaling is important for the production of cytokines necessary to attract leukocytes critical for viral clearance. Additionally, activation of TLR7 in keratinocytes has been shown to result in the migration of Langerhan cells from the initial site of infection within the skin into draining lymph nodes (44, 194). This is both positive, as these cells then traffic to lymph nodes and attract leukocytes, and negative, as this allows WNV to spread to new areas (77).

Studies analyzing the connection between the innate and adaptive immune responses have found that induction of a strong innate immune response can often have both positive and negative consequences during infection. While induction of interferon and other cytokines can increase trafficking of leukocytes to infected areas (44, 59, 77, 191), it is also thought to

increase the permeability of the blood-brain barrier, potentially providing the virus access to the brain and increasing neuro-pathogenesis (43, 44, 190). For example, increased production of cytokines activated through TLR-3 signaling in older mice resulted in an increase in inflammation in the brain during infection with WNV (85).

Although RIG-I is known to be an important component of the innate antiviral response to WNV, little is known about how the response is induced during infection. Identification of the PAMPs associated with WNV will provide important information regarding the ability of RIG-I to identify and respond to WNV RNA. In the present studies, we characterize the regions of the WNV genome that are capable of inducing a RIG-I mediated antiviral response. We also analyze the structure of one of these PAMPs in order to further explore the structural requirements for the induction of the antiviral response during WNV infection.

Chapter 2- Identification of Multiple RIG-I-Specific Pathogen Associated Molecular Patterns Within the West Nile Virus Genome and Antigenome

Introduction

West Nile virus (WNV) is a positive-sense, single-stranded RNA virus from the family *Flaviviridae*. The genome is ~11kb and consists of an open reading frame (ORF) flanked by 5' and 3' untranslated regions (UTRs). Within the UTRs, conserved sequences and predicted secondary structures encode the signals for negative strand synthesis, genome amplification, translation, and packaging. The incoming viral genomic RNA functions as a template for both translation, which produces a single polyprotein, and replication. The viral polyprotein is co- and post-translationally cleaved by host and viral proteases to generate ten individual proteins. The structural proteins, core (C), membrane (prM/M), and envelope (E), are involved in viral assembly, host cell binding, and entry. The seven nonstructural (NS) proteins (NS1, NS2A/B, NS3, NS4A/B, and NS5) support viral replication and evasion of the host antiviral response. Following polyprotein synthesis, genomic RNA is transcribed by the viral polymerase, NS5, to generate the complementary minus-strand antigenome, which serves as a template for synthesis of additional genomic RNA. Newly synthesized genomic RNA is either translated by the host cell or packaged into virus particles(21, 22, 29, 98).

In areas where WNV is endemic, such as the Middle East, Africa, and Asia, infection is typically asymptomatic or associated with a mild febrile illness known as West Nile fever(137). In contrast, recent outbreaks in the Western hemisphere have been marked by an increase in disease severity, including meningitis, encephalitis, and acute flaccid paralysis(67, 83, 121). Since its introduction into the United States in 1999, WNV has spread to every state within the continental United States, as well as parts of Canada, Mexico and the Caribbean (information found on the CDC website www.cdc.gov/ncidod/dvbid/westnile/index.htm). As of January 2012, yearly outbreaks of WNV have resulted in 13,229 reported cases with neurological complications and 1,263 deaths, making WNV the leading cause of mosquito-borne neuroinvasive disease in the United States.

The ability to rapidly sense an invading pathogen and respond appropriately is a critical factor influencing the outcome of infection. The intracellular pathogen recognition receptor (PRR) RIG-I plays a critical role in sensing a wide variety of viruses, including positive strand viruses such as WNV, Japanese encephalitis virus (JEV), hepatitis C virus (HCV), dengue virus and poliovirus, and negative strand RNA viruses such as paramyxoviruses, influenza, and vesicular stomatitis virus (VSV)(53, 80, 146, 152). The fact that RIG-I detects a wide variety of viruses spanning multiple families suggests that it is able to interact with multiple substrates. Recent evidence indicates that double stranded structures within viral RNAs function as primary activators of RIG-I during infection (12, 15, 79, 109), though 5' triphosphate (5'ppp) moieties

enhance detection of short dsRNAs (74, 140, 157, 158). Additionally, poly-UUC motifs in the genomes of HCV, measles, rabies and Ebola viruses are important for activating RIG-I (152). Once activated by a viral PAMP, RIG-I initiates a signaling cascade that results in the activation of latent transcription factors such as interferon regulatory factor 3 (IRF3)(69, 175, 180). Activation of IRF3 leads to the induction of type-I interferons (IFNs) as well as a subset of antiviral effector proteins such as IFN-stimulated gene 56 (ISG56) (69, 81, 175, 180). The induction of these IRF3 target genes results in the establishment of an antiviral state within the cell, which blocks viral replication.

As eukaryotes evolved strategies to combat invading pathogens, viruses have co-evolved processes to escape them. While many viruses actively impede the RIG-I signaling pathway (9, 20, 56, 99, 113, 134, 135), the pathogenic strain of WNV, WNV New York (WNV-NY), eludes detection at early times post-infection (52). However, the mechanism(s) by which WNV evades detection early during infection is currently unclear. We have previously demonstrated that cells treated with UV-inactivated WNV fail to induce an antiviral response, suggesting that RIG-I senses a product of viral replication. Furthermore, the WNV-NY genome lacks a poly-U/UC region, suggesting that RIG-I senses either dsRNA structures within the WNV genome or antigenome or an as of yet unidentified stimulatory motif. To distinguish between these possibilities, we undertook a systematic analysis of the WNV-NY genome and antigenome to define RIG-I-specific PAMPs. Multiple RIG-I stimulatory regions were identified throughout the WNV genome and antigenome. However, incorporation of these

regions into larger RNAs abolished their stimulatory potential, suggesting that the WNV PAMPs are masked in the context of the full genome and antigenome. This masking of the PAMPs likely accounts for WNV's ability to evade the innate immune response early during infection.

Results

WNV proteins do not induce an antiviral response.

Expression of the measles virus nucleocapsid protein alone has been shown to be sufficient to induce the host antiviral response (182). Therefore, we assessed the stimulatory capacity of WNV proteins from a pathogenic and nonpathogenic strain utilizing a luciferase reporter. Huh7 cells were transfected with a RIG-I-dependent luciferase reporter, ISG56-luc (182), and subsequently infected with Sendai Virus (SenV), a potent RIG-I-specific activator of the innate immune response, or transfected with plasmids encoding specific WNV genes. Cultures transfected in parallel were assessed for protein expression using western blot analysis (Table 3). Luciferase levels in cultures expressing WNV proteins were similar to mock transfection controls, suggesting that WNV proteins do not function as activators of the host antiviral response.

Table 3: Summary of WNV protein expression experiments.

WNV-NY Gene ^a	Protein Expression ^b	Luciferase Expression ^c	WNV-MAD78 Gene ^a	Protein Expression ^b	Luciferase Expression ^c
C	+	-	C	+	-
prM	+	-	prM	+	-
E	+	-	E	+	-
NS1	+	-	NS1	+	-
NS2a	+	-	NS2a	+	-
NS2b	+	-	NS2b	+	-
NS3	+	-	NS3	+	-
NS4a	+	-	NS4a	+	-
NS4b	+	-	NS4b	+	-
NS5	+	-	NS5	+	-

a) WNV gene. Cell lysates were prepared 8 hr post transfection and b) viral protein expression was assessed by western blot analysis +, protein expression, - no protein expression. c) +, luciferase levels were above the mock transfected control; -, luciferase levels similar to mock. Values represent the average luciferase expression compared to mock (\pm standard error) from a minimum of two independent experiments.

The 5' and 3' UTRs of WNV induce an antiviral response.

Because secondary structures within RNA are essential for recognition by and activation of RIG-I (12, 15, 74, 79, 105, 109, 120, 146, 157, 158), we hypothesized that the highly structured 5' and 3' UTRs of WNV stimulate RIG-I. Therefore, we assessed the capacity of these regions to stimulate a RIG-I-dependent antiviral response using a luciferase reporter assay. The assay was performed as previously described, but transfection with RNAs corresponding to the genomic (+) or antigenomic (-) 5' and 3' UTRs was used instead of plasmids encoding the WNV proteins. Cell lysates were recovered and analyzed for luciferase expression 8 hr after RNA transfection to ensure that the induction of luciferase expression was due to the primary activation of the RIG-I signal transduction pathway and not subsequent feedback amplification loops.

Significant induction of luciferase expression was detected in SenV-infected cells as well as cultures transfected with the WNV 5' (+) and 3' (-) UTRs (Figure 7A). In contrast, neither the WNV 3' UTR (+) nor WNV 5' UTR (-) fragments induced luciferase expression. In order to more accurately mimic the RNAs present during a native infection, the stimulatory capacity of the 5' UTR (+) containing a cap structure and the 5' UTR (-) containing a 5' PPP were also examined (Figure 7A). Neither the presence of a capped structure on the 5' UTR (+) nor a 5' PPP on the 5' UTR (-) altered the stimulatory capacity of these fragments.

The robust induction of the antiviral response by the capped 5' UTR (+) fragment suggested that the incoming viral genome is capable of functioning as a PAMP for RIG-I detection. However, the failure of WNV to initiate a rapid antiviral response indicates that this region is not accessible to RIG-I early in infection (52). Interactions between the 5' and 3' ends of the WNV genome have been shown to be essential for genome replication, suggesting that the 5' UTR does not function as an independent structural element during infection. Therefore, we generated a construct consisting of the 5' UTR to the conserved sequences (CS) element, located in the N- terminal coding region of the C gene, linked to the 3' UTR by the *egfp* reporter gene (5'UTR+CS-eGFP-3'UTR). Neither CIP-treated nor capped 5'UTR+CS-eGFP-3'UTR RNAs stimulated luciferase expression (Figure 7B), suggesting that the 5' UTR is not a functional PAMP when presented to the cell in this context.

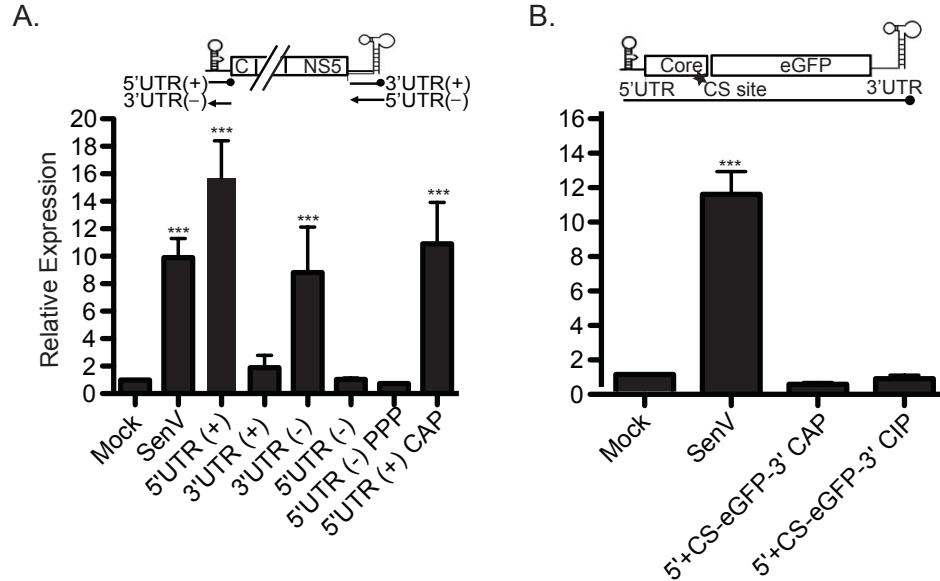


Figure 7: The 5' UTR (+) and 3' UTR (-) region of the WNV-NY genome induce an antiviral response. Huh7 monolayers were transfected with pISG56-luc and pCMV-*Renilla* 16 hr prior to infection with SenV or transfection with 500 ng of the indicated RNAs in triplicate. Cell lysates were prepared 8 hr post transfection and assayed for luciferase activity. Values represent the average luciferase expression compared to mock (\pm standard error) from a minimum of two independent experiments. Statistical analysis was performed using Dunnett's multiple comparison analysis, * $p < 0.05$, ** $p < 0.01$ *** $p < 0.001$. (A) Cells were transfected with RNA fragments corresponding to the genomic or antigenomic 5' and 3' UTRs. (B) Cells were transfected with 5'UTR+CS-eGFP-3'UTR RNAs.

Multiple regions of the WNV genome and antigenome induce the host antiviral response.

To determine whether other regions of the genome also harbor RIG-I PAMPs, the stimulatory capacity of RNAs corresponding to the individual WNV genes was assessed. While several fragments induced low to moderate levels of luciferase expression, only RNAs corresponding to NS2a (+), E (-), NS2a (-) and NS4a (-) functioned as potent stimulators of the antiviral response (Figure 8A & B). Thus, multiple regions within the WNV genome and antigenome are capable of stimulating an antiviral response.

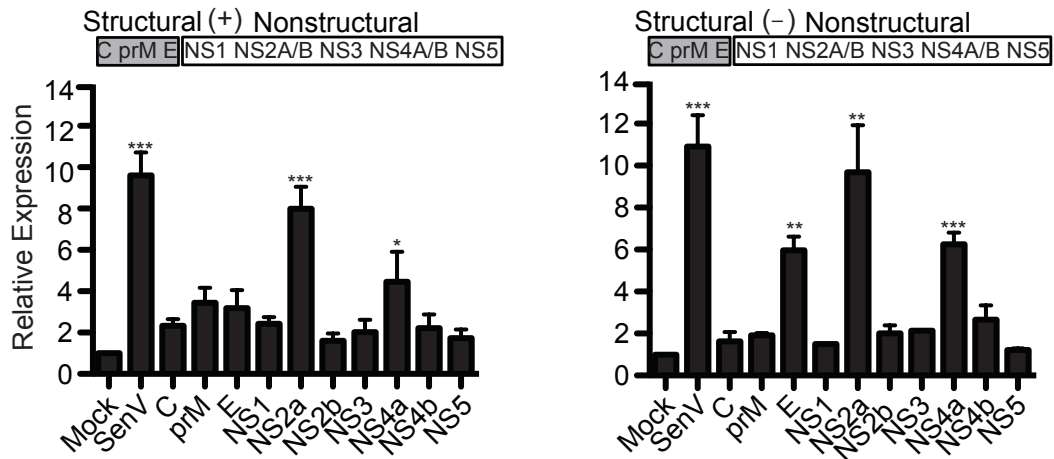


Figure 8: Multiple regions of the WNV genome and antigenome induce an antiviral response. Cells were transfected with ISG56-luc and pCMV-*Renilla* as described in Figure 7. Cultures were subsequently transfected with 500 ng of RNA fragments corresponding to genomic (A) or antigenome (B) orientation of WNV genes. Luciferase expression was assessed as described in Figure 7.

The antiviral response to WNV PAMPs is RIG-I-dependent.

The rapid and robust induction of luciferase expression by the 5' UTR (+), 3' UTR (-), NS2a (+), E (-), NS2a (-) and NS4a (-) RNAs was indicative of a RIG-I-dependent response. To confirm the specificity of this response, the ability of the identified PAMPs to form a stable complex with RIG-I was examined using limited trypsin digestion. This assay assesses the ability of a PAMP to induce conformational changes in RIG-I associated with the generation of the signaling-active form s(151, 152, 180). Incubation of *E.coli*-purified RIG-I with each of the WNV PAMPs identified above resulted in the accumulation of a 17-kDa trypsin resistant band indicative of the signaling-active form of RIG-I (Figure 9A). However, only a weak band was detected in the presence of the 5' UTR (+) fragment, suggesting that, unlike the other PAMPs, this fragment does not bind

tightly to RIG-I. We further verified the specificity of the identified PAMPs using the RIG-I-deficient Huh7.5 cell line (Figure 9B) (19, 177). High levels of luciferase expression were detected in control cells transfected with a constitutively active form of RIG-I, N-RIG. In contrast, WNV RNA fragments did not induce an antiviral response in the absence of functional RIG-I. Together, these findings indicated that the WNV PAMPs identified above induce a RIG-I-dependent antiviral response.

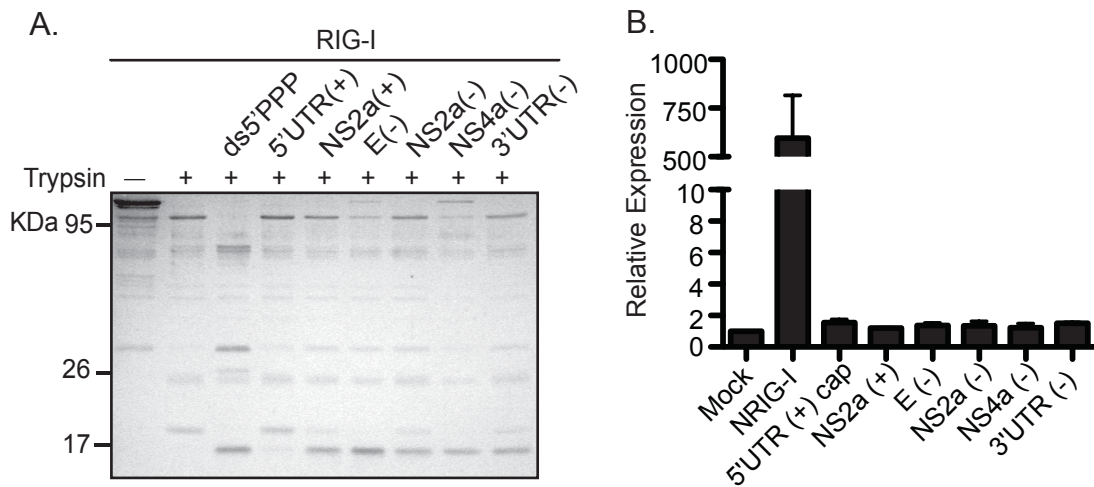


Figure 9: WNV PAMPs induce a RIG-I-specific antiviral response. (A) Purified RIG-I was incubated with control dsRNA or the indicated WNV RNA fragments prior to the addition of trypsin. Digestion products were separated on a 12.5% SDS polyacrylamide gel and visualized by Coomassie stain. (B) Huh7.5 monolayers were transfected with luciferase reporter constructs and 500 ng of the indicated RNAs or pEF-flagN-RIG, as described in Figure 7. Luciferase expression was assessed as described in Figure 7.

Incorporation of WNV PAMPs into larger RNAs masks their stimulatory capacity.

To determine whether WNV RNA sequences or structures spanning the individual genes are capable of stimulating RIG-I, we also tested the stimulatory capacity of overlapping segments of the viral genome and antigenome (Figure 10A & B). With the exception of the 5' UTR-prM (+) fragment, the overlapping segments failed to induce high levels of luciferase expression, despite the fact that several segments contained the highly stimulatory NS2a (+), E (-), NS2a (-) or NS4a (-) regions.

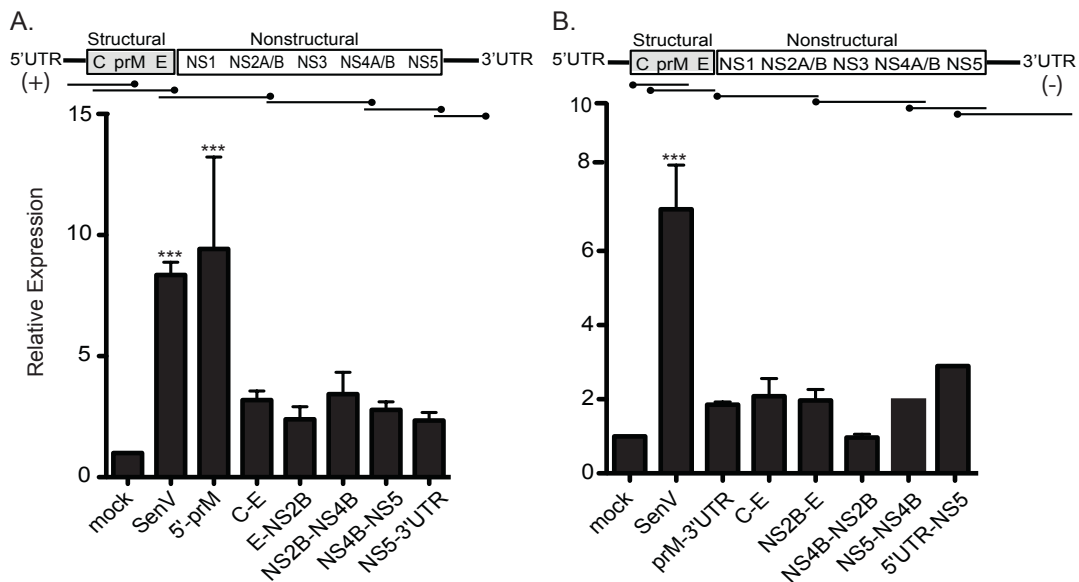


Figure 10: Larger RNAs containing WNV PAMPs fail to activate an antiviral response. Huh7 monolayers were transfected with ISG56-luc and pCMV-*Renilla* as described in Figure 7 and subsequently transfected with 500 ng of RNA fragments corresponding to the indicated sections of the WNV genome (A) or antigenome (B). Luciferase expression was assessed as in Figure 7.

In this experiment, we transfected cells with equivalent amounts of each of the RNAs based on mass. To ensure that the lack of stimulation by the larger fragments was not due to differences in the RNA copy number introduced into the cell, we also assessed the stimulatory capacity of these regions by transfecting equivalent moles of the various fragments. While similar levels of inductions were detected for the NS2a (+), E (-), NS2a (-) and NS4a (-) regions under these conditions, equal molar amounts of the larger RNA fragments did not induce luciferase expression (Figure 11). This suggests that RIG-I is unable to efficiently detect WNV PAMPs in the context of a larger RNA even when equivalent RNA copy numbers are introduced into the cell.

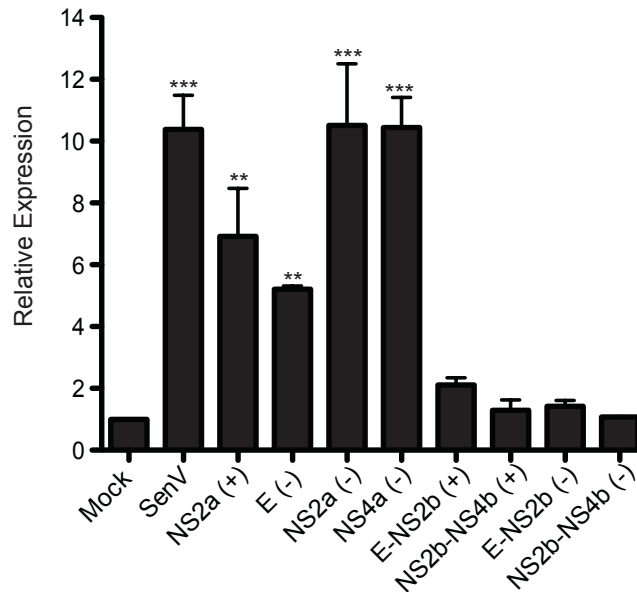


Figure 11: Larger RNAs containing WNV PAMPs fail to activate an antiviral response even with equivalent masses of RNA. Huh7 monolayers were transfected with ISG56-luc and pCMV-*Renilla* as described in Figure 7 and subsequently transfected with equal molar amounts (2pmol) of the indicated RNAs. Luciferase expression was assessed as described in Figure 7.

WNV genomic RNAs do not induce RIG-I activation.

The lack of RIG-I activation by the 5'UTR+CS-eGFP-3'UTR RNAs and the larger overlapping segments of the viral genome suggested that the stimulatory capacity of these PAMPs is masked in the context of full-length viral RNAs. Therefore, we assessed the stimulatory capacity of full-length genomic RNA isolated from culture supernatants (FL-WNV) or produced through *in vitro* transcription and capping (capped-FL-IT-WNV) (Figure 12). Both forms of genomic RNA failed to induce luciferase expression, further supporting the hypothesis that WNV PAMPs are masked in the context of the full genome.

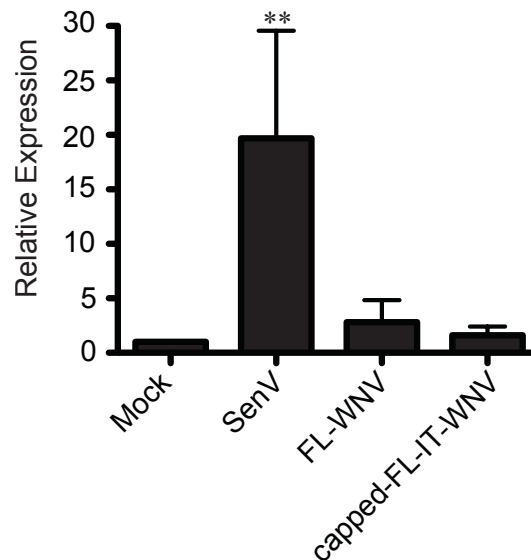


Figure 12: WNV genomic RNAs do not induce an antiviral response. Cells were transfected with ISG56-luc and pCMV-*Renilla* as described in Figure 7. Cultures were subsequently transfected with 500 ng of: (A) genomic RNA isolated from culture supernatants (FL-WNV), (B) full length *in vitro* transcribed and capped WNV genomic RNA (capped-FL-IT-WNV). Luciferase expression was assessed as described in Figure 7.

Processing by the host contributes to the production of RIG-I PAMPs

Our findings suggested that processing of the viral genome and antigenome is necessary to expose the identified RIG-I PAMPs. Alternatively, stimulation of the RIG-I pathway may require high levels of RNA expression, which was not re-capitulated in our assay system. To distinguish between these two possibilities, we examined the stimulatory capacity of a WNV RNA fragment over a longer time course (Figure 13). Cells were transfected with 5'-prM (+), which served as a positive control as it was the only overlapping fragment to show stimulation of RIG-I at 8 hours post transfection, or NS4b-2b (-). As previously observed, by 8 hours post transfection, 5'-prM (+) RNA induced luciferase expression, while NS4b-2b (-) did not. However, after 16 hours post transfection, both the 5'-prM (+) and NS4b-2b RNAs were able to induce luciferase expression, suggesting that cellular processing may be liberating PAMPs from the WNV genome capable of stimulating a RIG-I response.

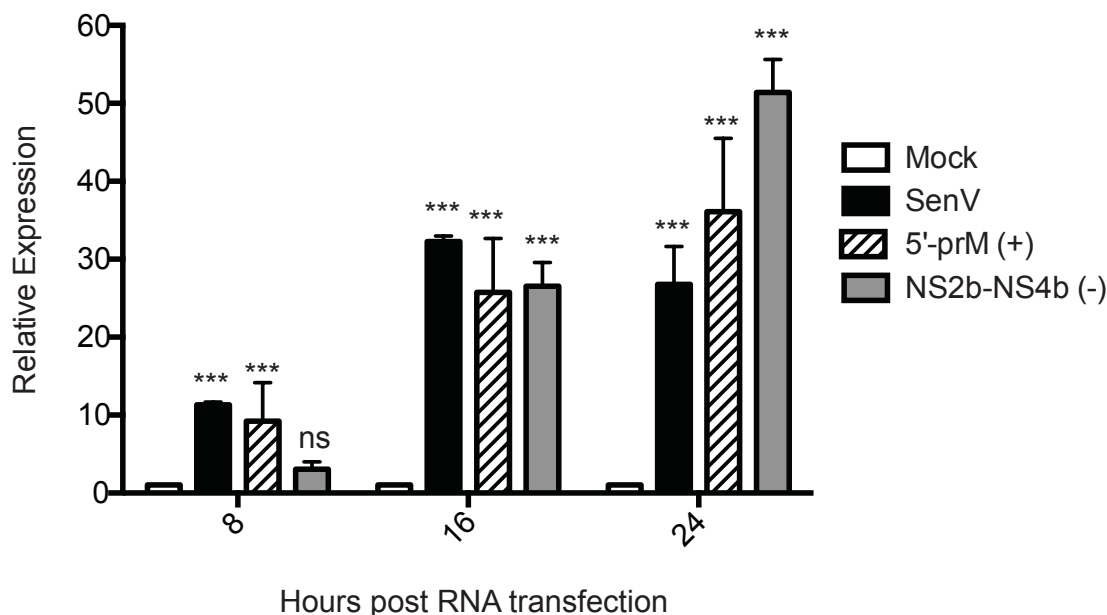


Figure 13: **Larger RNA containing WNV PAMPs induce an antiviral response over time.** Cells were transfected with ISG56-luc and pCMV-*Renilla* as described in Figure 7. Cultures were subsequently transfected with 500 ng of the indicated RNAs. Cell lysates were prepared 8, 16 and 24 hrs post transfection and assayed for luciferase activity. Values represent the average luciferase expression compared to mock (\pm standard error) from a minimum of two independent experiments. Statistical analysis was performed using Dunnett's multiple comparison analysis, * $p < 0.05$, ** $p < 0.01$ *** $p < 0.001$.

To confirm the activation detected at later time points post transfection was RIG-I specific, we assessed the stimulatory capacity of these RNAs over time in Huh7.5 cells (Figure 14). Luciferase expression was not detected at any point in cells transfected with NS4b-2b (-) RNA, confirming stimulation by this PAMP is RIG-I-dependent. Abrogation of RIG-I signaling also ablated luciferase expression in cells transfected with 5'-prM (+) at 8 hours. However, significant luciferase expression was detected at 24 hours post transfection, suggesting that other PRRs contribute to the antiviral response to WNV at later times post-infection.

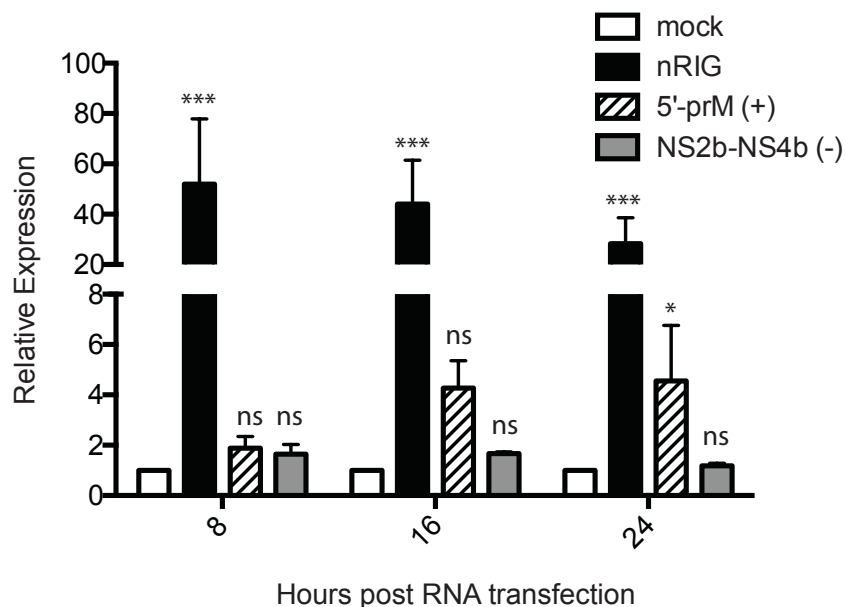


Figure 14: Stimulation by larger WNV RNAs over time is RIG-I specific. Huh7.5 Cells were transfected with ISG56-luc and pCMV-*Renilla* as described in Figure 7. Cultures were subsequently transfected with 500 ng of the indicated RNAs. Cell lysates were prepared 8, 16 and 24 hrs post transfection and assayed for luciferase activity. Values represent the average luciferase expression compared to mock (\pm standard error) from a minimum of two independent experiments. . Statistical analysis was performed using Dunnett's multiple comparison analysis, * $p < 0.05$, ** $p < 0.01$ *** $p < 0.001$.

Subgenomic flavivirus RNA does not induce RIG-I activation

We sought to further define the cellular processing pathways that contribute to PAMP production. During infection, incomplete digestion of genomic viral RNA by the 5'-3' exoribonuclease XRN1 results in the accumulation of a highly structured 3' UTR-derived monophosphorylated subgenomic RNA (sfRNA) (24, 55, 141). To determine if sfRNA can serve as PAMP, we tested the stimulatory capacity of both a CIP-treated and a monophosphorylated sfRNA construct. Although luciferase expression in cells transfected with either CIP-treated or monophosphorylated sfRNA was

consistently higher than background levels, the increase in luciferase expression did not reach statistical significance for either RNA (Figure 15). This finding suggests that sfRNA does not function as a major PAMP during WNV infection and is consistent with previous reports that the sfRNA promotes WNV pathogenesis (141, 159, 164).

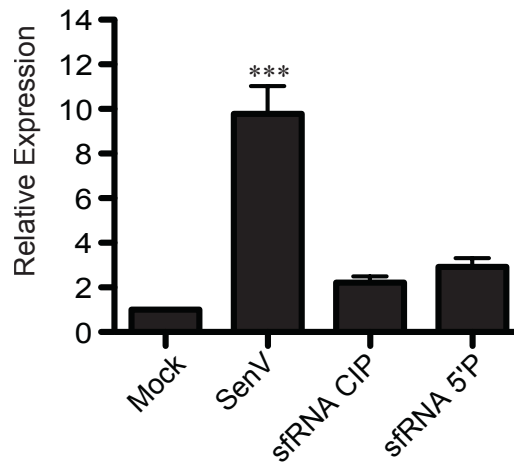


Figure 15: **WNV subgenomic RNAs do not induce an antiviral response.** Cells were transfected with ISG56-luc and pCMV-*Renilla* as described in Figure 7. Cultures were subsequently transfected with 500 ng of the indicated sfRNA constructs. Luciferase expression was assessed as described in Figure 7.

Discussion

In this study we utilized a systematic approach to identify RIG-I-dependent PAMPs present in the WNV genome and antigenome. Our findings demonstrated that WNV, in contrast to many other viruses (143, 152, 157, 188), encodes multiple segments located throughout the genome and antigenome that are capable of stimulating RIG-I. The lack of sequence similarity between the stimulatory regions suggests that RIG-I detects dsRNA structures within these

regions rather than a specific sequence motif. Secondary structural predictions indicate that the identified stimulatory regions within the WNV genome are highly structured (Figure 36-42, see appendix 5). While these structural predictions need to be tested experimentally, they provide a conceptual scaffold to begin defining the structural elements involved in RIG-I detection. Our finding also suggest that the intact the WNV genome and antigenome are poor activators of RIG-I. Larger RNA fragments as well as the full-length genomic RNA failed to induce the rapid activation of the antiviral response. These findings are consistent with a recent report demonstrating that RIG-I does not bind to the full-length genome of SenV (12).

Multiple factors may play a role in masking WNV PAMPs within full-length viral RNAs. It is possible that the secondary structures detected by RIG-I are altered or abolished in the context of the full genome. Alternatively, tertiary structures within the viral RNA may sterically hinder RIG-I's ability to bind the PAMPs. Comparison of the secondary structure predications for the 5'UTR alone and the 5'UTR in the context of the viral genome or the 5'UTR-prM fragment suggests that the structure of this region is not substantially altered when incorporated into larger RNAs (Figure 42). However, in the case of the incoming genome, the stimulatory capacity of the capped 5' UTR (+) may be obstructed by several additional factors. Upon entering cells, the viral genome undergoes cap-dependent translation to generate the viral polyprotein. Thus, host translational machinery may block RIG-I's access to this region. The viral genomic RNA also serves as a template for synthesis of the negative sense

antigenome, which requires interactions between the conserved sequence (CS) elements located within the 5' end of core and the 3' UTR as well as base pairing between a 5' UAR (upstream initiation AUG region element) and a 3' UAR. Therefore, long distance interactions between the 5' and 3' UTRs may sequester the stimulatory signals within the 5' UTR early in infection. The observations that the 5'UTR-prM fragment stimulated RIG-I, while the 5'UTR+CS-eGFP-3'UTR fragment did not, is consistent with this hypothesis.

Our findings suggested that WNV also evades detection at early times post-infection by sequestering potential PAMPs within the viral genome and antigenome. The mechanism(s) by which WNV PAMPs eventually become accessible to RIG-I during the course of infection are currently under investigation. As previously demonstrated for SenV and influenza virus, subgenomic defective interfering (DI) particles may play a role in stimulating RIG-I activation (12). The deletion of large segments from the viral genome may result in the exposure of WNV PAMPs that were previously buried within the full-length viral RNAs, thus providing the proper context for RIG-I recognition. In addition, the normal cellular processes of RNA degradation may be involved in the exposing of WNV PAMPs within the genome during the course of infection. This hypothesis is supported by the observation that when larger fragments of the WNV genome, which failed to induce a RIG-I response by 8 hours, are transfected into cells, RIG-I stimulation is observed 16 and 24 hours post transfection. The fact that the subgenomic sfRNA of WNV failed to substantially activate RIG-I suggested that the exonuclease XRN1 is not involved in liberating

RIG-I PAMPs. However, other cellular pathways, such as the “no-go” RNA degradation pathway, which is triggered by stalled ribosomal movement, may be involved in the processing of WNV viral RNAs (45, 183, 184). Furthermore, as has been demonstrated for HCV, activation of the OAS/RNaseL pathway later in infection may liberate additional PAMPs that help sustain and/or amplify the antiviral response (109, 156). In the case of the WNV antigenome, alternative RNA processing pathways may be required for the release of virally encoded PAMPs. The antigenome of WNV exists within the cell in two forms, the double-stranded replicative form (ds-RF) and the replicative intermediate (RI). The ds-RF consists of a nascent antigenome paired with the genome template, while the RI consists of a single copy of the viral antigenome and multiple strands of nascent genomic RNA being synthesized (58, 198). Detection of viral antigenome by the host cell may be limited due to the fact that the RI is sequestered within membrane invagination. However, processing the ds-RF by either the cell’s RNAi or ADAR/TSN pathway may liberate PAMPs from the WNV antigenome (154, 155, 186). These mechanisms, as well as other as of yet unknown cellular degradation pathways, may contribute, individually or in concert, to the liberation of PAMPs. Further analysis of the WNV RNAs produced both *in vitro* and *in vivo* will be necessary to more precisely map the WNV stimulatory regions with the viral genome and antigenome and to elucidate how PAMPs are produced over the course of infection.

Chapter 3 – Analysis of the WNV 5'UTR

Introduction

WNV is a (+) sense single stranded RNA virus of the family *Flaviviridae*. The WNV genome is ~11kb in length and encodes ten proteins. The genome is also flanked by 5' and 3' untranslated regions (UTRs). These regions have been previously reported to be critical for proper RNA translation and viral replication (32, 65, 95, 187, 213). The 5'UTR is either 96 or 97 nucleotides (nt) in length, depending on the strain (92). Several structure predictions, confirmed through mutational analysis, have determined that the 5'UTR is composed of 2 stem loop (SL) structures, identified as SLA and SLB. SLA is comprised of the first 70 nucleotides of the genome. SLB is located at the 3' end of the 5'UTR and contains the upstream AUG region (UAR). The 5' UAR interacts with a corresponding sequence in the 3'UTR and is critical for genome cyclization and RNA synthesis.

WNV has emerged in the past decade as a new public health threat in the Western hemisphere. Infection in regions where the virus was previously endemic typically results in a mild, febrile illness. However, strains that have recently emerged in the United States show a much higher incidence of severe neurological disease symptoms (111, 137). In the last year alone, there have been 5,387 reported cases in 2012, with 2,734 patients suffering severe

neurological disease and 234 deaths (Information from the CDC website, [www.http://www.cdc.gov/ncidod/dvbid/westnile/index.htm](http://www.cdc.gov/ncidod/dvbid/westnile/index.htm)). The factor(s) that contribute to the differences in pathogenicity between strains is poorly understood, although the induction of the host antiviral response may influence WNV pathogenicity.

The rapid induction of the innate immune response, mediated by pathogen recognition receptors (PRRs), is critical to limiting the scope and severity of infection. The cytoplasmic PRR retinoic acid inducible gene I (RIG-I) has been shown to be an important mediator of the innate immune response during WNV infection (53). Activated RIG-I is able to initiate a signaling cascade that results in the phosphorylation, dimerization and translocation of the transcription factor interferon regulatory factor 3 (IRF3) to the nucleus. IRF3 is able to directly induce the expression of several interferon-stimulated genes (ISGs), including ISG56 and ISG15 (61, 175). It also, in concert with other transcription factors, is able to induce the expression of interferon β (IFN- β) and thus initiate a type I IFN mediated antiviral response (69). We previously reported that WNV-New York (WNV-NY) is able to evade the innate immune response at early times post infection (52). This allows the virus to establish a productive infection and spread to neighboring cells prior to the induction of a robust innate antiviral response.

RIG-I and other PRRs are able to respond to viral infection by recognizing pathogen associated molecular patterns (PAMPs). Interaction of a RNA PAMP with the binding domain of RIG-I induces a conformational change that allows it to signal to downstream pathway components and subsequently induce the

expression of IFN (10, 39, 120). Recent structural analysis shows that blunt ended dsRNA containing a 5'triphosphate (5'PPP) is the most potent stimulator of RIG-I, although RNA lacking a 5'PPP can stimulate as well, despite a much weaker binding affinity (76, 84, 105, 106). Additionally, studies indicate that regions of dsRNA are required for strong binding, as affinity between RIG-I and ssRNA is poor. Poor binding affinity results in the inability to stimulate the RIG-I response, and indeed ssRNA is not stimulatory *in vivo*. This is not surprising, as many host cellular RNAs are single stranded. However, one model of RIG-I activation states the weak affinity for ssRNA allows RIG-I to constantly sample RNA within the cell, but only initiate antiviral signaling upon recognition of a PAMP structure (personal communication, Michael Gale). Thus, RNA with secondary structure and a 5'PPP is the most potent stimulator of the antiviral response, but other RNAs are also capable of binding to and possibly activating RIG-I.

Previous studies have demonstrated WNV is recognized by RIG-I during infection (53) and in chapter 2, we determined that several regions of the WNV genome and antigenome are capable of inducing a RIG-I mediated antiviral response. However, the specific structural features of WNV RNA involved in RIG-I activation still remain unknown. In order to gain further perspective on the RIG-I mediated antiviral response to WNV, we analyzed the structure and binding interactions with one of the identified PAMPs, the 5'UTR, utilizing selective 2'-hydroxyl acylation analysis by primer extension (SHAPE). SHAPE utilizes an electrophile, such as 1-methyl-7-nitroisatoic anhydride (1M7), to

selectively form adducts at the 2'hydroxyl position of RNA nucleotides that are unconstrained by base pairing. These adducts are identified as positions during primer extensions. The reverse transcriptase pauses, producing a product that is shifted one base upstream of the adduct-containing nucleotide. The product can then be resolved via denaturing polyacrylamide gel electrophoresis (PAGE) (115, 201, 202). Additionally, we sought to compare the structure of and the RIG-I response to the 5'UTR of a nonpathogenic viral strain, WNV-Madagascar78 (WNV-MAD78), as well as variations of the WNV-NY 5'UTR, including both a mutated and truncated RNA.

Our findings suggest that the WNV 5'UTR contains both secondary structural elements and regions of single stranded RNA. Additionally, both the WNV-NY and WNV-MAD78 5'UTR appear to be structurally similar and stimulated the RIG-I response to similar degree, despite a difference in sequence. Further analysis of RIG-I stimulation using mutated or truncated 5'UTRs revealed different stimulatory capacities. Despite the differences in stimulatory capacity between our RNAs, the steady state binding to RIG-I was not significantly different, indicating that binding of RIG-I to an RNA ligand alone is not sufficient to initiate the antiviral response.

Results

The WNV 5'UTR is highly structured

Our previous studies demonstrated that the WNV 5'UTR was capable of stimulating a RIG-I-mediated immune response. To understand the molecular determinants of the RIG-I response, we further analyzed the WNV 5'UTR through structural probing and binding assays with RIG-I. Several studies have provided predicted secondary structure models and mutational analysis has confirmed some of the predicted structures. However, structural probing of this RNA has yet to be performed. We analyzed the structures of different forms of the WNV 5'UTR, including the 5'UTR of the pathogenic WNV-NY, the nonpathogenic WNV-MAD78, and a mutated WNV-NY predicted to form a single SL structure (Figure 16).

We began by analyzing the full length (1-97nt) WNV 5'UTR (Figure 16 A). Resolution of our SHAPE reaction by PAGE revealed several de-protected bases at the 3' end of the fragment, primarily between bases 50 and 80. This region contained bases both strongly and weakly de-protected. There were additional de-protected bases clustered around base position 90, however, these bases were only weakly de-protected.

The 5'UTRs of different WNV strains are nearly identical and have been reported to contain the same secondary structures. However, there is a single base deletion at position 51 in the non-pathogenic WNV-MAD78 5'UTR as compared to a pathogenic WNV-NY strain. This small sequence difference may

contribute to a difference in the structures formed by the 5'UTR and result in differences in RIG-I binding. Therefore we probed the secondary structure of the WNV-MAD78 5'UTR using SHAPE (Figure 16B). The pattern of de-protected bases was similar to that seen with the WNV-NY, with several bases between positions 50 and 70 being de-protected, although only weakly.

In addition to examining the pathogenic and non-pathogenic strains of WNV, we also probed the structure of a WNV-NY 5'UTR mutated to form a single predicted SL structure (WNV-NY-SL). The SHAPE of WNV-NY-SL revealed several de-protected bases that suggest a stem loop (Figure 16C).

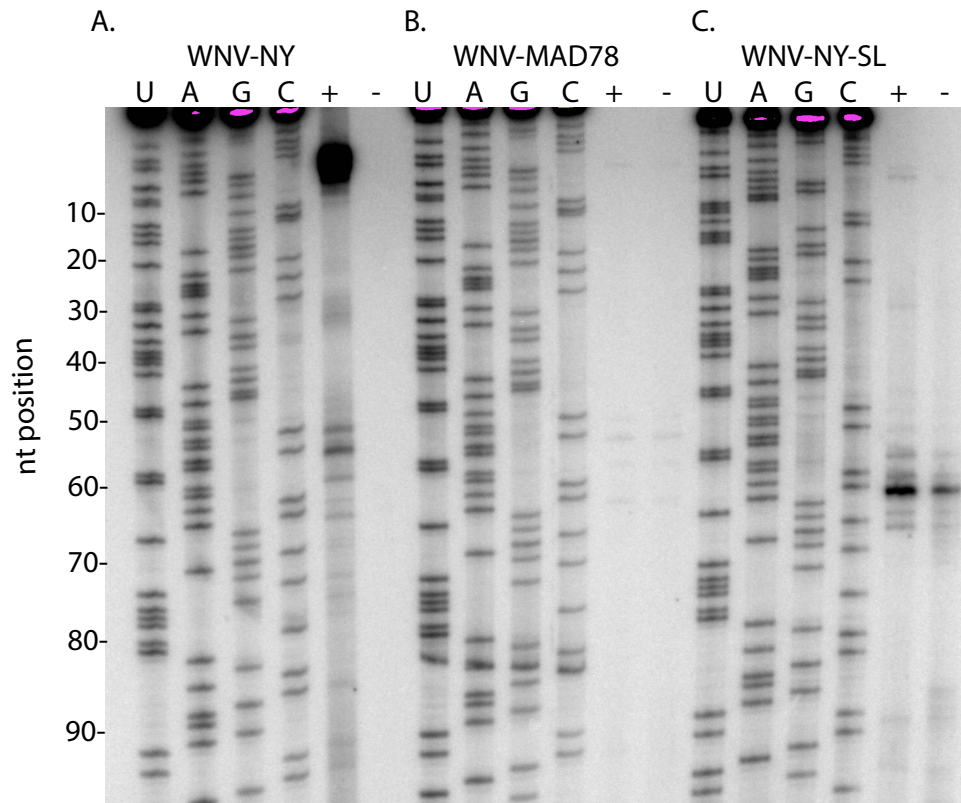


Figure 16: SHAPE analysis of the WNV 5'UTR. 2pmol of RNA was incubated with 1M7 (+) or DMSO (-) and then subjected to primer extension by reverse transcription. Products were analyzed by PAGE on a denaturing 8% polyacrylamide gel. A) WNV-NY 5'UTR. B) WNV-MAD78 5'UTR. C) WNV-NY 5'UTR predicted to form a single stem loop (SL).

In order to fully understand the implications of our SHAPE data, we next examined the data when mapped to the predicted secondary structures of our various RNAs. SHAPE of the WNV-NY 5'UTR results were mapped to secondary structure predictions generated using both the Nupack and mFold structure prediction program (Figure 17A & B). Structures that have been previously reported were generated using the MFold program. Nupack takes tertiary interactions into account when predicting folding, while MFold does not. When aligned to the predicted structures, the data suggests that there are regions that are de-protected, but these bases do not align to the previously proposed structures (25, 95, 171). This may indicate that there are tertiary interactions protecting bases, or that a stem loop structure is present but not in the location that was previously predicted. Regardless, several de-protected bases clustered near each other may result in an area of ssRNA, such as the top of a stem loop or a bulge within the hairpin structure. A majority of the de-protected bases are only weakly de-protected, as indicated by the grey circles, suggesting that interactions with these bases may be fluid and not produce a strong structure. The presence of only a limited number of de-protected bases suggests that the structure forms complex interactions, preventing adduct formation during chemical treatment.

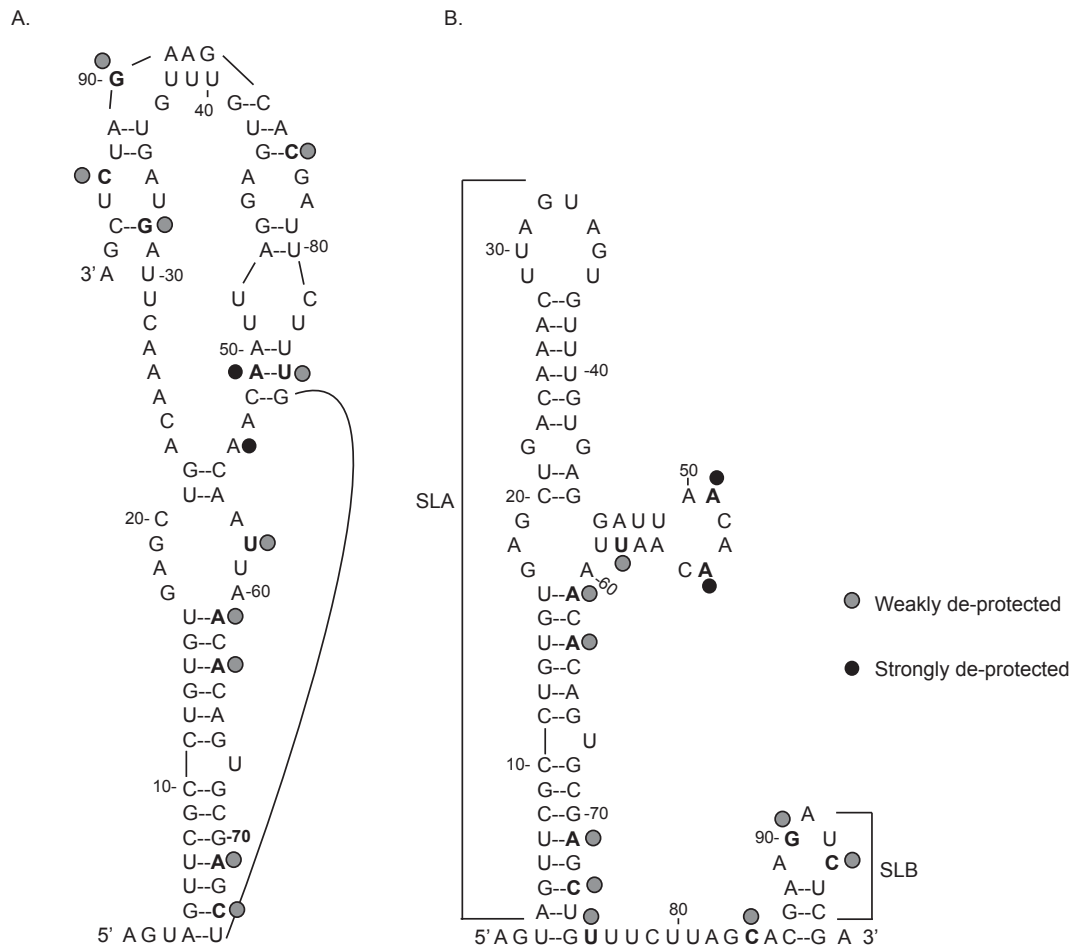


Figure 17: The WNV-NY 5'UTR forms tertiary interaction and contains ssRNA regions. Structural predictions were produced using the Nupack (211) (A) and Mfold (216) (B) prediction softwares. Black circles indicated strongly deprotected bases, gray circles indicate weakly deprotected bases. Predictions are given for structures with the lowest minimum free energy.

SHAPE analysis of the WNV-MAD78 5'UTR revealed a structure that was similar to the structure of the WNV-NY 5'UTR. When the SHAPE data was mapped to the predicted structures generated by Nupack and Mfold, the data indicated that, as with the WNV-NY 5'UTR, several bases are de-protected between positions 50-80nt (Figure 18A & B). The absence of any other de-protected bases suggests that there may also be tertiary interactions within the WNV-MAD78 5'UTR. One difference between the structures is the absence of de-protected bases clustered around base position 90, within the region predicted to form SLB, suggesting this SL is absent or buried in a tertiary interaction in the WNV-MAD78 5'UTR.

The WNV-MAD78 5'UTR is capable of stimulating an antiviral response.

The structures appear to be similar between the WNV-NY and -MAD78 strains but RIG-I stimulation has not been tested for the WNV-MAD78 5'UTR. In order to determine whether there is a difference in the RIG-I response between the two 5'UTRs, we compared RIG-I stimulation using a luciferase reporter assay (Fig 19). Huh7 cells were transfected with a RIG-I dependent luciferase reporter, ISG56-luc. Cells were subsequently infected with a potent inducer of the RIG-I specific antiviral response, SenV, or transfected with RNA corresponding to either the WNV-NY or -MAD78 5'UTR. The WNV-MAD78 5'UTR stimulated a RIG-I-mediated antiviral response that was similar to the response observed with the WNV-NY 5'UTR. Thus the structural differences seen between the two RNAs

do not significantly influence the ability of this RNA to induce an antiviral response.

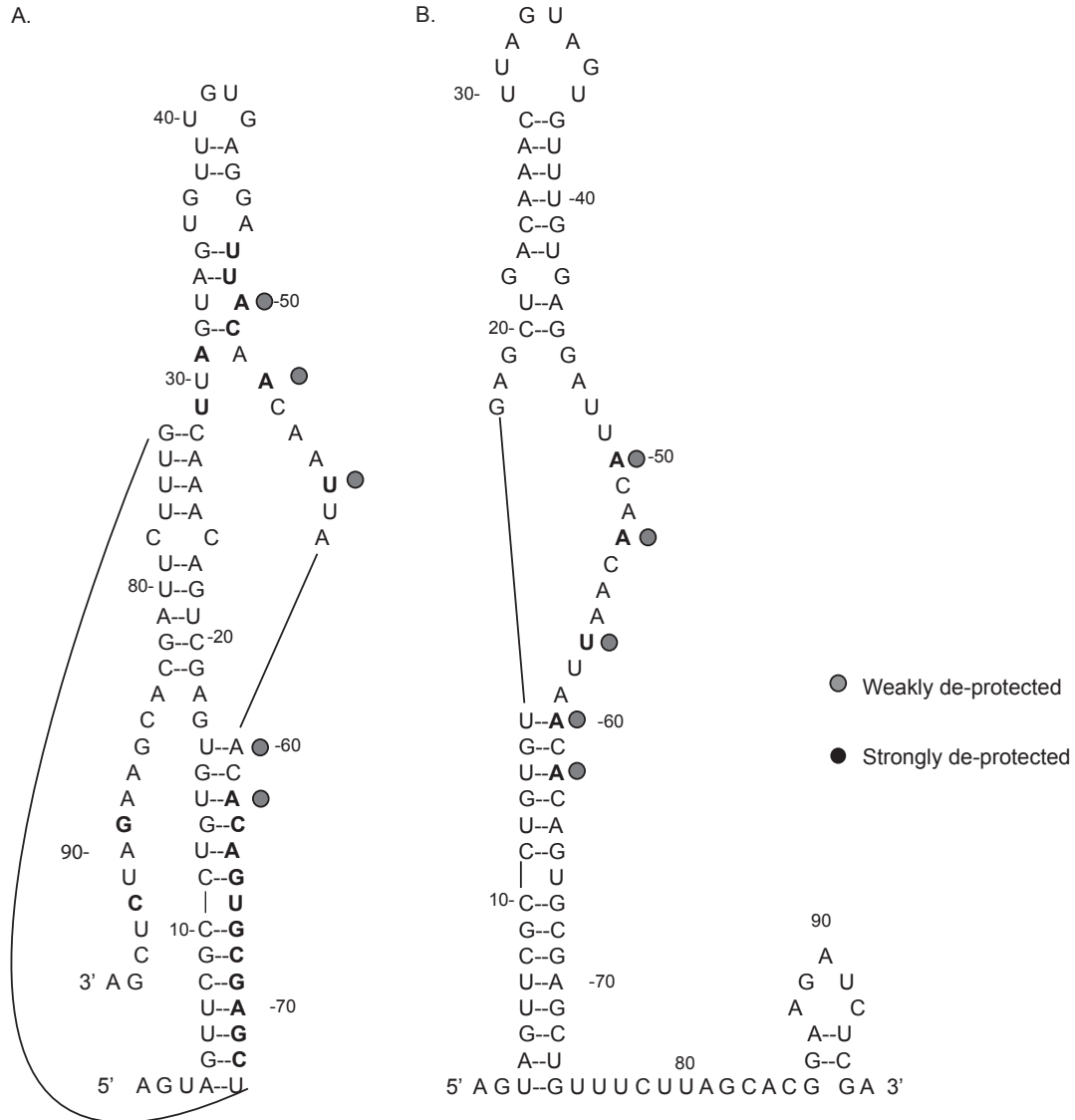


Figure 18: The WNV-MAD78 5'UTR forms tertiary interaction and contains ssRNA regions. Structural predictions were produced using the Nupack (A) and Mfold (B) prediction softwares. Black circles indicated strongly deprotected bases, gray circles indicate weakly deprotected bases. Predictions are given for structures with the lowest minimum free energy.

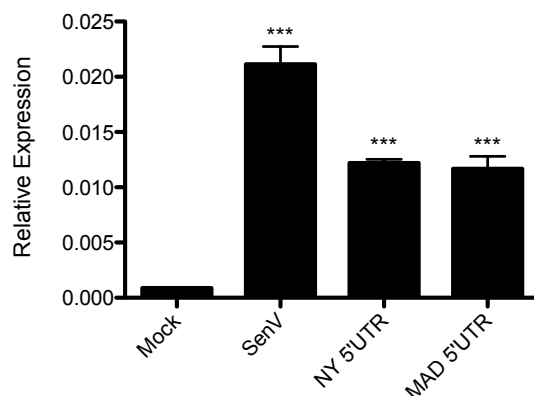


Figure 19: RIG-I stimulation is similar between the WNV-NY and WNV-MAD78 5'UTRs. Huh7 monolayers were transfected with pISG56-luc and pCMV-*Renilla* 16 hr prior to infection with SenV or transfection with 500 ng of the indicated RNAs in triplicate. Cell lysates were prepared 8 hr post transfection and assayed for luciferase activity. Values represent the average luciferase expression compared to mock (\pm standard error) from a minimum of two independent experiments. Statistical analysis was performed using Dunnett's multiple comparison analysis, * $p < 0.05$, ** $p < 0.01$ *** $p < 0.001$.

Mutation of the NY 5'UTR to form a single stem loop reduces its RIG-I stimulatory capacity

Our analyses of the WNV-NY and WNV-MAD78 5'UTRs suggested that these regions contain both a stem loop secondary structure and tertiary interactions. Additionally, these structures may result in regions of ssRNA. Our finding that RNAs containing these structures stimulates RIG-I expands on work from previous groups, who have demonstrated that RNA with a blunt-ended stem loop structure stimulates a robust RIG-I response (12, 146, 157). SHAPE analysis of the mutated 5'UTR SL suggested that the RNA formed a stem loop structure. However, when the SHAPE data was mapped to the Nupack or Mfold

predicted stem loop structure, which were virtually identical, the SHAPE data suggested that while the structure may form a stem loop, some bases may be involved in tertiary interactions, as suggested by the limited number of de-protected bases present (Figure 20). Also, The suggested structure appears to lack any significant regions of ssRNA, however.

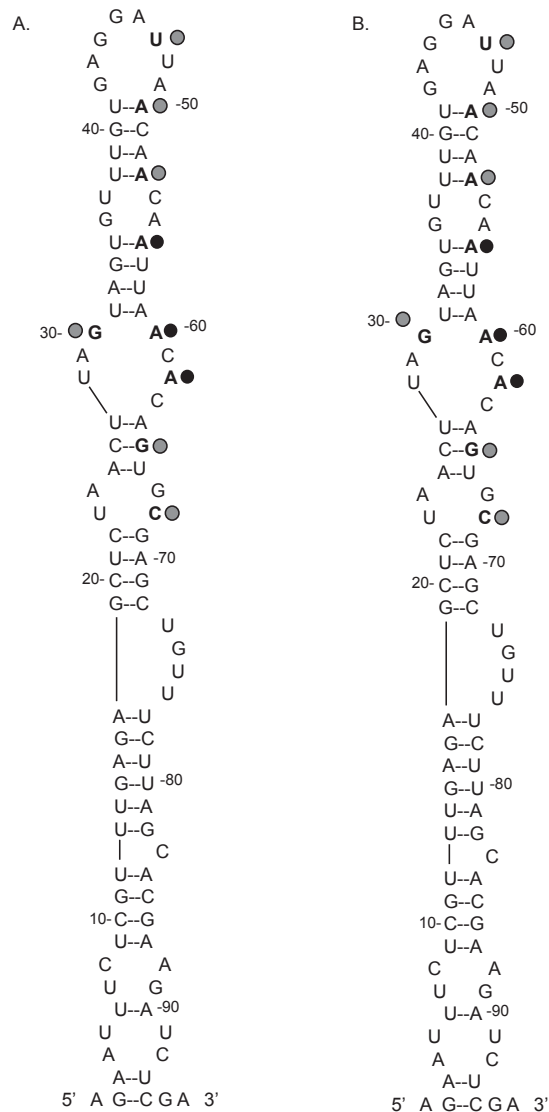


Figure 20: The WNV-NY-SL forms a complex structure. A structural prediction was produced using the Nupack A) and mFold B) structural prediction software. Black circles indicated strongly deprotected bases, gray circles indicate weakly deprotected bases. The prediction is given for structures with the lowest minimum free energy.

In order to examine the influence of the structures identified in WNV-NY and WNV-MAD78 on the ability of RIG-I to respond to the 5'UTR, we examined the ability of the mutated WNV-NY-SL 5'UTR to stimulate RIG-I using a luciferase reporter assay (Figure 21). The WNV-NY-SL 5'UTR was able to induce stimulation of the RIG-I response, but the response was reduced compared to that observed by wild type WNV-NY 5'UTR RNA.

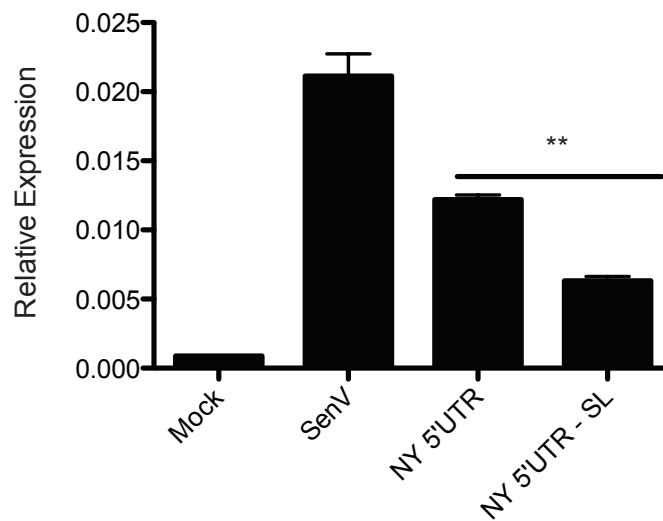


Figure 21: Stimulation by the WNV-NY-SL is reduced as compared to WNV-NY. Huh7 monolayers were transfected with pISG56-luc and pCMV-*Renilla* 16 hr prior to infection with SenV or transfection with 500 ng of the indicated RNAs in triplicate. Cell lysates were prepared 8 hr post transfection and assayed for luciferase activity. Values represent the average luciferase expression compared to mock (\pm standard error) from a minimum of two independent experiments. Statistical analysis was performed using Dunnett's multiple comparison analysis, * $p < 0.05$, ** $p < 0.01$ *** $p < 0.001$.

Truncation of the NY 5'UTR to fewer than 80 nucleotides abolishes RIG-I signaling capacity

To define the minimal stimulatory element in the 5'UTR, we generated 3' deletion mutants of WNV-NY 5'UTR in order to determine the minimum number of bases required for induction of the RIG-I response (Figure 22A) and analyzed their stimulatory capacity using a luciferase reporter assay (Figure 22B). While the 90 nucleotide 5'UTR construct retained its stimulatory capacity, the 80 nucleotide construct did not. Structural predictions were generated of the truncation mutants in order to determine if there are any readily identifiable structural variances between the 1-80nt fragment and the 1-90nt fragment to account for the differences in stimulatory capacity. The 1-90nt fragment is predicted to form a tertiary interaction, but is not predicted to contain a region of ssRNA (Figure 23A). The 1-80nt fragment is also predicted to contain some tertiary interaction, which occurs in the middle of a ssRNA bulge. However, the interaction at this position is only mediated by 3 bases and is therefore considered to be very weak. Given the weakness of this interaction, the tertiary interaction predicted to occur within the 1-80nt fragment is very unlikely to occur (Figure 23B).

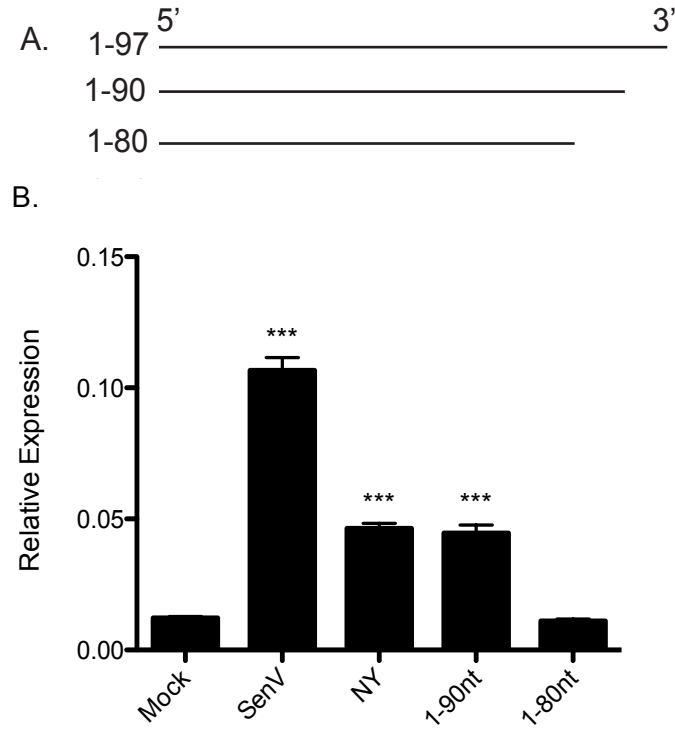


Figure 22: Truncation of the WNV-NY 5'UTR affects stimulation of RIG-I. A) Diagram illustrating the truncations produced of the WNV-NY 5'UTR. B) Huh7 monolayers were transfected with pISG56-luc and pCMV-*Renilla* 16 hr prior to infection with SenV or transfection with 500 ng of the indicated RNAs in triplicate. Cell lysates were prepared 8 hr post transfection and assayed for luciferase activity. Values represent the average luciferase expression compared to mock (\pm standard error) from a minimum of two independent experiments. Statistical analysis was performed using Dunnett's multiple comparison analysis, * $p < 0.05$, ** $p < 0.01$ *** $p < 0.001$.

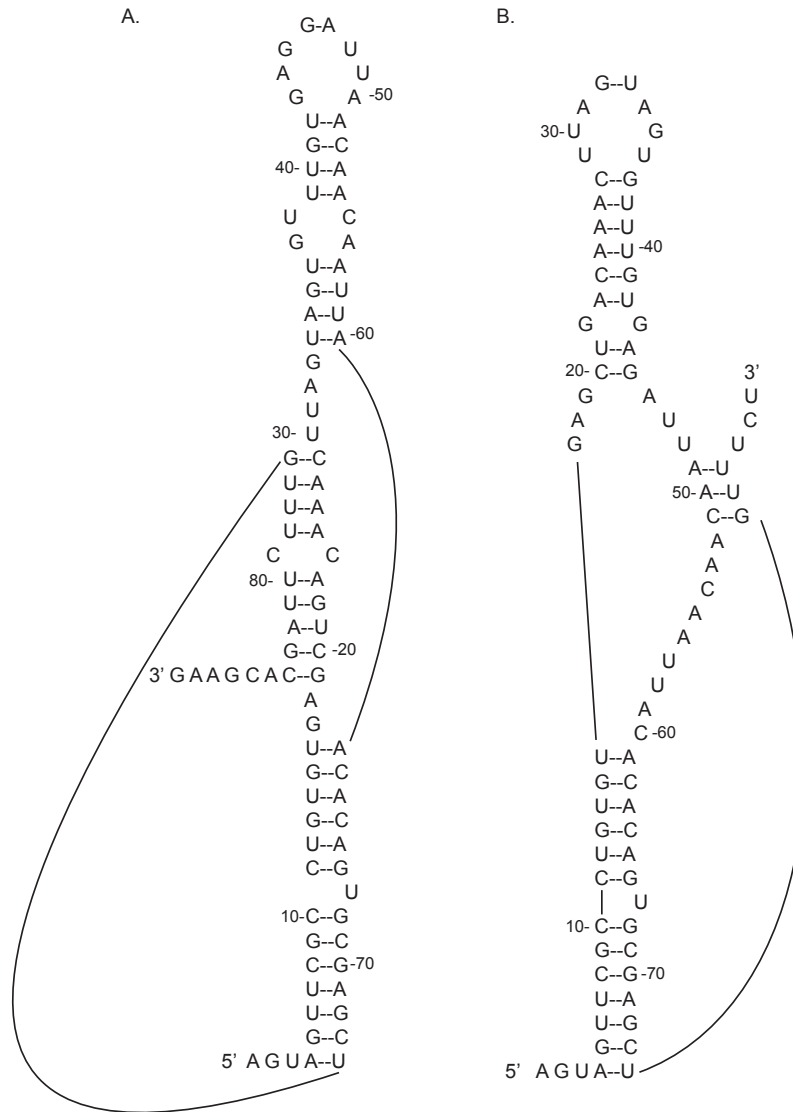


Figure 23: Truncation of the WNV-NY 5'UTR is predicted to alter the secondary structures. Structural predictions were made of the WNV-NY 1-90nt (A) and WNV-NY 1-80nt (B) fragments using the Nupack structure prediction software. Predictions are given for structures with the lowest minimum free energy.

Binding affinity of the WNV 5'UTR for RIG-I does not correlate with stimulatory capacity

In order to determine whether RIG-I activation correlated to binding of RIG-I to RNA, we examined the steady state binding of RIG-I to the various RNA species using the newly described Differential Radial Capillary Action of Ligand Assay (DRaCALA) (Figure 24) (46, 144, 147). DRaCALA is based on the principle that proteins are immobilized in a nitrocellulose matrix, while RNA will diffuse. Radiolabeled RNA bound to a protein will be localized in the center of the diffusion circle, creating a dark spot within the center of the total circle. The fraction bound can be calculated by determining the fraction of signal retained in the central circle as compared to the total signal and the dissociation constant (K_d) of the reaction determined by plotting fraction bound versus protein concentration. The K_d for the full length WNV-NY, WNV-MAD78 5'UTR and the mutated WNV-NY-SL were determined to be $270 \text{ nM} \pm 50 \text{ nM}$, $\sim 800 \text{ nM} \pm 130 \text{ nM}$ and $\sim 500 \text{ nM} \pm 100 \text{ nM}$, respectively. When the binding curves of WNV-NY and WNV-MAD78 were compared, the total fraction of RNA bound was higher in WNV-MAD78, at $\sim 30\%$, than the WNV-NY, which was only at 20% , despite the fact that the WNV-NY had a lower K_d (Figure 25A). In contrast, comparison of the WNV-NY and the WNV-NY-SL indicated that the total fraction bound in both samples was similar, at $\sim 20\%$, despite WNV-NY having a lower K_d . This suggests that while affinity for the WNV-MAD78 is lower, the total amount of RNA bound is greater than for WNV-NY or WNV-NY-SL. The differences seen in stimulation as related to binding affinity may indicate that stimulation of RIG-I,

which was similar between the WNV-MAD78 and WNV-NY, is not solely determined by binding affinity but can also be influenced by the percent of RNA that is bound.

We next examined the steady state binding of the WNV-NY 5'UTR truncations using DRaCALA (Figure 26). The K_d of 1-80nt fragment was $\sim 200 \text{ nM} \pm 50 \text{ nM}$, while the K_d of the 1-90nt fragment was much higher, at $\sim 420 \text{ nM} \pm 50 \text{ nM}$ (Figure 26). Comparison of the binding curves between full length WNV-NY (1-97nt), the 1-90nt fragment and the 1-80nt fragment revealed that while the K_d s of the WNV-NY and the 1-90nt fragments were higher than the 1-80nt fragment, the total fraction bound for the 1-80nt fragment was less.

Overall, the differences in K_d observed between the RNA species examined do not correlate with stimulation. This suggests that while slight structural differences may exist between the analyzed 5'UTR fragments, and these fragments have differential stimulatory capacity, the differences are not purely at the level of binding of the RNA to RIG-I.

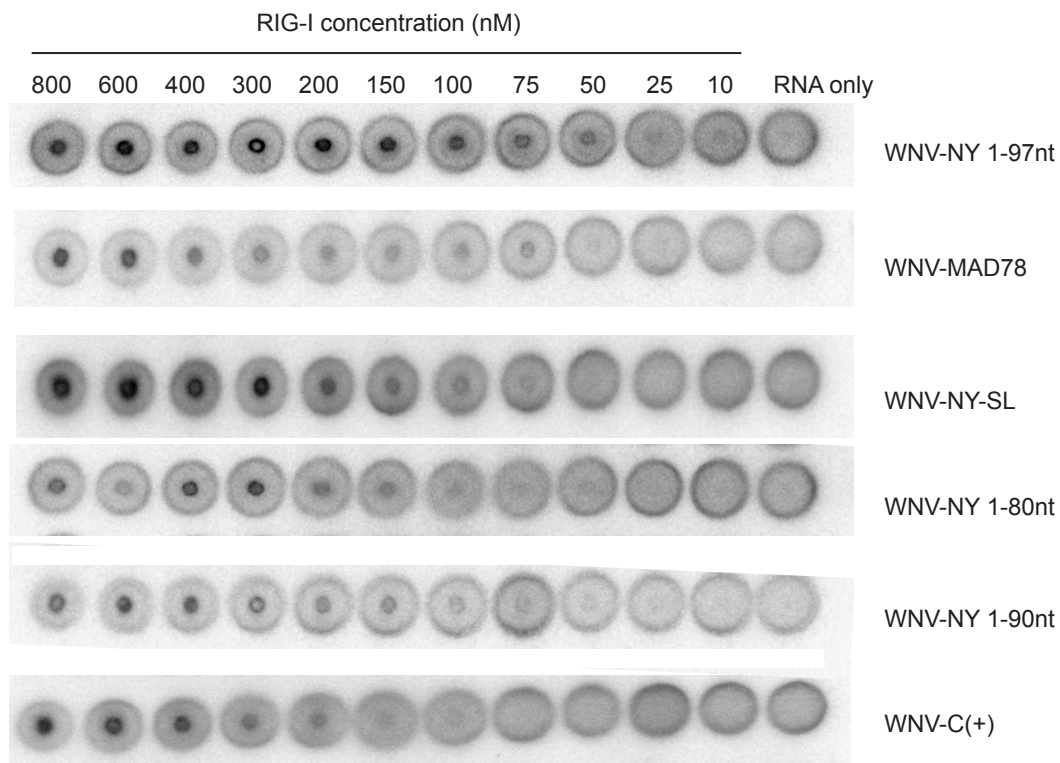


Figure 24: Representative DRaCALA images used for K_d determination. Purified RIG-I was incubated with the indicated radiolabeled RNAs and Differential Radial Capillary Action of Ligand Assays were performed. Protein-RNA complexes were spotted onto nitrocellulose and examined using a FLA-5000 phosphorimager. Protein concentrations were consistent between the RNAs tested, as indicated.

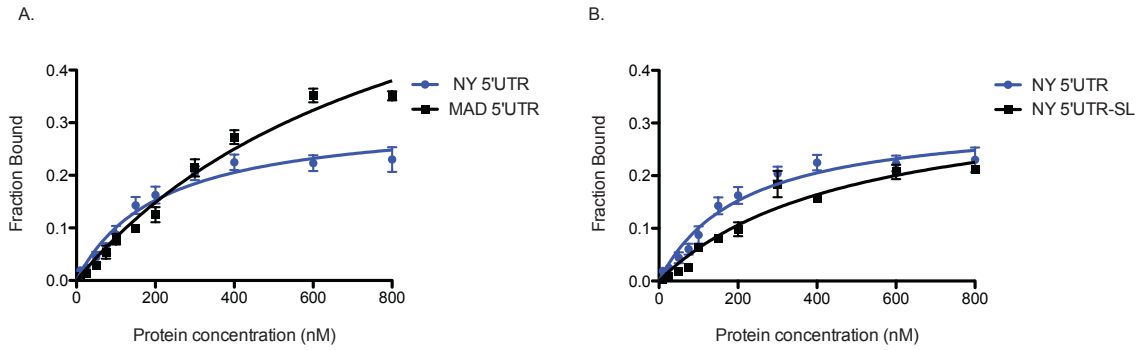


Figure 25: Steady state binding of RIG-I to the WNV-NY 5'UTR is similar to WNV-MAD78 and WNV-NY-SL. Purified RIG-I was incubated with the indicated radiolabeled RNAs and Differential Radial Capillary Action of Ligand Assays were performed. Protein-RNA complexes were spotted onto nitrocellulose and examined as compared to WNV-MAD78 (A) and WNV-NY-SL (B). Values are representative of duplicate biological replicates performed at least in triplicate.

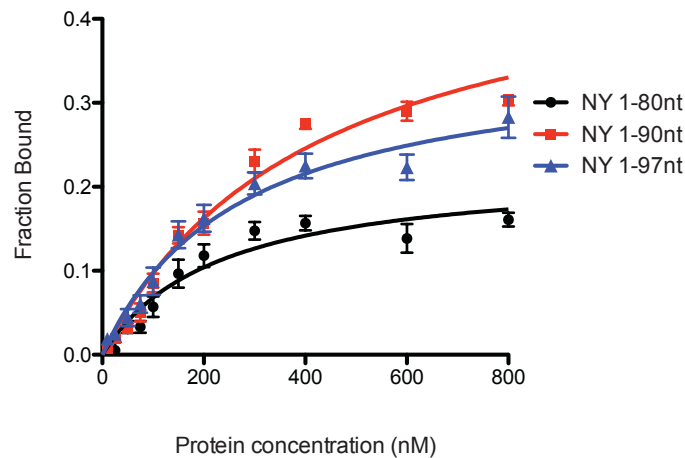


Figure 26: Steady state binding of RIG-I to the full length WNV-NY 5'UTR RNA is similar to the 1-90nt fragment but not the 1-80nt fragment. Purified RIG-I was incubated with the indicated radiolabeled RNAs and Differential Radial Capillary Action of Ligand Assays were performed. Protein-RNA complexes were spotted onto nitrocellulose and examined. Values are representative of duplicate biological replicates performed at least in triplicate.

The WNV C(+) RNA does not bind to RIG-I

In order to confirm RIG-I/RNA binding was specific in our DRaCALA experiments, we examined the steady state binding of a non-stimulatory WNV-NY RNA, C(+) (Chapter 2). The WNV-NY C(+) RNA did not induce RIG-I stimulation in our previous assays. If stimulation is dependent on specific binding by RIG-I, the C(+) should not bind, and indeed our data indicates that the binding is non-specific (Figure 27). The non-specific binding of C(+) to RIG-I, which was unable to stimulate the RIG-I response, confirms that the binding observed with our 5'UTR species is specific.

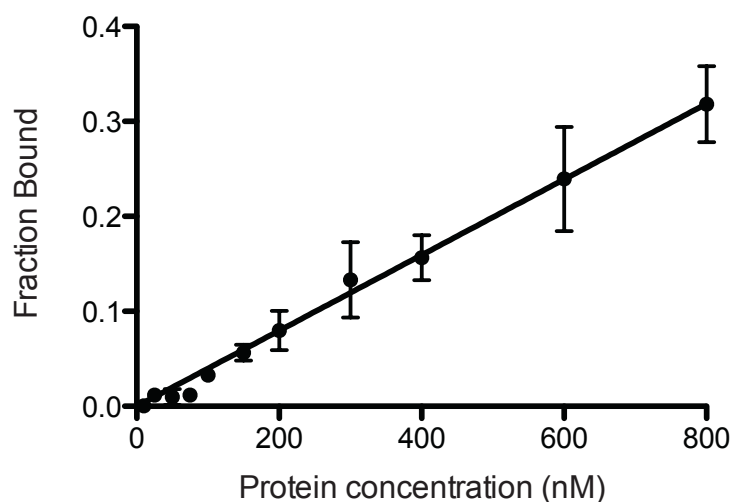


Figure 27: RIG-I binding of WNV C(+) is non-specific. Purified RIG-I was incubated with the indicated radiolabeled RNAs and Differential Radial Capillary Action of Ligand Assays were performed. Protein-RNA complexes were spotted onto nitrocellulose and examined. Values are representative of duplicate biological replicates performed at least in triplicate.

Discussion

Stimulation of the RIG-I mediated antiviral response is an important step in controlling viral infection. The ability of the host to respond rapidly to infection can influence disease outcome. In the case of WNV, different strains of the virus demonstrate variable levels of pathogenicity. The factors that influence this difference are poorly understood, but may include differences in innate immune response to the virus, as previous work has demonstrated different disease outcomes can be dependent on the immune response to WNV (40, 85, 185, 195). In order to define the structures that are important for RIG-I recognition of WNV PAMPs, we performed structure probing and binding studies of the WNV 5'UTR, a previously determined viral PAMP.

SHAPE analysis provided insight into the structure formed by an established RIG-I PAMP, the WNV 5'UTR. Structure probing suggested that both the WNV-NY and WNV-MAD78 5'UTRs formed structures in which few bases were de-protected, suggesting complex tertiary interactions occur within these RNAs, and that only small regions of ssRNA were present. Furthermore, only minor differences in structure were suggested between the WNV-MAD78 and WNV-NY 5'UTRs as a result of a single nucleotide deletion from WNV-MAD78, and there was no difference in the ability of WNV-MAD78 5'UTR to stimulate RIG-I. Thus RIG-I is likely interacting with conserved structural elements between the NY and MAD78 5'UTRs. Additionally, ssRNA regions may be an important factor in RIG-I interaction, as regions of ssRNA were suggested in both the WNV-NY and WNV-MAD78 5'UTR, but not in the WNV-NY-SL. Structural probing suggested that the WNV-NY-SL RNA may also contain tertiary

interactions similar to the WNV-NY and –MAD78 RNA, which may account for the ability of this RNA to stimulate RIG-I, albeit less robustly. WNV-NY 5'UTR truncation mutants were predicted to contain tertiary interactions. However, the predicted interaction in the 1-80nt fragment was very weak, with only 3 bases interacting, thus tertiary interactions may be lost during normal RNA breathing. If the tertiary interactions within this RNA are lost, this also creates a significant ssRNA bulge, which was predicted to be absent in the 1-90nt fragment. The inability of the 1-80nt fragment to stimulate suggests that even if this ssRNA bulge is sufficient for binding, tertiary interactions are required to induce signaling, as the 1-80nt fragment did not stimulate RIG-I. Structure probing of the 1-80nt and 1-90nt fragments will help to clarify the structural requirements necessary to stimulate RIG-I.

When the binding of the RNA species to RIG-I was analyzed, the Kds were higher than previously reported Kd values for RIG-I ligands. A blunt-ended 14 bases dsRNA was shown to have a Kd of 5 nM (84), as compared to the WNV-NY 5'UTR, at ~270nM. This increase in the Kd value may be a reflection of the increased length of the RNA, as the NY 5'UTR is 97 bases in length. Size alone does not account for the ability of RIG-I to bind or be stimulated by an RNA, however, as truncation of the NY 5'UTR to 80 nucleotides in length abolished signaling, while decreasing the Kd. Crystal structures of RIG-I bound to RNA have revealed that only 9 base pairs of the dsRNA bound can fit in the RIG-I binding pocket, with the remaining sequence extended out beyond (76, 84, 94, 106). This suggests that the structures adopted by the various 5'UTR species

are influencing how the region of RNA that is bound within this binding pocket are able to interact.

Another possible explanation of the differential binding and stimulation seen amongst the RNA species examined is due to the limited number of bases required in order to facilitate binding. Multiple copies of RIG-I have been shown to bind to a single RNA molecule, especially those of longer length (<200nt) (18, 136). It is possible that the structural confirmation adopted by those RNAs that show more stimulation of the RIG-I response allow for a greater number of RIG-I proteins to bind, thus increasing the signaling strength to the downstream target IPS-1. Binding to internal regions of the dsRNA molecule have been shown to have a much lower affinity than binding interactions which occur at the 5' end of the molecule (76). This weak binding affinity is proposed to facilitate RIG-I binding to RNA in order to “scan” for PAMP characteristics, thereby enabling RIG-I to survey the cell without being in a signaling-active state. The weak affinity for RIG-I associated with the examined RNAs may indicate one or both of these mechanisms of RIG-I binding and stimulation may be contributing to the induction of the antiviral response.

This study examined the structure of RIG-I specific WNV PAMPs and assed the steady state binding of these WNV PAMPs to RIG-I. Our data suggests that affinity is not necessarily a reflection of stimulatory capacity and that structures present or absent within the PAMP RNA can greatly alter the ability of RIG-I to induce a response.

Chapter 4 – DDX3 as a potential antiviral protein during WNV infection

Introduction

The DExD/H-box helicases belong to a large group of proteins within the superfamily 2. The members of this family are generally involved in a variety of roles related to RNA metabolism. One DExD/H-box helicase that has been recently defined is DDX3. DDX3 has been shown to be involved in a variety of normal cellular processes involving RNA, including mRNA splicing and export from the nucleus, regulation of both transcription and translation, and RNA decay (28, 57, 68, 90, 91, 161). Due to its involvement in a wide variety of cellular processes, especially RNA processing, DDX3 can be localized to both the nucleus and cytoplasm and is constitutively expressed. DDX3 contains both a helicase domain and an ATPase domain (82), similar to other DExD/H-box helicases, such as the pattern recognition receptors (PRRs) RIG-I and MDA5. However, RIG-I and MDA5 also contain a CARD-signaling domain, which is necessary to initiate the antiviral response to viral RNA

Due to the variety of cellular functions performed by DDX3, it makes an attractive target for viruses, and has been shown to be co-opted to serve as a pro-viral protein, as well as as regulated to limit anti-viral activities. For example, HIV and HCV have both been shown to utilize DDX3 for replication. HIV takes

advantage of DDX3's role in mRNA export from the nucleus. The viral Rev protein acts in concert with DDX3 to export the HIV mRNA into the cytoplasm (100, 123). Although the specific role that DDX3 plays in this export is not fully understood, the helicase domain of DDX3 is required in order to achieve proper export. The requirement of a functional helicase suggests that DDX3 may have a role in disrupting secondary structures within the viral RNA prior to export (207). The HCV core protein has been shown by several groups to interact with the C-terminal domain of the DDX3 protein (5, 131, 133). Further studies have suggested that the interaction between the core and DDX3 is critical for the virus, and it has been suggested that helicase function of DDX3 may be important in unwinding the viral RNA to facilitate replication. There is also work to suggest that direct interaction of the core with DDX3 is not required for replication, as mutation in core that disrupt its interaction with DDX3 did not affect the production of viral RNA or infectious particles (4). However, further data from this study indicated that knock down of DDX3 in cells infected with a virus unable to bind to DDX3 resulted in a reduction in viral particles and RNA replication, indicating that DDX3 is necessary for HCV replication. Thus, the requirement for interaction between the HCV core and DDX3 is still unclear, although the predominance of evidence suggests that DDX3 is necessary for HCV replication.

DDX3 has also recently been implicated in serving in an antiviral capacity through the innate, intracellular antiviral response. Recent studies have begun to define an antiviral role of DDX3 as both a sensor of viral RNA and as an interacting partner of several proteins involved in the downstream RIG-I/MDA5

and TLR3 signaling cascades. It was first noted that vaccinia virus encodes a protein, K7, which serves to inhibit several of the PRR proteins, also targets DDX3 (78). Additionally, it was demonstrated that knock down of DDX3 during vaccinia virus infection led to a decrease in IFN- β expression. This suggested that in addition to a role in RNA processing and production, DDX3 may also have antiviral activity. Later studies found DDX3 co-immunoprecipitates with the TBK1/Ik ϵ protein complex, which is activated by both RIG-I and TLR3 signaling (163). Further studies have demonstrated that DDX3 can bind synthetic RNA (polyI:C) as well as short double stranded RNA segments, giving it a potential role as an RNA sensor (132). A role in antiviral activity is further supported by the observation that, in contrast to RIG-I and MDA5, which are expressed at low levels in the cell, DDX3 is constitutively expressed. Therefore, DDX3 is present at high enough levels to serve as an initial RNA sensor or interacting partner to other cellular PRRs. Indeed, DDX3 has been shown to interact with both RIG-I/MDA5 and IPS-1 to enhance the RIG-I mediated response. Finally, there is also some evidence implicating DDX3 as a transcription factor, as DDX3 was shown to associate with the IFN- β promoter.

This mounting evidence supports the role of DDX3 as either an initial sensor of RNA or an enhancer of the antiviral response during viral infection. Although DDX3 may be an important component of the innate intracellular immune response, its role as an RNA sensor and mediator of the antiviral response has not been clearly defined for a number of viruses. We therefore examined the role that DDX3 plays during WNV infection.

Results

DDX3 co-localizes with WNV proteins during infection

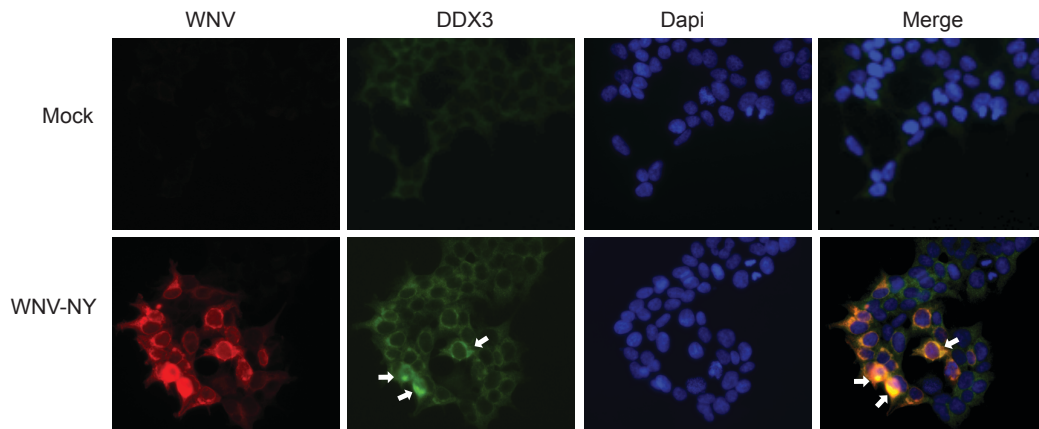
DDX3 has been shown to interact with HCV core protein in order to promote viral replication. Therefore, we assessed whether DDX3 co-localized with WNV proteins. Mock- or WNV-infected cells were examined for protein localization by immunofluorescence assay (IFA) at 24 hours post infection (Figure 30). In two different cell types, 293T (Figure 28A) and Huh7 (Figure 28B) cells, DDX3 was observed in the cytoplasm in mock infected cells. In both cell types, at 24 hours post WNV infection, DDX3 could be detected in both the cytoplasm and the nucleus. Additionally, DDX3 proteins appear to be co-localized with WNV proteins, and the relative intensity of the DDX3 staining was enhanced when it colocalized with WNV protein (white arrows) as compared to the DDX3 intensity in un-infected cells. This suggest that WNV proteins may interact with DDX3 at 24 hpi.

DDX3 does not a have pro-viral effect during WNV infection

Due to the apparent co-localizaiton of DDX3 with WNV proteins, we examined if DDX3 may have pro-viral effects during infection. Therefore, we analyzed the effect of DDX3 expression in a WNV replicon-bearing cell line (Figure 29). A BHK cell line harboring a subgenomic WNV replicon encoding a

renilla luciferase was transfected with DDX3. Although lacking the structural genes required to produce virions, the replicon contains the 5' UTR through to the CS sequence within C, and the 3'UTR, enabling viral replication and protein translation to take place. The effects on viral replication and protein expression were examined by monitoring the production of luciferase, which would be enhanced if DDX3 was playing a pro-viral role.

A.



B.

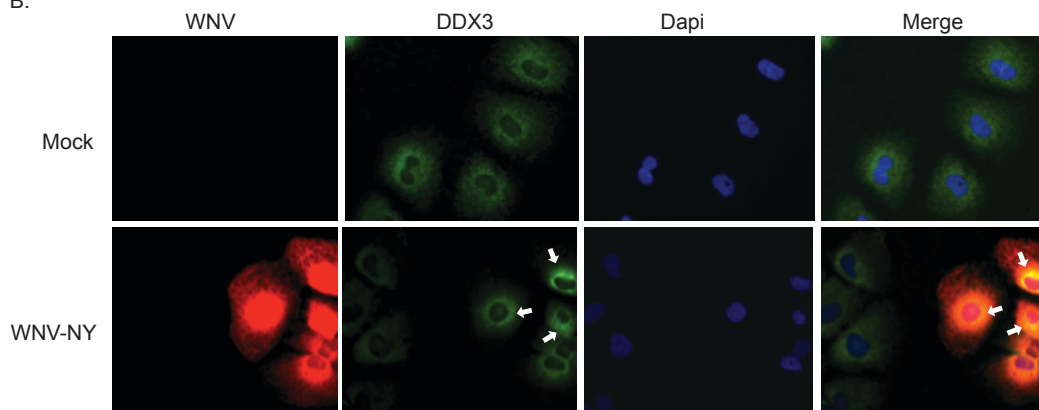


Figure 28: WNV protein colocalized with DDX3 during infection in multiple cell types. 293T cell (A) and Huh7 cell (B) monolayers were mock infected or infected with WNV-NY at an MOI of 1. At the indicated time points, cells were fixed and analyzed by IFA for WNV and DDX3 protein expression. Cells were visualized at 40x magnification.

The levels of renilla luciferase produced, however, were consistent between mock-transfected cells and cells transfected with either an empty control vector or the DDX3 containing plasmid. Therefore, additional DDX3 expression had no effect on replication of the viral genome or protein expression, suggesting DDX3 does not have a pro viral role during WNV infection.

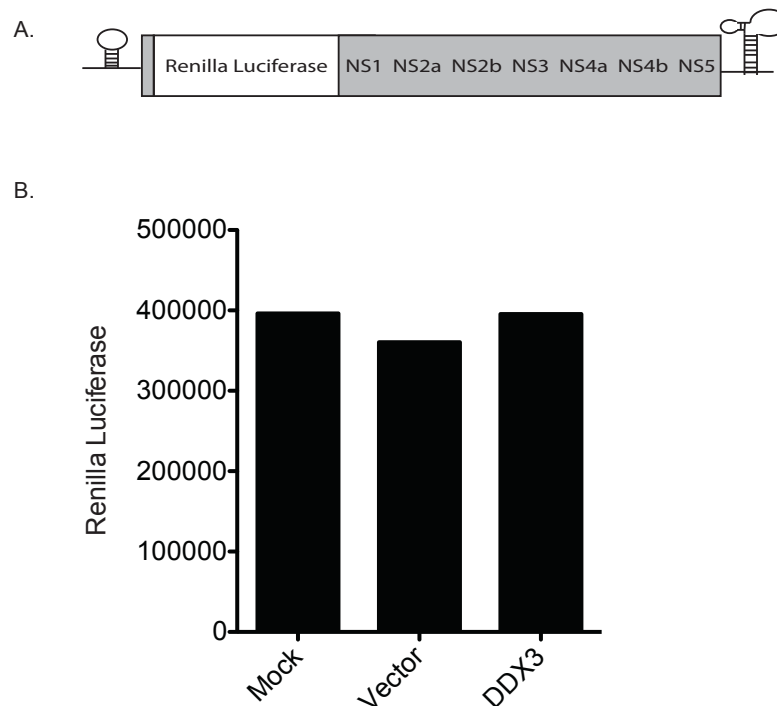


Figure 29: DDX3 overexpression does not affect replication or protein expression of a WNV replicon. A) Diagram illustrating the WNV replicon. Gray shading indicates WNV sequence. B) BHK cells bearing a WNV replicon were transfected with 500 ng DDX3. Cell lysates were prepared 24 hrs post transfection and assayed for luciferase activity. Values represent the average luciferase expression compared to mock (\pm standard error) from a representative experiment done in triplicate.

DDX3 expression is reduced at late points post WNV infection

To further characterize the potential interaction of DDX3 with WNV, we examined if DDX3 protein levels change over time during infection. Cell lysates from WNV-NY infected 293T cells were probed with DDX3 and WNV antibodies (Figure 30). DDX3 protein levels decreased between 48 and 72 hours post infection. Although this time point also corresponds with a high degree of cell death within this cell type, levels of the loading control, GAPDH, are still consistent at 72 hours. This data suggests that DDX3 expression may be modulated at very late points post WNV infection in this cell type.

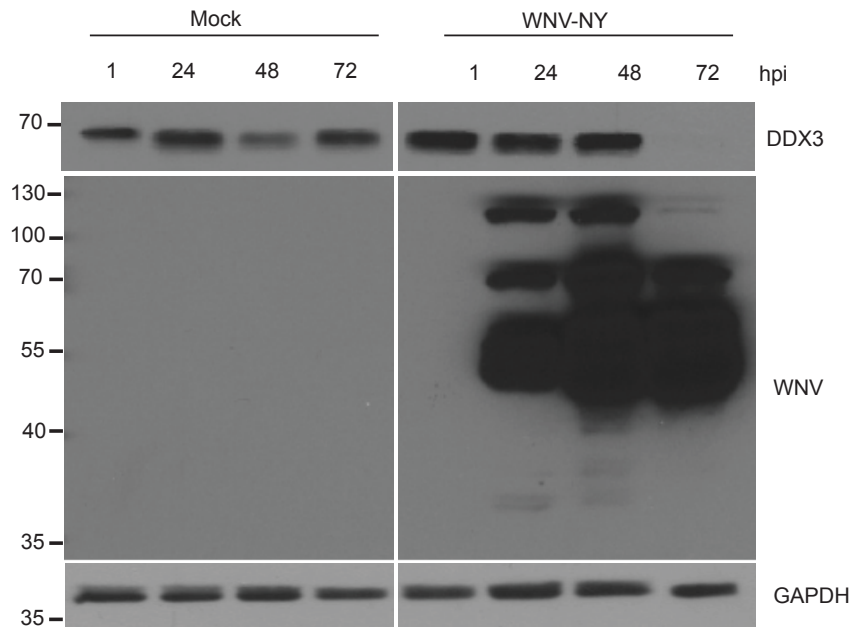


Figure 30 DDX3 expression is reduced by late points in WNV infection. 293T cells were mock infected or infected with WNV-NY at an MOI of 1. Lysates were collected at the indicated time points and subjected to immunoblot analysis. Blots were examined for DDX3, WNV and GAPDH protein expression. Data is representative of 2 experiments.

Overexpression of DDX3 does not alter viral replication or the antiviral response

DDX3 appears to localize with WNV proteins, and DDX3 protein levels appear to decrease over time in the cell, indicating that WNV may be negatively regulating DDX3 expression. As DDX3 is proposed to play a role in the antiviral response, we wanted to determine if DDX3 overexpression was capable of inducing an antiviral state through interaction with IPS-1. We examined the effect of overexpression of DDX3 and IPS-1 together in the presence of IRF3-inducible luciferase reporter construct (Figure 31A). In cells transfected with IPS-1 alone, the RIG-I response was stimulated, but DDX3 alone did not induce luciferase expression. However, in cells co-transfected with IPS-1 and DDX3, there is an increase in luciferase expression, indicating that DDX3 expression was capable of enhancing an IPS-1 stimulated antiviral response.

We next examined the affect of DDX3 overexpression in cells infected with WNV to determine whether increasing available DDX3 would enhance the antiviral response to WNV. We infected DDX3 overexpressing cells with WNV at an MOI of 1 (Figure 31B & C). DDX3 overexpression did not alter ISG56 protein levels, an antiviral protein directly induced as a result of IPS-1 activation. Additionally, there was no difference in the expression of WNV protein at either 24 or 48 hours post infection in either the vector expressing or DDX3 expressing cells (Figure 33 B). Overexpression of DDX3 also had no effect on WNV titers at 24 or 48 hours post infection (Figure 33C). Thus, overexpression of DDX3 did not

alter the antiviral response to WNV, nor did it enhance viral replication, further supporting the data that DDX3 is not pro viral.

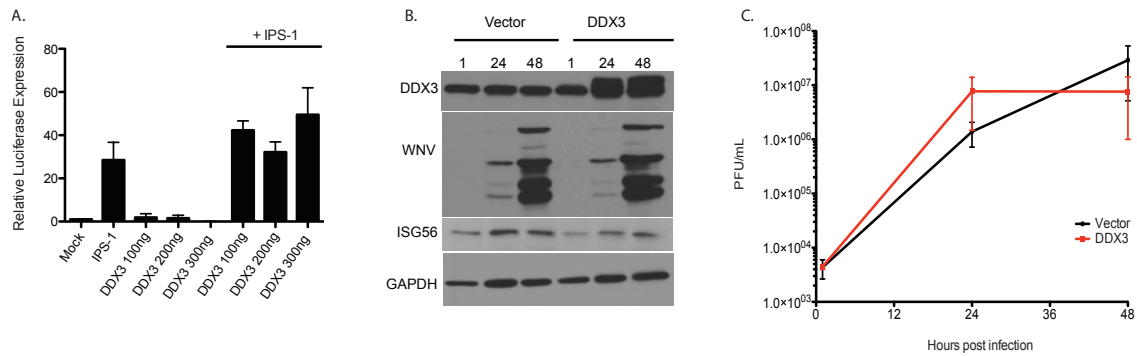


Figure 31: DDX3 overexpression does not affect the antiviral response to WNV infection or viral replication. A) Huh7 cells were transfected with IPS-1, DDX3 and pISG56-luc in triplicate. Cell lysates were prepared 24 hrs post transfection and assayed for luciferase activity as described in Figure 7. B, C) 293T cells were mock infected or infected with WNV-NY at an MOI of 1. Cell lysates were collected for immunoblot analysis (B) and supernatants were collected for viral plaque assay (C) at the indicated time points post infection. All values are representative of duplicate experiments.

Discussion

DDX3 carries out a number of functions related to RNA production, transport and degradation, and is therefore a potential target for exploitation by viruses. It has also been implicated as a component of the RIG-I mediated antiviral pathway, and even as a PRR itself. Several viruses have been shown to actively impede the antiviral activity of DDX3. The vaccinia virus K7 protein targets DDX3 by directly binding to it, preventing it from interacting with the Ikk ϵ /TBK1 complex and activating IRF3 and consequently inducing IFN- β expression (78, 128). Other viruses such as HIV and HCV utilize DDX3 in their

life cycle. HIV takes advantage of the function of DDX3 in export of RNA from the nucleus. The viral Rev protein acts in concert with DDX3 and the cellular CRM1 protein to export un-spliced and/or partially spliced viral RNAs from the nucleus, an essential part of the HIV replication scheme (100, 123, 207). HCV is suggested to require DDX3 for viral replication, although the specific mechanisms underlying this requirement are still unknown (5). DDX3 has also been shown to interact directly with the core protein, although it is unclear if this interaction is required for viral replication (4, 133). There is some data to indicate that binding of the HCV core protein prevents DDX3 from interacting with IPS-1 and thereby impedes the antiviral transduction pathway (131). Here we evaluated the role DDX3 may play during the course of WNV infection.

We first sought to characterize its localization and determine the affect of DDX3 on viral replication. DDX3 appeared co-localized with WNV protein by IFA, suggesting that WNV may be interacting with DDX3. One of the most recently defined roles of DDX3 is as a component of the translation pre-initiation complex. DDX3 binds to the translation complex component eIF4G within stress granules; therefore it is possible that co-localization of DDX3 with WNV proteins is simply due to the fact that as infection progresses, more DDX3 is recruited to and is found to interact with WNV proteins as a consequence of viral translation. When DDX3 was overexpressed in a cell line containing a WNV replicon encoding renilla luciferase, there was no increase in the production of renilla, suggesting that WNV does not utilize the increased available DDX3 to enhance replication or protein translation. However, the cells containing the replicon are

BHK cells, a hamster kidney line, and therefore it is possible that the human DDX3 used in the experiment does not properly interact with the hamster translation proteins. This seems unlikely, however, as the sequence conservation between the hamster and human DDX3 proteins is 100% on the amino acid level. Even so, examining the ability of DDX3 to promote WNV protein translation in a human cell line would ensure that the results were not influenced by potential differences between the human and hamster cellular proteins.

Another proposed role for DDX3 is as an enhancer of the antiviral response, and so we examined the ability of DDX3 expression to enhance the IPS-1 mediated antiviral response. Expression of DDX3 and IPS-1 together enhanced IPS-1 activation of IRF-3, indicating that DDX3 is able to contribute to this antiviral pathway. This is consistent with previous work demonstrating that DDX3 interacts directly with IPS-1, and this interaction enhances IFN- β promoter expression (132). However, when the expression of the IRF3 inducible antiviral protein ISG-56 was monitored in DDX3 overexpressing cells, there was no difference in the protein levels between those infected with WNV infected and mock-infected. The similar levels of ISG-56 suggest that overexpression of DDX3 is unable to enhance the antiviral response during WNV infection. Repetition of these IPS-1/DDX3 co-transfection experiments in the context of a WNV infection would reveal if WNV prevents DDX3 from interacting with IPS-1 in the antiviral response, either directly or as a consequence of utilizing DDX3 for other functions related to viral replication.

We also examined the effects of overexpression of DDX3 on viral replication and viral protein production. We observed no difference in WNV viral protein expression or viral replication when DDX3 was overexpressed, further suggesting that DDX3 does not play a pro-viral role during WNV infection. The decrease in DDX3 expression at 72 hours post infection suggests that WNV is negatively regulating DDX3 protein expression. One possibility is that as infection progresses, the cell begins to respond by inducing the degradation of viral proteins. The Jab1 protein has been shown to associate with the WNV C protein, resulting in the export to the cytoplasm and eventual degradation of C (129). Given that DDX3 has been shown to bind to the related HCV C, it is possible that DDX3 binds the WNV C protein as well. If this is the case, it may be that DDX3 is degraded as a consequence of association as is the case with Jab1 induced degradation of WNV C. Identification of which viral or cellular proteins DDX3 is bound to or associates with will begin to clarify why there is a reduction in protein level at late times in infection.

DDX3 was observed to co-localize with and WNV proteins at 24 hours post infection. While there is no indication that this interaction is antiviral, it is possible that by this point in infection the virus has already subverted any antiviral activity DDX3 possess. It is also possible that the virus is utilizing DDX3 specifically for its role as a component of the ribosome/translational machinery or one of its other RNA-related cellular functions at this point in infection. In order to determine if DDX3 is interacting with other antiviral proteins during WNV infection, DDX3 protein expression and localization patterns should be examined

in relation to other antiviral pathway components, especially the RIG-I pathway members via immunofluorescence. Likewise, analysis of co-immunoprecipitation experiments to see what binding partners DDX3 is associated with during WNV infection could help identify which cellular proteins or the specific WNV protein DDX3 is interacting with during infection.

Experiments utilizing the overexpression of DDX3 failed to increase the antiviral response or reduce the viral titer to any significant level. This is not to say, however, that knock down of the protein would not have more readily apparent consequences during infection. Indeed, other studies have looked at the knock down of processing body (p-body) associated proteins, including DDX3, during WNV infection and found a correlation to viral replication (27). P-bodies are vesicles formed as a consequence of cellular stresses, including viral infection, where mRNA is stored and degraded. When DDX3 was knocked down, there was a reduction of WNV viral RNA replication and the production of viral particles. Repeating experiments to analyze whether the absence of DDX3 during infection can affect the antiviral response would clarify the role this protein is playing during WNV infection.

Our work thus far suggests that DDX3 may co-localize with WNV protein and that WNV infection affects DDX3 protein levels by late time points during infection. However, the protein does not appear, according to our initial experiments, to possess a clear pro- or antiviral function. The precise role of DDX3 during WNV infection remains unknown, and its potential involvement as an antiviral cascade partner or viral RNA sensor has yet to be defined. Further

studies to examine the antiviral potential of DDX3 will need to be performed in order to determine what role, if any, it plays in the RIG-I mediated antiviral pathway.

Chapter 5 – Discussion

Within the past decade, WNV has established itself as a serious public health concern within the United States. The increased incidence of neurological disease combined with the establishment of yearly epidemics has made gaining a full understanding of the factors that contribute to virulence a priority. The host response to a viral infection can be critical in defining the severity of infection. A rapid and robust antiviral response, such as that mediated by the PRR RIG-I, can serve to constrain viral replication at the site of infection and trigger activation of the adaptive immune response to promote viral clearance thereby, moderating disease symptoms. The RIG-I response is a critical component of the innate immune response to WNV infection, but as with many other viruses, the PAMPs activating this pathway remain undefined. The work described in this dissertation begins to define the components of the WNV genome and antigenome that serve as viral PAMPs recognized by RIG-I. Additionally, these studies begin to provide insight into the RNA structures that may be involved in activating RIG-I. This work also describes preliminary data analyzing the role of DDX3, a protein with proposed antiviral activity associated with the RIG-I response, during WNV, although the exact function of the protein remains to be defined.

Identification of WNV-NY PAMPs

This work has defined several regions of the WNV genome capable of serving as PAMPs during infection. The 5'UTR and NS2a from the positive

sense genome and the 3'UTR, E NS2a and NS4a of the negative sense antigenome were all capable of stimulating a RIG-I mediated antiviral response. However, incorporation of these regions into larger RNA fragments or the entire genome abolished the stimulatory capacity, suggesting these PAMP regions need to be liberated from the viral genome and antigenome to induce an antiviral response. Indeed, when larger WNV RNAs were transfected into cells, RIG-I stimulation was detected over time, further supporting the hypothesis that PAMPs can be liberated by the host cell during the course of infection. Degradation of the WNV RNA via the host's RNA processing pathways may be contributing to PAMP production, thus we began to examine methods of RNA degradation. The endonuclease XRN1 has been previously shown to degrade WNV RNA and produce a discrete RNA fragment, the sfRNA. When examined, the WNV sfRNA did not stimulate a RIG-I response. This is not surprising, as other studies have concluded that the sfRNA serves to promote WNV neuroinvasiveness and thus serve as a pathogenicity factor (142, 164). Mutation of the WNV 3'UTR such that the sfRNA is not produced reduces the lethality of the virus. There is also data to suggest that the sfRNA may be acting as an inhibitor of RNAi, another cellular RNA degradation mechanism and important antiviral pathway, leading to an increase in virulence (159). It remains possible that XRN1 may liberate other PAMPs during degradation of the viral genome, and examining knock down of XRN1 during WNV infection will provide information about the extent of this enzyme's role in PAMP production.

Potential pathways involved in PAMP liberation

Along with the XRN1, several other RNA degradation mechanisms have been defined that process viral RNAs. The RNaseL pathway is an antiviral mechanism induced by viral RNA and is important in the liberation of RNA PAMPs over the course of HCV infection (109). 2'5'-linked oligoadenylate synthase (OAS) responds to viral dsRNA PAMPs by producing 2'5'-linked oligoadenyltic acid, which serves to activate RNaseL, a ribonuclease that degrades RNA in the cell, including viral genomes (47). Previous work has determined RNaseL is activated during WNV infection (156), therefore it would be of interest to examine the potential WNV PAMP producing capacity of this pathway. However, OAS expression is IFN-dependent and requires an active antiviral response in order to initiate this particular RNA degradation mechanism. PAMPs recognized by RIG-I may result in the expression IFN and therefore lead to the activation the RNaseL pathway. Therefore, the OAS, RNase L pathway is likely to play a role in enhancing the antiviral response rather than serving to produce the initial PAMPs. Therefore, the RNaseL pathway does not readily account for the induction of the initial antiviral response and the PAMPs recognized by RIG-I.

The RNA interference (RNAi)/Dicer pathway is an evolutionarily conserved pathway in eukaryotes used to control gene expression by regulating RNA post-transcriptionally. The pathway utilizes small, interfering RNAs (siRNA) and micro RNAs (miRNA) for a variety of regulatory functions, including normal cellular gene expression, development and also as an antiviral control mechanism (186).

siRNAs are produced by the cleavage of exogenous, long, dsRNAs into small (~20nt), single stranded fragments by the cellular ribonuclease Dicer. These siRNAs are then loaded into the RISC complex, which facilitates the base pairing of the siRNAs to corresponding regions of mRNA and inhibit translation. The RNA is then degraded. miRNAs are host cell, non-coding RNAs that are similarly processed by Dicer, loaded into the RISC complex and then serve to regulate gene expression. Viruses induce the RNAi pathway due to the prevalence of dsRNA species formed during the course of replication (63). As a consequence, several viruses have evolved mechanisms to defend against the RNAi pathway. Many viruses encode viral proteins that function as suppressors of RNAi silencing (SRS), or have RNA regions that can serve in a similar SRS capacity (64, 172). The sfRNA of WNV is proposed to serve as an SRS in both insect and mammalian cells. Degradation of viral RNA by Dicer to form siRNA may, in addition to serving its function in the RNAi pathway, liberate potential PAMPs to be recognized by other PRRs in the host cell cytoplasm. If the Dicer pathway is important for PAMP production, the finding that the sfRNA interferes with it during the course of infection may also provide insight into how WNV is able to avoid detection by the host cell.

Another potential mechanism involved in the formation of viral PAMPs is the adenosine deaminase that act on RNA (ADAR) proteins. In mammals, there are three ADAR proteins, numbered 1, 2 and 3. The ADARs act by deaminating adenosines found in dsRNA molecules to form inosine, a process referred to as hyper-editing. This conversion can result in a destabilization of the RNA, as the

uridine base paired to the edited adenosine is not able to bind as readily to the converted inosine, resulting in degradation of the RNA molecule (125, 155). While the ADAR proteins normally act in cells in order to regulate gene expression, especially during development, they can also serve as antiviral proteins, given their specificity for dsRNA (153). Of the ADAR family members, ADAR-1 is IFN inducible, implicating it as an antiviral effector molecule. There is also evidence to suggest that hyper-editing by ADAR and the consequential destabilization of the RNA molecule can provide a target RNA for cleavage by Dicer, implicating ADAR-1 as a factor in the production of siRNAs and contributing to RNAi (154). In the case of several paramyxoviruses, hyper-editing by ADAR-1 reduces virulence in cells and results in less-infectious viral particles (193). However, ADAR can also act in a pro-viral manner (62, 139, 153). During measles virus infection, hyper-editing of the matrix gene is found to be associated with a decrease in infectious particle production in CNS; however, these less infectious particles result in a persistent infection and can induce encephalitis, a serious neurological disease state (203). Given the evidence for ADAR activity, both in an anti- and pro-viral capacity and its connection to the RNAi pathway, it is reasonable to investigate whether ADAR-1 editing in WNV infection may result in the production of RNAs able to serve as PAMPs identified by RIG-I.

The final pathway for consideration during the initial investigation of the cellular RNA processing mechanisms that may contribute to PAMP production is the ER stress-induced inositol-requiring enzyme-1 (IRE-1) pathway. This

pathway is traditionally associated with degradation of proteins that are unfolded in the ER lumen as part of the unfolded protein response (UPR) (148, 184). Activated IRE-1 induces the cleavage of the mRNA *xbp1*, allowing it to be translated into an active X-box protein-1 (XBP-1) able to serve as a transcription factor for other stress induced proteins. The cytoplasmic domain of the IRE-1 protein encodes the endoribonuclease responsible for this cleavage. Other work has shown that in addition to the specific cleavage of *xbp1*, IRE-1 can cleave cellular mRNAs during stress responses (72, 73). Infection of the cell induces membrane rearrangement, especially on the ER, to form platforms for viral replication, bringing IRE-1 into close association with the viral replication complex. Indeed, WNV has been previously shown to modulate the IRE-1 pathway, and several other viruses inhibit IRE-1 to avoid activation of the UPR, although there is no evidence connecting IRE-1 to viral RNA cleavage or processing (3, 138, 205, 212). However, IRE-1 associated with these membranes can come into contact with viral RNAs and the domain of the protein that contains endoribonuclease function could potentially cleave viral genomic RNA, making it a potential contributor to RIG-I PAMP production.

In the case of all of the RNA degradation pathways/mechanisms listed, an examination of the effect of knock down of these proteins/pathways on WNV replication and the kinetics of the antiviral response would help to illuminate their role in the production of RIG-I PAMPs. Reduced activation of RIG-I pathway components, such as IRF-3, in knock down cells infected with WNV could indicate a failure to induce the RIG-I response. Additionally, an increase in viral

replication and a delay in IFN production in knock down cells could be indicative of this pathway's importance in the antiviral response to WNV. Further analysis of pathways identified through initial knock down experiment would then serve to tease apart the specific proteins/steps within the pathway that are required for PAMP production and/or the induction of the RIG-I mediated antiviral response.

Examination of PAMPs during a native infection

Examination of RNAs pulled down along with RIG-I in the context of WNV infection would be the most direct way to identify PAMPs *in vivo*. Analysis of RNA species bound to RIG-I in infection through RNAseq has been done with influenza A and SENV, revealing information concerning the structures required for RIG-I recognition of these viral PAMPs (12). Determining such basic characteristics, including size and structural features of the RNA, can help define the pathway responsible for PAMP production, further confirming studies examining RNA processing. It would also provide general information regarding RNA PAMPs and the features required for RIG-I binding and activation, thus increasing our knowledge about this critical antiviral protein. The development of antiviral therapies based on stimulating the RIG-I pathway during infection is a possible consequence of a greater understanding of the PAMPs required to stimulate this antiviral response.

Analysis of WNV PAMPs

Differences in WNV PAMPs between strains may account for differential activation of the antiviral response

The work presented begins to define the structural characteristics required for a WNV RNA to serve as a RIG-I PAMP. During the course of analyzing the WNV-NY 5'UTR, a comparison to the WNV-MAD78 5'UTR was made to examine the effects of a single base deletion from WNV-NY to WNV-MAD78. This revealed that the WNV-MAD78 5'UTR is a potent stimulator of the RIG-I response, consistently stimulating at the same level as the WNV-NY 5'UTR. However, preliminary analysis of the total viral genome suggests that there are differences in which regions can serve as PAMPs between the two viruses strains (Appendix 1). Initial luciferase reporter assays suggest WNV-MAD78 NS3 (+) stimulates RIG-I. In contrast, WNV-MAD78 NS2a (+ and -), both of which stimulated in WNV-NY, do not appear to induce a RIG-I response. The WNV-MAD78 RNAs stimulate as robustly as the identified WNV-NY PAMPs, indicating a strong RIG-I response to both WNV-NY and WNV-MAD78 PAMPs, when they are accessible. Further analysis of the WNV-MAD78 genome for potential PAMP regions will fully define the regions capable of stimulating a RIG-I response. Additionally, studies constructing chimeric viruses combining regions of the WNV-NY and WNV-MAD78 will indicate which regions are critical for the RIG-I response.

ssRNA and tertiary interactions may influence RIG-I stimulation

The full length WNV-NY 5'UTR, WNV-MAD78 5'UTR and WNV-NY 1-90 fragment were all capable of stimulating a robust RIG-I response, while the WNV-NY-SL stimulated to a lesser degree and WNV-NY 1-80nt fragment failed to stimulate RIG-I. Structural analysis of the WNV-NY and WNV-MAD78 5'UTRs suggest regions of single stranded RNA present in these structures. Such a region is suggested to be absent in the WNV-NY-SL and structural prediction of the WNV-NY 1-90 fragment also suggests this ssRNA region is absent. However, regions of ssRNA are not an absolute requirement for RIG-I activation as constructs lacking single stranded regions still stimulatory. However, all RNAs capable of inducing RIG-I are predicted to contain regions of tertiary interaction within the RNA. Combined, the ssRNA region and the tertiary interaction may be required for optimal stimulation of RIG-I. Indeed, one proposed mechanism of action for RIG-I is a "scanning model," whereby RIG-I constantly scans cellular RNAs and is only activated once it contacts a specific PAMP (personal communication, Michael Gale). RIG-I may be binding to the ssRNA regions of the 5'UTR initially while scanning, but is only activated once the protein encounters a region of dsRNA or a structure formed by tertiary interaction, denoting a viral PAMP. Analysis of mutations producing ssRNA regions or disrupting tertiary interactions may further characterize the importance of these structural features for RIG-I stimulation. Structural analysis of other identified PAMP regions of both WNV-NY and WNV-MAD78 will also provide information about the requirements of RIG-I/PAMP interaction, which will in

general provide useful information in the identification of viral PAMPs from other viral species. It may also elucidate how viruses may circumvent the RIG-I response by altering or otherwise masking crucial structures required for proper binding to RIG-I during the course of infection.

Steady state binding does not indicate RIG-I stimulatory capacity

We observed that steady-state binding of the 5'UTR RNA to RIG-I varies between species and that affinity does not correlate with stimulatory ability. The WNV-NY and –MAD78 5'UTRs were both able to robustly stimulate RIG-I but both had much higher K_d values as compared to the 1-80nt fragment, which did not stimulate. It is possible that the secondary structures within the RNA can also serve to bind multiple copies of RIG-I, which has been previously shown to occur, enhancing signaling of RIG-I through a multimerization effect and resulting in a more potent antiviral response overall (75, 87). Therefore, if the WNV-MAD78 RNA has weaker binding affinity but is able to bind more RIG-I per molecule than WNV-NY RNA, inducing a stronger response, this may account for ability of the host to clear the WNV-MAD78 virus and prevent serious pathology as compared to WNV-NY. Further examination of the binding of WNV RNAs and RIG-I through x-ray crystallography may serve to clarify these interactions.

The role of DDX3 during WNV infection

The DEAD/H helicase DDX3 has recently been characterized as playing a role in the RIG-I mediated antiviral response. DDX3 has been suggested to serve as a sensor of viral RNA, interact with and activate RIG-I, or/and serve as

an activator of downstream signaling components such as IPS-1 and the TBK1/Ikkε complex (132, 162, 163). DDX3 also plays a role in a variety of normal cellular processes involving RNA, such as export from the nucleus and as a part of the translation pre-initiation complex (33, 57, 68, 91, 167). The work presented here suggests that DDX3 may co-localize with WNV proteins during infection, and infection results in the reduction of DDX3 protein levels at later time points. However, there is no discernible difference in either viral replication or the antiviral response to WNV when DDX3 is overexpressed. Co-localization studies and immunoprecipitation of DDX3 with RIG-I pathway members will help to illuminate the antiviral role of DDX3 during WNV infection. Recent work has demonstrated that knock down of DDX3 negatively affects WNV replication, but the impact of knock down on the antiviral response to WNV has yet to be determined. If DDX3 normally participates in the RIG-I mediated antiviral response but is prevented from functioning in this capacity, either by an active repression by WNV or because the virus is utilizing DDX3 for one of its other cellular roles, it could provide an attractive target for the development of antiviral therapies.

It remains to be seen if the DDX3 protein, which has been implicated as a viral RNA sensor and as a component of the RIG-I mediated antiviral pathway, is active in this capacity during WNV infection. Further work to fully characterize which regions of the WNV genome can stimulate RIG-I will need to be done to determine if differences in the PAMPs produced between strains are contributing to a differential activation of the RIG-I response. The use of artificial ligands

designed based on information obtained by studying native ligands of RIG-I can be utilized for antiviral therapies. These artificial RIG-I PAMPs help to increase the antiviral response and may result in a more rapid clearance of the virus. Studies testing such RIG-I ligands for use during HCV infection are ongoing (personal communication, Michael Gale). Development of such broad-spectrum antiviral therapies would be beneficial for the treatment of numerous viral infections, including WNV.

The work presented here begins to analyze WNV PAMPs. It is important to gain a proper understanding of how WNV is able to stimulate the antiviral response, how this response varies between strains, and to characterize the specific components required for the proper activation of the antiviral response. This information allows us to gain perspectives on treatment for infected individuals and to apply this knowledge more generally in analyzing infection with other viruses, again leading to more effective treatments during infection and potential prophylactic treatment or vaccines to prevent infection.

Chapter 6 – Materials and Methods

Cells and Viruses. Huh7, Huh7.5 (Apath) and 293T (GeneHunter, Nashville TN) cells were propagated in Dulbecco's modified Eagle's medium (DMEM) supplemented with 10% FBS, 2 mM L-glutamine, 1 mM sodium pyruvate, 1 mM non-essential amino acids and antibiotic/antimycotic solution (complete DMEM). Sendai virus (SenV), Cantell strain was obtained from Charles River.

Plasmids. pFL-WNV (166) was used as a template for PCR-amplification of the indicated segments of the WNV-NY genome (Table 1). Primer sequences are listed in Appendix 2. Amplified segments were cloned into pCAGGS, pVL-blunt (a gift from Dr. Vincent Lee), pBluKSM or pWSK29 (a gift from Dr. Sydney Kushner, (189) and the sequence confirmed. The reporter plasmids pISG56-luc (a gift from Dr. Ganes Sens)(61) and pCMV-Renilla (Promega) encode the firefly luciferase gene under transcriptional control of the ISG56 promoter and the Renilla luciferase gene under the constitutively active cytomegalovirus (CMV) early promoter, respectively. pEF-flag-N-RIG encodes the constitutively active N-terminus of RIG-I (208). DDX3 was cloned into pEFBOS (117). Construct produced are detailed in Appendix 3 and 4.

Plasmid transfection. Subconfluent monolayers of Huh7 cells in a 12-well plate 200ng of pCAGGs construct encoding one gene of the WNV genome.

For DDX3 overexpression, subconfluent monolayers of 293T cells in a 6-well plate or BHK cells containing a WNV replicon (reference) in a 48-well plate were transfected with 500ng of pEFBOS-DDX3. For IPS-1 cotransfection, subconfluent monolayers of Huh7 cells in a 48-well plate were transfected with 200ng of pCDNA3.1-IPS-1 and 100, 200 or 300ng of pEFBOS-DDX3. All transfections were done using Lipofectamine 2000 transfection reagent (Invitrogen).

RNA fragments. *In vitro* transcribed RNA fragments were generated according to the manufacturer's protocol (Ampliscribe T3 and T7 kits; Epicentre). Briefly, a 20 µl reaction mixture containing 1 µg of linearized plasmid encoding the indicated RNAs was incubated at 42°C for 2 hr. DNA template was subsequently removed from the reaction by treating with DNase I. RNA was recovered by phenol/chloroform extraction followed by ethanol precipitation. Unless otherwise indicated, RNAs were treated with calf alkaline phosphatase (CIP) to remove free 5' triphosphates (New England Biolabs). The purity of the RNAs was confirmed by polyacrylamide gel electrophoresis. The NS2b fragment was further purified on a 6% polyacrilamide gel containing 8 M urea. The RNA was eluted overnight at 4°C from the excised gel fragments in buffer containing 200mM NaCl, 10mM Tris-HCl pH 7.5, 1mM EDTA. The eluted RNA was precipitated with ethanol, aliquoted and stored at -80°C. The Amplicap kit (Epicentre) was used to generate the capped 5' UTR segment and full length genomic RNA. Monophosphorylated sub-genomic WNV RNA (sfRNA) was generated by incubating CIP-treated *in vitro* transcribed sfRNA with T4

polynucleotide kinase according to the manufacturer's instructions (NEB). WNV genomic RNA was isolated from culture supernatants recovered from WNV-NY infected cells. Cell debris was removed by low speed centrifugation at 1500 rpm for 5 min and genomic RNA was recovered by Trizol (Invitrogen) extraction.

Luciferase Reporter Assays. Subconfluent monolayers of Huh7 or Huh7.5 cells in a 48 well plate were transfected with 100 ng of ISG56-luc and 20 ng of pCMV-Renilla using Lipofectamine 2000 transfection reagent (Invitrogen). Where indicated, cells were also transfected with 200 ng of pEF-flagN-RIG or pCAGGs encoding a single WNV gene. For protein expression experiments, cells lysates were prepared 24 hours post transfection. For RNA transfections, at 16 hr post-transfection, cells were mock-transfected, transfected with 500 ng or 2 pmol of the indicated RNAs using TransMessenger transfection reagent (Qiagen), or infected with SenV (100 HA units), in triplicate. Cell lysates were prepared 8 hr after RNA transfection or infection with SenV and luciferase levels were detected using a dual luciferase kit according to the manufacturer's protocol (Promega). Luciferase activity was quantified using a Berthold Centro XS3 LB960 luminometer. Normalized luciferase levels were determined by dividing firefly luciferase levels by control *Renilla* luciferase levels. Values represent the average luciferase expression compared to mock (\pm standard error) from a minimum of two independent experiments. Statistical analysis was performed using Dunnett's multiple comparison analysis.

Trypsin Digestion. Control dsRNA (Invivogen) or the indicated WNV RNA fragments (30 pmol) were incubated with purified *E. coli*-produced RIG-I (15

pmol) for 15 min at room temperature. The RNA/RIG-I mixtures were digested with trypsin (0.83 mg) for 15 min at 37°C. Trypsin was inactivated by the addition of protease inhibitor (Sigma) and the digestion products were separated on a 12.5% SDS polyacrylamide gel. Bands were visualized using Imperial Protein Stain (Thermo scientific).

SHAPE analysis. Selective 2'-hydroxyl acylation probed by primer extension was performed as previously described (115, 201). Briefly, 2 pmol of RNA was incubated at 37°C in buffer (333 mM HEPES, pH 8.0, 333 mM NaCl, 30 mM MgCl₂) for 20 min. RNA was then treated with either 60 mM 1M7 or DMSO for 10 min at 37°C. RNA was ethanol precipitated and then used in primer extension with P³² radiolabeled primers using Superscript III reverse transcriptase (Invitrogen). Sequencing reactions were also run concurrently with the DNA template used for *in vitro* transcription using the Thermosequenase cycle sequencing kit (USB). Extension products were separated on an 8% polyacrylamide 8M Urea gel and analyzed using a FLA-5100 phosphoimager.

RIG-I binding. Binding interactions were analyzed by Differential Radial Capillary Action of Ligand Assay (DRaCALA) as previously described (46, 147). Briefly, 1 nM P³² radiolabeled RNA was incubated with varying concentrations of *E. coli* purified RIG-I protein in binding buffer (100mM Tris, pH 7.5, 10mM NaCl) for 10 minutes. Mixtures were then spotted onto dry nitrocellulose membrane and allowed to dry. Results were imaged using a Kodak FLA-5000 phosphoimager. Quantification was done using the Multi Gauge software v3.0. Fraction Bound was calculated by measuring area and PSL intensity of the total

spot (A_{total} and I_{total} , respectively) and the area and PSL intensity of the inner spot (A_{inner} and I_{inner} , respectively) and utilizing the following equation:

$$\frac{I_{inner} - A_{inner} * \left(\frac{I_{total} - I_{inner}}{A_{total} - A_{inner}} \right)}{I_{total}}$$

Radiolabeled primers and RNA. Primer used for primer extension (Appendix 2) and RNAs used for binding assays were labeled with γ - ^{32}P -ATP using T4 Polynucleotide Kinase at 30 μCi /50pmol of RNA. Unincorporated label was removed using an Illustra Microspin G-25 column (GE Healthcare).

Immunofluorescence Assay. Subconfluent Huh7 or 293T monolayers were grown on a microscope coverslip in a 35mm dish and then infected with WNV-NY at an MOI of 1. At the indicated times post infection, cells were washed with 1x PBS and then fixed in 3% paraformaldehyde for 30 minutes. Cells were permeabilized (0.2% TritonX-100, 1x PBS) and incubated at room temperature in blocking solution (1x PBS, 10% normal goat serum) for 1 hour. Cells were incubated for 1 hour with polyclonal mouse-anti WNV (1:1000, Arbovirus Research Center, T35570) and a polyclonal rabbit-anti DDX3 (1:1000, Bethyl Laboratories, A300-475A) in antibody diluent (1x PBS, 0.5% Tween-20, 3% bovine serum albumin). Cells were then washed (1x PBS, 0.5% Tween-20) and incubated with goat anti-rabbit immunoglobulin G-Alexa 488 antibody conjugate (1:800, Molecular Probes) or goat anti mouse immunoglobulin G-rhodamine antibody conjugate (1:800, Jackson ImmunoResearch). Coverslips were inverted

onto microscope slides and overlaid with Vectasheild solution (Vector Labs). Slides were visualized on an Olympus IX51 equipped with a digital camera.

Immunoblots. 293T cells were infected at an MOI of 1. Cells were lysed in RIPA buffer (10 mM Tris pH 7.4, 150 mM NaCl, 0.02% NaN₃, 1% sodium deoxycholate, 1% Triton X-100, 0.1% sodium dodecyl sulfate [SDS], and 1X protease inhibitors [Sigma]) at the indicated times post infection. 10-20 ug of total protein were separated by 10% SDS-polyacrylamide gel electrophoresis (PAGE) and transferred to a nitrocellulose membrane. Membranes were blocked in blocking buffer (1x PBS, 5% milk, 0.1% Tween-20) and then incubated with primary antibodies to the following: polyclonal rabbit-anti DDX3 (1:5000), polyclonal mouse-anti WNV (1:1000) or polyclonal rabbit-anti GAPDH (1:5000, Abcam, ab36845). Goat anti rabbit and goat anti mouse secondary antibodies were peroxidase conjugated. Blots were visualized using ECL Plus Western blotting detection reagents (Amersham Biosciences) followed by exposure to film.

Virus Infection. Subconfluent monolayers of 293T or Huh7 cells were washed once with DMEM and infected with WNV at a multiplicity of infection (MOI) of 1. After 1 hour at 37°C, the inoculum was replaced with complete DMEM and cells were incubated at 37°C. Supernatants were collected at the indicated time points.

Plaque Assays. Monolayers of Vero cells in a six-well plate were washed with DMEM followed by addition of serial dilutions of viral samples. Cells were incubated in a 5% CO₂ incubator for 1 hour at 37°C with rocking. The inoculum was then removed and a 0.9% agarose-complete DMEM overlay was added. Cells were then incubated for 48 hours and a second overlay of agarose-DMEM containing 0.003% neutral red (MP Biochemicals) was applied. Plaques were counted 4 days after initial inoculation.

Appendix 1: Preliminary WNV-MAD78 PAMP data

WNV-MAD78 is a strain of WNV isolated in Madagascar in 1978. In mice, this strain is considered non-pathogenic, as it does not result in neurological symptoms when injected at a peripheral site. In contrast, infection with WNV-NY, a strain that has recently emerged in the western hemisphere, at peripheral sites can result in neurological symptoms and therefore, this strain is considered pathogenic (13). Despite these differences in disease pathology, there is only a limited understanding of the factors that contribute to the differences in pathogenicity between strains.

In order to compare the antiviral response between WNV-NY and WNV-MAD78, the WNV-MAD78 genome is being examined for potential PAMPs. RNA corresponding to the ten genes of the WNV-MAD78 genome were generated by *in vitro* transcribed and we are currently in the process of being tested for their stimulatory capacity. Preliminary data indicates that, as with the WNV-NY genome, several WNV-MAD78 RNAs are capable of inducing an antiviral response (Figure 32). NS3(+) appears to be stimulatory and E(+) may also stimulate, albeit weakly. Conversely, regions that were stimulatory in WNV-NY, including NS2a(+) and NS2a(-), were not stimulatory from WNV-MAD78.

When experiments have been completed, a more definitive statement concerning the stimulatory capacity of these regions can be made. However, the preliminary data suggests that different regions are capable of stimulating the innate immune response between the various strains of WNV. Understanding the differences in PAMP regions between these strains may help to clarify the RIG-I mediated response during infection, and help to elucidate if and how the innate antiviral response is a contributing factor to the differences in pathogenicity between strains.

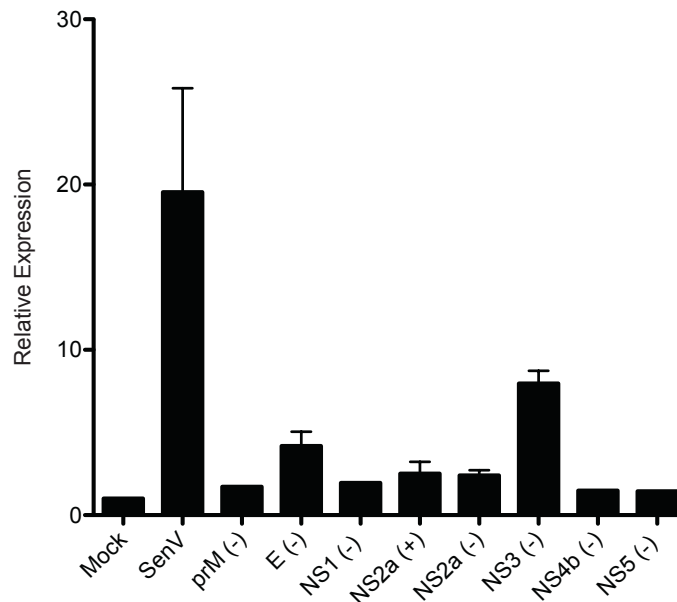


Figure 32: Stimulatory capacity of WNV-MAD78 RNA. Huh7 monolayers were transfected with pISG56-luc and pCMV-*Renilla* 16 hr prior to infection with SenV or transfection with 500 ng of the indicated RNAs in triplicate. Cell lysates were prepared 8 hr post transfection and assayed for luciferase activity. Values represent the average luciferase expression compared to mock (\pm) standard error.

Appendix 2: Oligonucleotides

Table 3: List of Oligonucleotides used for various experiments.

Name	Sequence
PCR products	
WNV-NY 5' w/T7 promoter (s)	TAATACGACTCACTATAGAGTAGTTCGCCTG
1-90nt(as)	CTTCGTGCTAAGAAACAGCTCGC
1-80nt(as)	AGAAACAGCTCGCACTGTG
WNV 97(as)	CGAGATCTTCGTGCTAAGAAACAG
T7 (sfRNA) 10504 (s) +Gs	TAATACGACTCACTATAGGGAAGTCAGGCCG GGAAG
Site directed mutagenesis	
WNV-NY 5' knot #1 mutation	TAATACGACTCACTATAGAGAATTTCTCGTTTG AGACAAACTTAG
Cloning	
WNV-NY	
WNV-NY 5'UTR s	ATCGGCTAGCAGTAGTTCGCCTGTGTGAGCT G
WNV 5-UTR BamHI) as	GATCGGATCCGAGATCTTCGTGCTAAGAA
WNV-TX EcoRI-(C) s	GGGAATTCGCCATGTCTAAGAAACCAGGAGG
WNV-TX (C)-KpnI as	CCGGTACCCCTCTTTTCTTTTGTTTGAGC
WNV-TX EcoRI-(prM) s	GCGAATTCCATGAAAAGAGGAGGAAAGACCG
WNV-TX (prM)-KpnI as	ATGGTACCCCGCTGTAAGCTGGGGCCAC
WNV-TX EcoRI-(E) s	GCGAATTCATGAGCAACACCATGCAGAGAGTT G
WNV-TX (E)-KpnI as	TTGGTACCCAGCATGCACGTTACGG
WNV-TX EcoRI-(NS1) s	GGGAATTCATGATAGCTCTCACGTTTCTCGCA

	G
WNV-TX (NS1)-KpnI as	ACGGTACCCCAGCATTCACTTGTGACTGCA
WNV-TX SacI-(NS2a) s	CCGAGCTCATGTATAATGCTGATATGATTGA
WNV-TX (NS2a)-KpnI as	ATGGTACCCCGCGTTTACGGTTGG
WNV-TX EcoRI-(NS2b) s	AAGAATTCATGGGATGGCCCGCAACTG
WNV-TX (NS2b)-KpnI as	CCGGTACCCCTCTCTTTGTGTATTGGAGAG
WNV-TX EcoRI-(NS3) s	GAGAATTCATGGGAGGCGTGTTGTGGGACAC
WNV-TX (NS3)-NsiI as	ACCATGCATCCACGTTTTCCCGAGGCG
WNV-TX EcoRI-(NS4a) s	CCGAATTCATGTCTCAGATAGGGCTCATTGA
WNV-TX (NS4a)-KpnI as	ATGGTACCCCCTTCTCTGGCTCAGGAATTA
WNV (NS4b) 7680a	GCCTCTAGATCATCTTTTTAGTCCTGGTTTTTC C
WNV (NS4b) 7680a	GCCTCTAGATCATCTTTTTAGTCCTGGTTTTTC C
WNV-NY NS5 (ClaI)s	GATCATCGATATGGGTGGGGCAAAGGACGC
WNV-NY NS5 (SmaI)a	GCATCCCGGGCAGTACTGTGTCCTCAACC
WNV-NY 3'UTR/NotI (s)	ATCGGCGGGCCGCTAGATATTTAATCAATTG
WNV-NY 3'UTR as	AACAATCTAGAGATCCTGTGTTCTCGCACCAC
WNV-NY 5'UTR+CS(BamHI195)as	AAGGATCCAGCCCTCTTCAGTCCAATC
WNV-NY E (XbaI-979)s	AGTCTAGAGGAATGAGCAACAG
WNV-NY 2b(EcoRV)s	CCTCTAGAACTGAAGTGATGAC
WNV-NY 2b(EcoRV)as	TGGATATCTCTCTTTGTGTATTGG
WNV-NY 4b(XbaI)s	GGTCTAGAAACGAGATGGGTTG
WNV-NY 4b(EcoRV)as	CTGATATCTCTTTTTAGTCCTTTTTCC
WNV-NY 5(EcoRV)	AAGATATCGGTGGGGCAAAGG
WNV-NY 5(RV-10389)as	ACGATATCTGTGTCCTCAACC
T7 3'UTR (as) +Gs	TAATACGACTCACTATAGGGAGATCCTGTGTT CTCGCACCAC
WNV-MAD78	
WNV-MAD EcoRI-(C) s	GCGAATTCACCATGTCTAAGAAACCAGGAGG
WNV-MAD (C)-KpnI as	ACGGTACCCCTCTTTTCTTTTGTGTTTGC
WNV-MAD (anchC)-KpnI as	ATGGTACCCCAGCGCCTGCGCAG
WNV-MAD EcoRI-(prM) s	GCGAATTCATGAAAAGAGGAGGTACAGCGG
WNV-MAD (prM)-KpnI as	ATGGTACCCCACTGTATGCCGGCGCTACTA
WNV-MAD EcoRI-(E) s	AAGAATTCATGAGCAACACGATGCAGCGAG
WNV-MAD (E)-KpnI as	TAGGTACCCCGCATGGACGTTAACTGAGA
WNV-MAD EcoRI-(NS1) s	CCGAATTCATGATTGCTATGACGTTCTTGCT G
WNV-MAD (NS1)-KpnI as	AAGGTACCCCGCATTCACTCTCGATTGCA

WNV-MAD SacI-(NS2a) s	CCGAGCTCATGTACAATGCTGACATGATTGAT CC
WNV-MAD (NS2a)-KpnI as	TTGGTACCCCCCGCTTGCGGTTAGGGT
WNV-MAD EcoRI-(2b) s	TTGAATTCATGGGATGGCCTGCTACAG
WNV-MAD (NS2b)-KpnI as	TTGGTACCCACGTTTCGTGTATTGAAG
WNV-MAD SacI-(NS3) s	TTGAGCTCATGGGTGGTGTCTTGTGGGAC
WNV-MAD (NS3)-KpnI as	AAGGTACCCCGCGTTTCCCCGATGC
WNV-MAD EcoRI-(NS4a) s	GGAATTCATGTCACAAATTGGGCTTGT
WNV-MAD (NS4a)-KpnI as	TTGGTACCCCCTTTTCAGGTTCTGGAATCA
WNV-MAD (4b) sigseq fwd	GCGAATTCACCATGCAGCGCTCACAGACTGAT AAC
WNV-MAD (4b) rev	TACCATGCATCGTCTCTTCAGGCCAGGCTTCT CC
WNV-MAD EcoRI-(NS5) s	AAGAATTCATGGGTGGGGCCAAAGGAC
WNV-MAD (NS5)-KpnI as	CCGGTACCCCCAAAACAGTGTCCTCTACAA
DDX3	
hDDX3 (Nhe)s	GGCTAGCTCAGGGATGAGTCATGTGG
hDDX3 (Xho)as	ATCTCGAGTCAGTTACCCACACAGTC

Appendix 3: Constructs used for protein expression

Table 4: Constructs used for protein expression experiments. Nucleotide positions are based on the sequence from GenBank accession: a, AF404756; b, DQ176636; c, AF061337

Construct	Vector	Restriction sites	Position in the genome
WNV-NY ^a			
pCAGGS-NY-C	pCAGGS	EcoRI/XmaI	98-465
pCAGGS-NY-prM	pCAGGS	EcoRI/XmaI	406-965
pCAGGS-NY-E	pCAGGS	EcoRI/XmaI	904-2469
pCAGGS-NY-NS1	pCAGGS	EcoRI/XmaI	2407-3525
pCAGGS-NY-NS2a	pCAGGS	KpnI/SacI	3525-4218
pCAGGS-NY-NS2b	pCAGGS	EcoRI/XmaI	4219-4611
pCAGGS-NY-NS3	pCAGGS	EcoRI/XmaI	4612-6468
pCAGGS-NY-NS4a	pCAGGS	EcoRI/XmaI	6469-6915
pCAGGS-NY-NS4b	pCAGGS	EcoRI/XmaI	6916-7680
pCAGGS-NY-NS5	pCAGGS	EcoRI/XmaI	7681-10395
WNV-MAD78 ^b			
pCAGGS-MAD-C	pCAGGS	KpnI/EcoRI	96-464
pCAGGS-MAD-prM	pCAGGS	KpnI/EcoRI	465-965
pCAGGS-MAD-E	pCAGGS	KpnI/EcoRI	966-2468
pCAGGS-MAD-	pCAGGS	KpnI/EcoRI	2469-3524

NS1			
pCAGGs-MAD-NS2a	pCAGGs	KpnI/SacI	3525-4217
pCAGGs-MAD-NS2b	pCAGGs	KpnI/EcoRI	4218-4610
pCAGGs-MAD-NS3	pCAGGs	KpnI/SacI	4611-6467
pCAGGs-MAD-NS4a	pCAGGs	KpnI/EcoRI	6468-6913
pCAGGs-MAD-NS4b	pCAGGs	KpnI/EcoRI	6915-7682
pCAGGs-MAD-NS5	pCAGGs	KpnI/EcoRI	7683-10397
DDX3 ^c			
pEFBOS-DDX3	pEFBOS	NheI/XhoI	1-2202

Appendix 4: Constructs used for *in vitro* transcription

Table 5: Constructs used for *in vitro* transcription. Nucleotide positions are based on the sequence from GenBank accession numbers: a, AF404756; b, DQ176636

Construct	Vector	Restriction sites for cloning	Parental virus	Position WNV genome
WNV-NY ^a				
NY-5'UTR	pBLuKSM	KpnI/SacI	WNV-NY	1-97
NY-C	pBLuKSM	EcoRI/XmaI	WNV-NY	98-465
NY-prM	pBLuKSM	EcoRI/XmaI	WNV-NY	406-965
NY-E	pBLuKSM	EcoRI/XmaI	WNV-NY	904-2469
NY-NS1	pBLuKSM	EcoRI/XmaI	WNV-NY	2407-3525
NY-NS2a	pBLuKSM	KpnI/SacI	WNV-NY	3525-4218
NY-NS2b	pBLuKSM	EcoRI/XmaI	WNV-NY	4219-4611
NY-NS3	pBLuKSM	EcoRI/XmaI	WNV-NY	4612-6468
NY-NS4a	pBLuKSM	EcoRI/XmaI	WNV-NY	6469-6915
NY-NS4b	pBLuKSM	EcoRI/XmaI	WNV-NY	6916-7680
NY-NS5	pBLuKSM	EcoRI/XmaI	WNV-NY	7681-10395
NY-3'UTR	pBLuKSM	XbaI/NotI	WNV-NY	10396-11029
NY-5'UTR+CS	pBLuKSM	BamHI/SacI	WNV-NY	1-196
NY-5'UTR+prM	pBLuKSM	KpnI/NotI	WNV-NY	1-966
NY-C-E	pWSK29	XbaI/EcoRV	WNV-NY	98-2467
NY-E-NS2b	pBLuKSM	Clal/XbaI	WNV-NY	979-4102
NY-NS2b-NS4b	pBLuKSM	EcoRV/XbaI	WNV-NY	4231-7679
NY-NS4b-NS5	pBLuKSM	EcoRV/XbaI	WNV-NY	6916-10389

NY-NS5-3'UTR	pBLuKSM	XbaI/ClaI	WNV-NY	7681-11029
NY-5'UTR+Cs-eGFP-3'UTR	pCDNA3.1	BamHI/SacI, XbaI/NotI	WNV-NY	1-196, 10396-11029
WNV-MAD78 ^b				
MAD-C	pBLuKSM	KpnI/EcoRI	WNV-MAD78	96-464
MAD -prM	pBLuKSM	KpnI/EcoRI	WNV-MAD78	465-965
MAD-E	pBLuKSM	KpnI/EcoRI	WNV-MAD78	966-2468
MAD-NS1	pBLuKSM	KpnI/EcoRI	WNV-MAD78	2469-3524
MAD-NS2a	pBLuKSM	KpnI/SacI	WNV-MAD78	3525-4217
MAD-NS2b	pBLuKSM	KpnI/EcoRI	WNV-MAD78	4218-4610
MAD-NS3	pBLuKSM	KpnI/SacI	WNV-MAD78	4611-6467
MAD-NS4a	pBLuKSM	KpnI/EcoRI	WNV-MAD78	6468-6913
MAD-NS4b	pBLuKSM	KpnI/EcoRI	WNV-MAD78	6915-7682
MAD-NS5	pBLuKSM	KpnI/EcoRI	WNV-MAD78	7683-10397
PCR products w/ T7 promoter				
WNV-NY-sfRNA	N/A	N/A	WNV-NY	10504-11029
WNV-MAD78 5'UTR	N/A	N/A	WNV-MAD78	1-96
WNV-NY-SL	N/A	N/A	WNV-NY	1-97
WNV-NY 1-90nt	N/A	N/A	WNV-NY	1-90
WNV-NY 1-80nt	N/A	N/A	WNV-NY	1-80

Appendix 5: Structural predictions of WNV-NY PAMPs

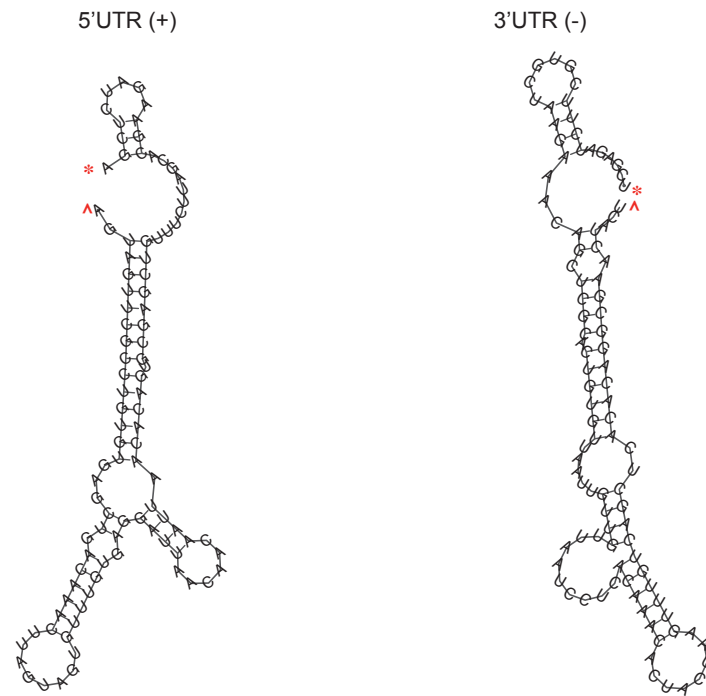


Figure 33: Structural predictions of the WNV-NY 5'UTR (+) and 3'UTR (-). Structures produced with the sfold prediction software (206). *, 5' end; ^ 3' end

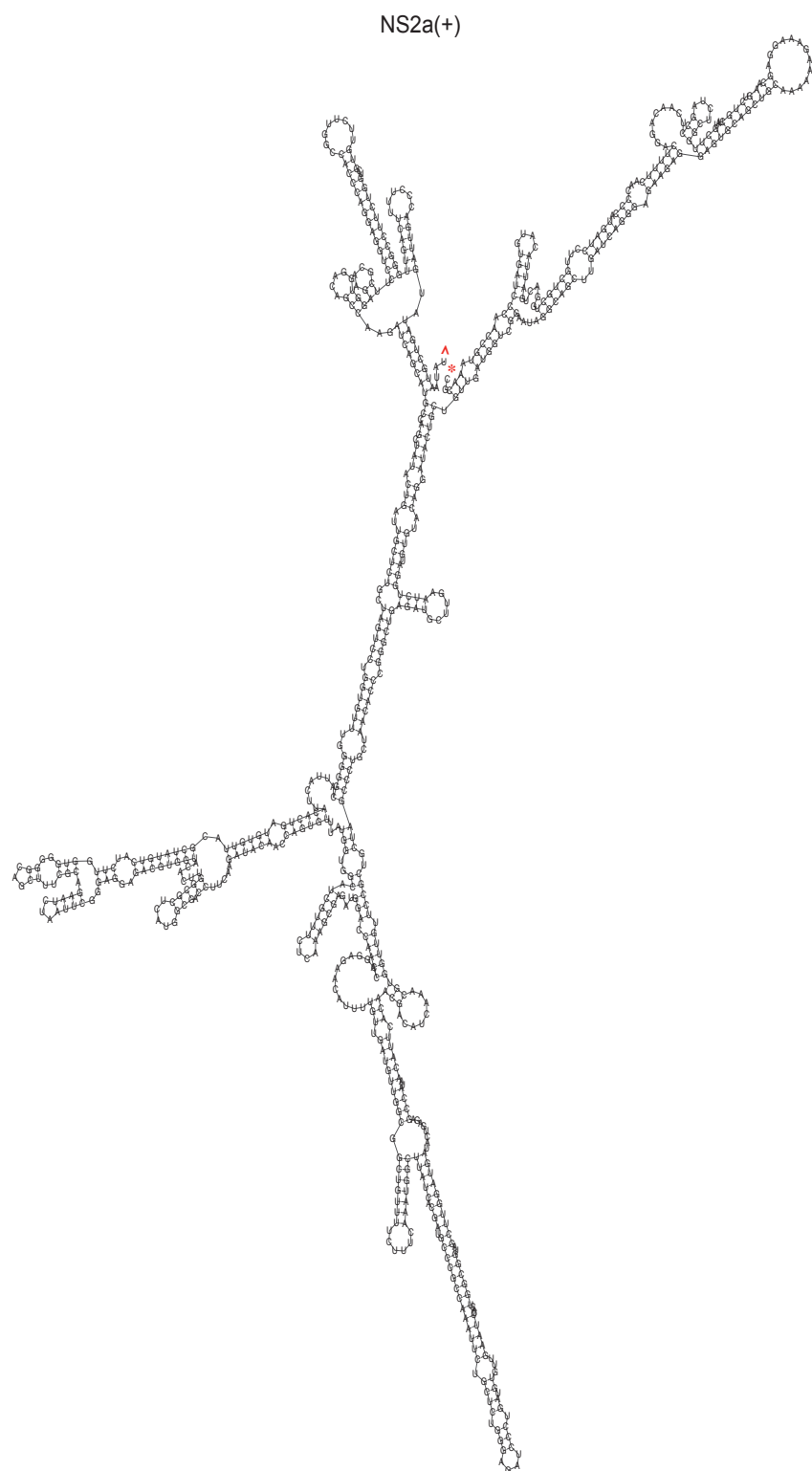


Figure 34 Strucutral predictions of the WNV-NY NS2a(+). Structures produced with the sfold prediciton software. *, 5' end; ^ 3' end

E(-)

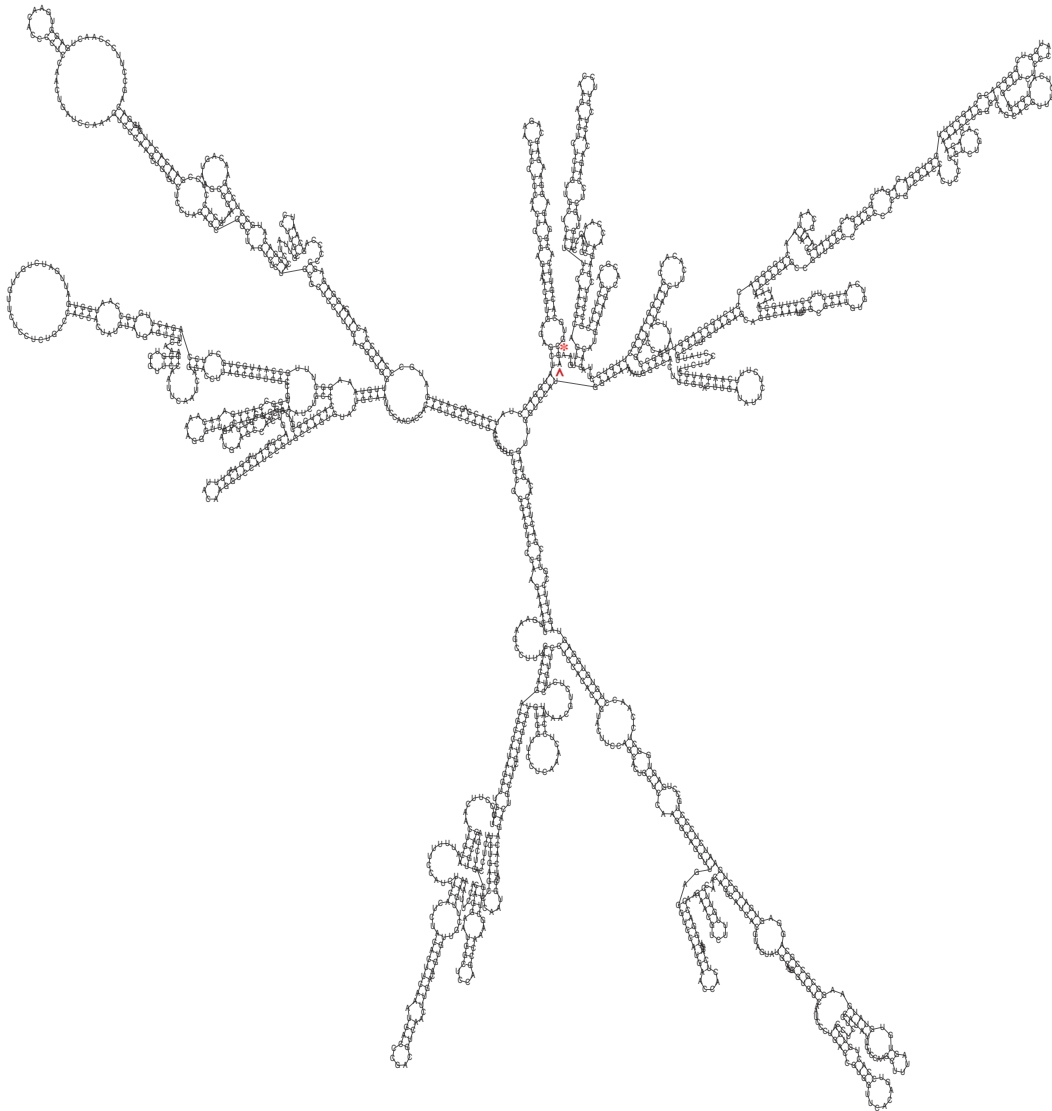


Figure 35: Structural predictions of the WNV-NY E(-). Structures produced with the sfold prediction software. *, 5' end; ^ 3' end

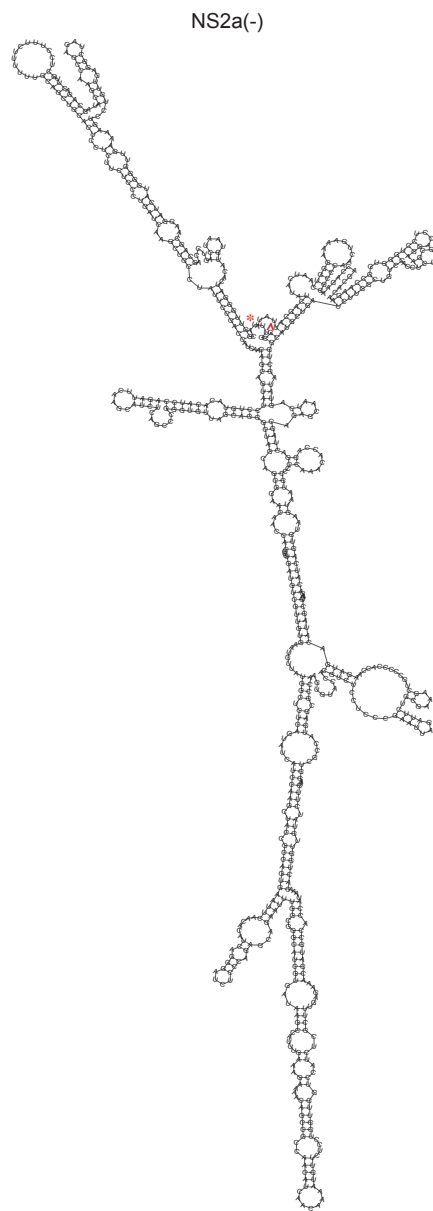


Figure 36: Structural predictions of the WNV-NY NS2a(-). Structures produced with the sfold prediction software. *, 5' end; ^ 3' end

NS4a(-)



Figure 37 Strucutral predictions of the WNV-NY NS4a(-). Structures produced with the sfold prediciton software. *, 5' end; ^ 3' end

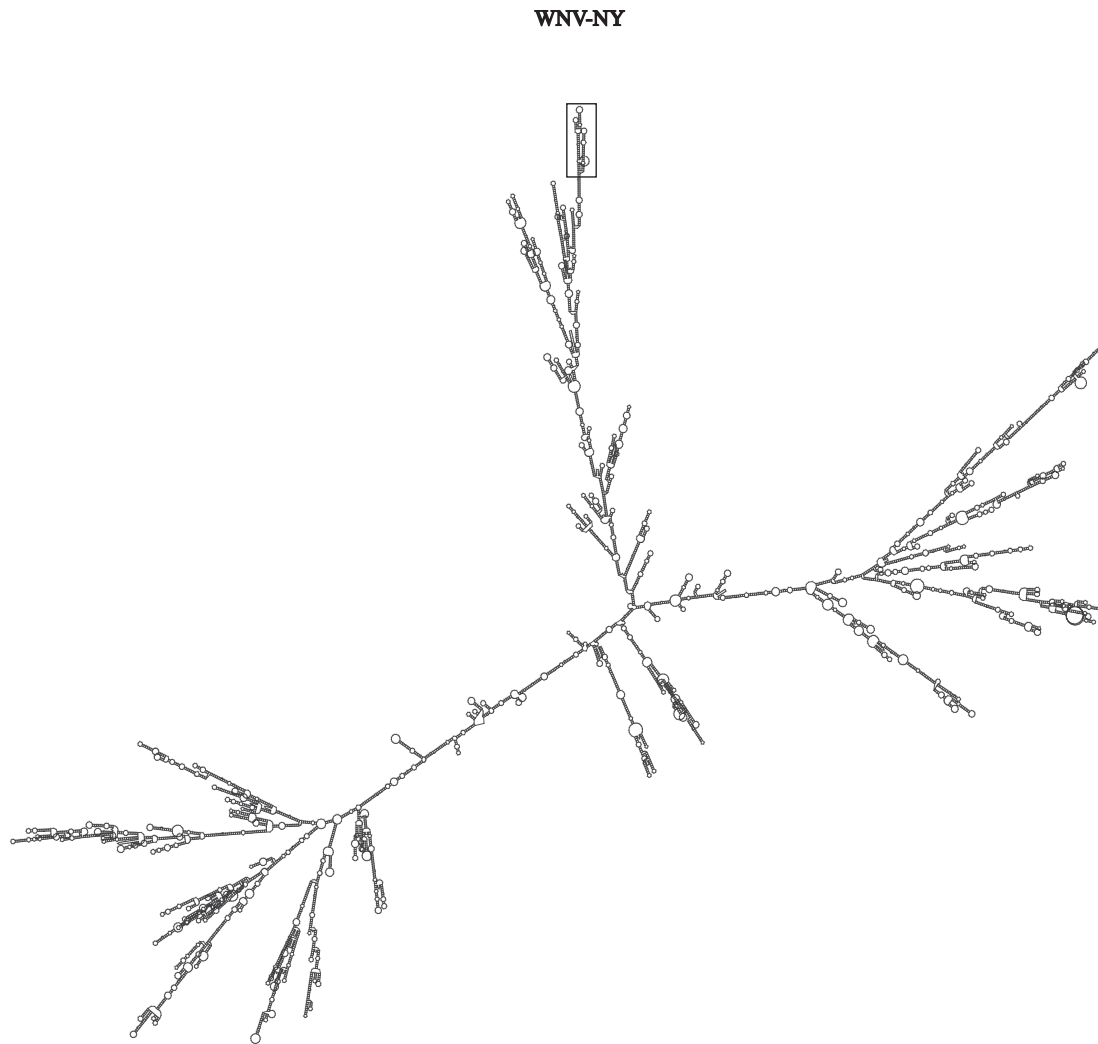


Figure 38 Strucutral predictions of the full WNV-NY genome. Structures produced with the sfold prediciton software. Box indicates 5'UTR region.

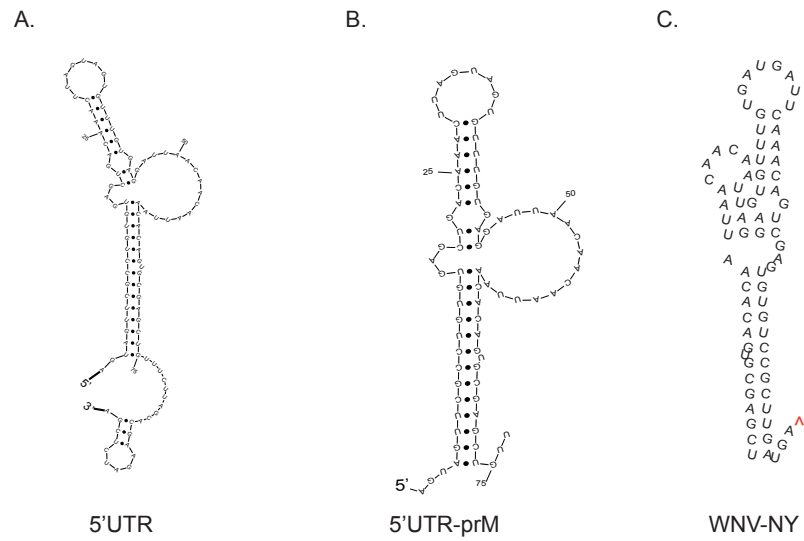


Figure 39 Structural predictions of the WNV-NY 5'UTR (+) alone, within the 5'-prM and within the full genome. Structures of the WNV-NY 5'UTR alone (A), within the context of the 5'-prM RNA (B) or within the context of the full WNV-NY genome (C). Structures A & B were produced with the sfold prediction software, structure C was produced with mfold. ^, 3' end

Works Cited

1. **Ackermann M, Padmanabhan R.** 2001. De novo synthesis of RNA by the dengue virus RNA-dependent RNA polymerase exhibits temperature dependence at the initiation but not elongation phase. *The Journal of biological chemistry* **276**:39926–37.
2. **Alcon-LePoder S, Sivard P, Drouet MT, Talarmin A, Rice C, Flamand M.** 2006. Secretion of flaviviral non-structural protein NS1: from diagnosis to pathogenesis. *Novartis Foundation symposium* **277**:233–47; discussion 247–53.
3. **Ambrose RL, Mackenzie JM.** 2011. A conserved peptide in West Nile virus NS4A protein contributes to proteolytic processing and is essential for replication. *Journal of virology* **85**:11274–82.
4. **Angus AGN, Dalrymple D, Boulant S, McGivern DR, Clayton RF, Scott MJ, Adair R, Graham S, Owsianka AM, Targett-Adams P, Li K, Wakita T, McLauchlan J, Lemon SM, Patel AH.** 2010. Requirement of cellular DDX3 for hepatitis C virus replication is unrelated to its interaction with the viral core protein. *The Journal of general virology* **91**:122–32.
5. **Ariumi Y, Kuroki M, Abe K, Dansako H, Ikeda M, Wakita T, Kato N.** 2007. DDX3 DEAD-box RNA helicase is required for hepatitis C virus RNA replication. *Journal of virology* **81**:13922–6.
6. **Arpaia N, Barton GM.** 2011. Toll-like receptors: key players in antiviral immunity. *Current opinion in virology* **1**:447–54.
7. **Avirutnan P, Hauhart RE, Somnuek P, Blom AM, Diamond MS, Atkinson JP.** 2011. Binding of flavivirus nonstructural protein NS1 to C4b binding protein modulates complement activation. *Journal of immunology* (Baltimore, Md. : 1950) **187**:424–33.
8. **Avirutnan P, Punyadee N, Noisakran S, Komoltri C, Thiemmecca S, Auethavornanan K, Jairungsri A, Kanlaya R, Tangthawornchaikul N, Puttikhunt C, Pattanakitsakul S-N, Yenchitsomanus P-T, Mongkolsapaya J, Kasinrerk W, Sittisombut N, Husmann M, Blettner M, Vasanawathana S, Bhakdi S, Malasit P.** 2006. Vascular leakage in severe dengue virus infections: a potential role for the nonstructural viral protein NS1 and complement. *The Journal of infectious diseases* **193**:1078–88.
9. **Barral PM, Sarkar D, Fisher PB, Racaniello VR.** 2009. RIG-I is cleaved during picornavirus infection. *Virology* **391**:171–6.

10. **Barral PM, Sarkar D, Su ZZ, Barber GN, DeSalle R, Racaniello VR, Fisher PB.** 2009. Functions of the cytoplasmic RNA sensors RIG-I and MDA-5: key regulators of innate immunity. *Pharmacol Ther*, 2009/07/21 ed. **124**:219–234.
11. **Basu M, Brinton MA.** West Nile virus (WNV) genome RNAs with up to three adjacent mutations that disrupt long distance 5'-3' cyclization sequence basepairs are viable. *Virology*, 2011/02/05 ed. **412**:220–232.
12. **Baum A, Sachidanandam R, Garcia-Sastre A.** 2010. Preference of RIG-I for short viral RNA molecules in infected cells revealed by next-generation sequencing. *Proc Natl Acad Sci U S A*, 2010/09/02 ed. **107**:16303–16308.
13. **Beasley DWC, Li L, Suderman MT, Barrett ADT.** 2002. Mouse neuroinvasive phenotype of West Nile virus strains varies depending upon virus genotype. *Virology* **296**:17–23.
14. **Beasley DWC, Whiteman MC, Zhang S, Huang CY-H, Schneider BS, Smith DR, Gromowski GD, Higgs S, Kinney RM, Barrett ADT.** 2005. Envelope protein glycosylation status influences mouse neuroinvasion phenotype of genetic lineage 1 West Nile virus strains. *Journal of virology* **79**:8339–47.
15. **Berg RK, Melchjorsen J, Rintahaka J, Diget E, Søby S, Horan KA, Gorelick RJ, Matikainen S, Larsen CS, Ostergaard L, Paludan SR, Mogensen TH.** 2012. Genomic HIV RNA Induces Innate Immune Responses through RIG-I-Dependent Sensing of Secondary-Structured RNA. *PLoS ONE* **7**:e29291.
16. **Berthet F, Zeller H, Drouet M, Rauzier J, Digoutte J, Deubel V.** 1997. Extensive nucleotide changes and deletions within the envelope glycoprotein gene of Euro-African West Nile viruses. *J. Gen. Virol.* **78**:2293–2297.
17. **Bieback K, Lien E, Klagge IM, Avota E, Schneider-Schaulies J, Duprex WP, Wagner H, Kirschning CJ, Ter Meulen V, Schneider-Schaulies S.** 2002. Hemagglutinin protein of wild-type measles virus activates toll-like receptor 2 signaling. *Journal of virology* **76**:8729–36.
18. **Binder M, Eberle F, Seitz S, Mücke N, Hüber CM, Kiani N, Kaderali L, Lohmann V, Dalpke A, Bartenschlager R.** 2011. Molecular mechanism of signal perception and integration by the innate immune sensor retinoic acid-inducible gene-I (RIG-I). *The Journal of biological chemistry* **286**:27278–87.

19. **Blight KJ, McKeating JA, Rice CM.** 2002. Highly permissive cell lines for subgenomic and genomic hepatitis C virus RNA replication. *J Virol* **76**:13001–13014.
20. **Bowie AG, Unterholzner L.** 2008. Viral evasion and subversion of pattern-recognition receptor signalling. *Nature reviews. Immunology* **8**:911–22.
21. **Brinton MA.** 2001. Host factors involved in West Nile virus replication. *Ann N Y Acad Sci*, 2002/01/19 ed. **951**:207–219.
22. **Brinton MA.** 2002. The molecular biology of West Nile Virus: a new invader of the western hemisphere. *Annu Rev Microbiol*, 2002/07/27 ed. **56**:371–402.
23. **Brinton MA, Dispoto JH.** 1988. Sequence and secondary structure analysis of the 5'-terminal region of flavivirus genome RNA. *Virology*, 1988/02/01 ed. **162**:290–299.
24. **Brinton MA, Fernandez AV, Dispoto JH.** 1986. The 3'-nucleotides of flavivirus genomic RNA form a conserved secondary structure. *Virology*, 1986/08/01 ed. **153**:113–121.
25. **Brinton MA, Dispoto JH.** 1988. Sequence and secondary structure analysis of the 5'-terminal region of flavivirus genome RNA. *Virology* **162**:290–299.
26. **Burzyn D, Rassa JC, Kim D, Nepomnaschy I, Ross SR, Piazzon I.** 2004. Toll-like receptor 4-dependent activation of dendritic cells by a retrovirus. *Journal of virology* **78**:576–84.
27. **Chahar HS, Chen S, Manjunath N.** 2012. P-body components LSM1, GW182, DDX3, DDX6 and XRN1 are recruited to WNV replication sites and positively regulate viral replication. *Virology*.
28. **Chalupníková K, Lattmann S, Selak N, Iwamoto F, Fujiki Y, Nagamine Y.** 2008. Recruitment of the RNA helicase RHAU to stress granules via a unique RNA-binding domain. *The Journal of biological chemistry* **283**:35186–98.
29. **Chambers TJ, Hahn CS, Galler R, Rice CM.** 1990. Flavivirus genome organization, expression, and replication. *Annual review of microbiology* **44**:649–88.
30. **Chawla-Sarkar M, Lindner DJ, Liu Y-F, Williams BR, Sen GC, Silverman RH, Borden EC.** 2003. Apoptosis and interferons: role of

interferon-stimulated genes as mediators of apoptosis. *Apoptosis : an international journal on programmed cell death* **8**:237–49.

31. **Chen YC, Wang SY, King CC.** 1999. Bacterial lipopolysaccharide inhibits dengue virus infection of primary human monocytes/macrophages by blockade of virus entry via a CD14-dependent mechanism. *Journal of virology* **73**:2650–7.
32. **Chiu W-W, Kinney RM, Dreher TW.** 2005. Control of translation by the 5'- and 3'-terminal regions of the dengue virus genome. *Journal of virology* **79**:8303–15.
33. **Choi Y-J, Lee S-G.** 2012. The DEAD-box RNA helicase DDX3 interacts with DDX5, co-localizes with it in the cytoplasm during the G2/M phase of the cycle, and affects its shuttling during mRNP export. *Journal of cellular biochemistry* **113**:985–96.
34. **Chu JJH, Ng ML.** 2004. Infectious entry of West Nile virus occurs through a clathrin-mediated endocytic pathway. *Journal of virology* **78**:10543–55.
35. **Chu JJ-H, Ng M-L.** 2004. Interaction of West Nile virus with alpha v beta 3 integrin mediates virus entry into cells. *The Journal of biological chemistry* **279**:54533–41.
36. **Civril F, Bennett M, Moldt M, Deimling T, Witte G, Schiesser S, Carell T, Hopfner K-P.** 2011. The RIG-I ATPase domain structure reveals insights into ATP-dependent antiviral signalling. *EMBO reports* **12**:1127–34.
37. **Cleaves GR, Dubin DT.** 1979. Methylation status of intracellular dengue type 2 40 S RNA. *Virology* **96**:159–165.
38. **Compton T, Kurt-Jones EA, Boehme KW, Belko J, Latz E, Golenbock DT, Finberg RW.** 2003. Human cytomegalovirus activates inflammatory cytokine responses via CD14 and Toll-like receptor 2. *Journal of virology* **77**:4588–96.
39. **Cui S, Eisenacher K, Kirchhofer A, Brzozka K, Lammens A, Lammens K, Fujita T, Conzelmann KK, Krug A, Hopfner KP.** 2008. The C-terminal regulatory domain is the RNA 5'-triphosphate sensor of RIG-I. *Mol Cell*, 2008/02/05 ed. **29**:169–179.
40. **Daffis S, Samuel MA, Keller BC, Gale M, Diamond MS.** 2007. Cell-specific IRF-3 responses protect against West Nile virus infection by interferon-dependent and -independent mechanisms. *PLoS pathogens* **3**:e106.

41. **Dal Col J, Mastorci K, Faè DA, Muraro E, Martorelli D, Inghirami G, Dolcetti R.** 2012. Retinoic acid/alpha-interferon combination inhibits growth and promotes apoptosis in mantle cell lymphoma through Akt-dependent modulation of critical targets. *Cancer research* **72**:1825–35.
42. **Davis CW, Nguyen H-Y, Hanna SL, Sánchez MD, Doms RW, Pierson TC.** 2006. West Nile virus discriminates between DC-SIGN and DC-SIGNR for cellular attachment and infection. *Journal of virology* **80**:1290–301.
43. **de Vries HE, Blom-Roosemalen MCM, Oosten M van, de Boer AG, van Berkel TJC, Breimer DD, Kuiper J.** 1996. The influence of cytokines on the integrity of the blood-brain barrier in vitro. *Journal of Neuroimmunology* **64**:37–43.
44. **Diamond MS, Shrestha B, Mehlhop E, Sitati E, Engle M.** 2003. Innate and adaptive immune responses determine protection against disseminated infection by West Nile encephalitis virus. *Viral immunology* **16**:259–78.
45. **Doma MK, Parker R.** 2006. Endonucleolytic cleavage of eukaryotic mRNAs with stalls in translation elongation. *Nature* **440**:561–4.
46. **Donaldson GP, Roelofs KG, Luo Y, Sintim HO, Lee VT.** 2012. A rapid assay for affinity and kinetics of molecular interactions with nucleic acids. *Nucleic acids research* **40**:e48.
47. **Dong B, Niwa M, Walter P, Dong B, Niwa M, Walter P, Silverman RH.** 2001. Basis for regulated RNA cleavage by functional analysis of RNase L. Basis for regulated RNA cleavage by functional analysis of RNase L and Ire1p. *Spring* 361–373.
48. **D’Arcy A, Chaillet M, Schiering N, Villard F, Lim SP, Lefevre P, Erbel P.** 2006. Purification and crystallization of dengue and West Nile virus NS2B-NS3 complexes. *Acta crystallographica. Section F, Structural biology and crystallization communications* **62**:157–62.
49. **Elshuber S.** 2003. Cleavage of protein prM is necessary for infection of BHK-21 cells by tick-borne encephalitis virus. *Journal of General Virology* **84**:183–191.
50. **Erbel P, Schiering N, D’Arcy A, Renatus M, Kroemer M, Lim SP, Yin Z, Keller TH, Vasudevan SG, Hommel U.** 2006. Structural basis for the activation of flaviviral NS3 proteases from dengue and West Nile virus. *Nature structural & molecular biology* **13**:372–3.

51. **Foy E, Li K, Wang C, Sumpter R, Ikeda M, Lemon SM, Gale M.** 2003. Regulation of interferon regulatory factor-3 by the hepatitis C virus serine protease. *Science (New York, N.Y.)* **300**:1145–8.
52. **Fredericksen BL, Gale Jr. M.** 2006. West Nile virus evades activation of interferon regulatory factor 3 through RIG-I-dependent and -independent pathways without antagonizing host defense signaling. *J Virol*, 2006/02/28 ed. **80**:2913–2923.
53. **Fredericksen BL, Keller BC, Fornek J, Katze MG, Gale Jr. M.** 2008. Establishment and maintenance of the innate antiviral response to West Nile Virus involves both RIG-I and MDA5 signaling through IPS-1. *J Virol*, 2007/11/06 ed. **82**:609–616.
54. **Friebe P, Shi P-Y, Harris E.** 2011. The 5' and 3' downstream AUG region elements are required for mosquito-borne flavivirus RNA replication. *Journal of virology* **85**:1900–5.
55. **Funk A, Truong K, Nagasaki T, Torres S, Floden N, Balmori Melian E, Edmonds J, Dong H, Shi PY, Khromykh AA.** 2011. RNA structures required for production of subgenomic flavivirus RNA. *J Virol*, 2010/08/20 ed. **84**:11407–11417.
56. **Gack MU, Albrecht RA, Urano T, Inn K, Huang I, Carnero E, Farzan M, Inoue S, Jung J, García-Sastre A.** 2009. Influenza A virus NS1 targets the ubiquitin ligase TRIM25 to evade recognition by the host viral RNA sensor RIG-I. *Cell host & microbe* **5**:439–49.
57. **Geissler R, Golbik RP, Behrens S-E.** 2012. The DEAD-box helicase DDX3 supports the assembly of functional 80S ribosomes. *Nucleic acids research* **40**:4998–5011.
58. **Gillespie LK, Hoenen A, Morgan G, Mackenzie JM.** 2010. The endoplasmic reticulum provides the membrane platform for biogenesis of the flavivirus replication complex. *Journal of virology* **84**:10438–47.
59. **Glass WG, Lim JK, Cholera R, Pletnev AG, Gao J-L, Murphy PM.** 2005. Chemokine receptor CCR5 promotes leukocyte trafficking to the brain and survival in West Nile virus infection. *The Journal of experimental medicine* **202**:1087–98.
60. **Gorbalenya AE, Donchenko AP, Koonin E V, Blinov VM.** 1989. N-terminal domains of putative helicases of flavi- and pestiviruses may be serine proteases. *Nucleic acids research* **17**:3889–97.

61. **Grandvaux N, Servant MJ, tenOever B, Sen GC, Balachandran S, Barber GN, Lin R, Hiscott J.** 2002. Transcriptional Profiling of Interferon Regulatory Factor 3 Target Genes: Direct Involvement in the Regulation of Interferon-Stimulated Genes. *Journal of Virology* **76**:5532–5539.
62. **Gélinas J-F, Clerzius G, Shaw E, Gatignol A.** 2011. Enhancement of replication of RNA viruses by ADAR1 via RNA editing and inhibition of RNA-activated protein kinase. *Journal of virology* **85**:8460–6.
63. **Haasnoot J, Berkhout B.** 2011. RNAi and cellular miRNAs in infections by mammalian viruses. *Methods in molecular biology (Clifton, N.J.)* **721**:23–41.
64. **Haasnoot J, Westerhout EM, Berkhout B.** 2007. RNA interference against viruses: strike and counterstrike. *Nature biotechnology* **25**:1435–43.
65. **Hahn CS, Hahn YS, Rice CM, Lee E, Dalgarno L, Strauss EG, Strauss JH.** 1987. Conserved elements in the 3' untranslated region of flavivirus RNAs and potential cyclization sequences. *J Mol Biol* **198**:33–41.
66. **Hanna SL, Pierson TC, Sanchez MD, Ahmed AA, Murtadha MM, Doms RW.** 2005. N-linked glycosylation of west nile virus envelope proteins influences particle assembly and infectivity. *Journal of virology* **79**:13262–74.
67. **Hayes EB, Gubler DJ.** 2006. West Nile virus: epidemiology and clinical features of an emerging epidemic in the United States. *Annual review of medicine* **57**:181–94.
68. **Hilliker A, Gao Z, Jankowsky E, Parker R.** 2011. The DEAD-box protein Ded1 modulates translation by the formation and resolution of an eIF4F-mRNA complex. *Molecular cell* **43**:962–72.
69. **Hiscott J.** 2007. Triggering the innate antiviral response through IRF-3 activation. *J Biol Chem*, 2007/03/31 ed. **282**:15325–15329.
70. **Hiscott J, Lin R, Nakhaei P, Paz S.** 2006. MasterCARD: a priceless link to innate immunity. *Trends Mol Med*, 2006/01/13 ed. **12**:53–56.
71. **Hoenen A, Liu W, Kochs G, Khromykh AA, Mackenzie JM.** 2007. West Nile virus-induced cytoplasmic membrane structures provide partial protection against the interferon-induced antiviral MxA protein. *The Journal of general virology* **88**:3013–7.

72. **Hollien J, Lin JH, Li H, Stevens N, Walter P, Weissman JS.** 2009. Regulated Ire1-dependent decay of messenger RNAs in mammalian cells. *The Journal of cell biology* **186**:323–31.
73. **Hollien J, Weissman JS.** 2006. Decay of endoplasmic reticulum-localized mRNAs during the unfolded protein response. *Science (New York, N.Y.)* **313**:104–7.
74. **Hornung V, Ellegast J, Kim S, Brzozka K, Jung A, Kato H, Poeck H, Akira S, Conzelmann KK, Schlee M, Endres S, Hartmann G.** 2006. 5'-Triphosphate RNA is the ligand for RIG-I. *Science*, 2006/10/14 ed. **314**:994–997.
75. **Hou F, Sun L, Zheng H, Skaug B, Jiang Q-X, Chen ZJ.** 2011. MAVS forms functional prion-like aggregates to activate and propagate antiviral innate immune response. *Cell* **146**:448–61.
76. **Jiang F, Ramanathan A, Miller MT, Tang G-Q, Gale M, Patel SS, Marcotrigiano J.** 2011. Structural basis of RNA recognition and activation by innate immune receptor RIG-I. *Nature* **479**:423–7.
77. **Johnston LJ, Halliday GM, King NJ.** 2000. Langerhans cells migrate to local lymph nodes following cutaneous infection with an arbovirus. *The Journal of investigative dermatology* **114**:560–8.
78. **Kalverda AP, Thompson GS, Vogel A, Schröder M, Bowie AG, Khan AR, Homans SW.** 2009. Poxvirus K7 protein adopts a Bcl-2 fold: biochemical mapping of its interactions with human DEAD box RNA helicase DDX3. *Journal of molecular biology* **385**:843–53.
79. **Kato H, Takeuchi O, Mikamo-Satoh E, Hirai R, Kawai T, Matsushita K, Hiiragi A, Dermody TS, Fujita T, Akira S.** 2008. Length-dependent recognition of double-stranded ribonucleic acids by retinoic acid-inducible gene-I and melanoma differentiation-associated gene 5. *J Exp Med*, 2008/07/02 ed. **205**:1601–1610.
80. **Kato H, Takeuchi O, Sato S, Yoneyama M, Yamamoto M, Matsui K, Uematsu S, Jung A, Kawai T, Ishii KJ, Yamaguchi O, Otsu K, Tsujimura T, Koh CS, Reis e Sousa C, Matsuura Y, Fujita T, Akira S.** 2006. Differential roles of MDA5 and RIG-I helicases in the recognition of RNA viruses. *Nature*, 2006/04/21 ed. **441**:101–105.
81. **Kawai T, Takahashi K, Sato S, Coban C, Kumar H, Kato H, Ishii KJ, Takeuchi O, Akira S.** 2005. IPS-1, an adaptor triggering RIG-I- and Mda5-mediated type I interferon induction. *Nat Immunol*, 2005/08/30 ed. **6**:981–988.

82. **Kim YS, Lee SG, Park SH, Song K.** 2001. Gene structure of the human DDX3 and chromosome mapping of its related sequences. *Molecules and cells* **12**:209–14.
83. **Klee AL, Maidin B, Edwin B, Poshni I, Mostashari F, Fine A, Layton M, Nash D.** 2004. Long-term prognosis for clinical West Nile virus infection. *Emerg Infect Dis* **10**:1405–11.
84. **Kolakofsky D, Kowalinski E, Cusack S.** 2012. A structure-based model of RIG-I activation. *RNA* (New York, N.Y.).
85. **Kong K-F, Delroux K, Wang X, Qian F, Arjona A, Malawista SE, Fikrig E, Montgomery RR.** 2008. Dysregulation of TLR3 impairs the innate immune response to West Nile virus in the elderly. *Journal of virology* **82**:7613–23.
86. **Koonin E V.** 1991. The phylogeny of RNA-dependent RNA polymerases of positive-strand RNA viruses. *The Journal of general virology* **72** (Pt 9):2197–206.
87. **Kowalinski E, Lunardi T, McCarthy AA, Louber J, Brunel J, Grigorov B, Gerlier D, Cusack S.** 2011. Structural basis for the activation of innate immune pattern-recognition receptor RIG-I by viral RNA. *Cell* **147**:423–35.
88. **Kuhn RJ, Zhang W, Rossmann MG, Pletnev S V., Corver J, Lenches E, Jones CT, Mukhopadhyay S, Chipman PR, Strauss EG.** 2002. Structure of Dengue Virus Implications for Flavivirus Organization, Maturation, and Fusion. *Cell* **108**:717–725.
89. **Kurt-Jones EA, Chan M, Zhou S, Wang J, Reed G, Bronson R, Arnold MM, Knipe DM, Finberg RW.** 2004. Herpes simplex virus 1 interaction with Toll-like receptor 2 contributes to lethal encephalitis. *Proceedings of the National Academy of Sciences of the United States of America* **101**:1315–20.
90. **Lai M-C, Chang W-C, Shieh S-Y, Tarn W-Y.** 2010. DDX3 regulates cell growth through translational control of cyclin E1. *Molecular and cellular biology* **30**:5444–53.
91. **Lai M-C, Lee Y-HW, Tarn W-Y.** 2008. The DEAD-box RNA helicase DDX3 associates with export messenger ribonucleoproteins as well as tip-associated protein and participates in translational control. *Molecular biology of the cell* **19**:3847–58.
92. **Lanciotti RS, Ebel GD, Deubel V, Kerst AJ, Murri S, Meyer R, Bowen M, McKinney N, Morrill WE, Crabtree MB, Kramer LD, Roehrig JT.**

2002. Complete Genome Sequences and Phylogenetic Analysis of West Nile Virus Strains Isolated from the United States, Europe, and the Middle East. *Virology* **298**:96–105.
93. **Laurent-Rolle M, Boer EF, Lubick KJ, Wolfinbarger JB, Carmody AB, Rockx B, Liu W, Ashour J, Shupert WL, Holbrook MR, Barrett AD, Mason PW, Bloom ME, García-Sastre A, Khromykh AA, Best SM.** 2010. The NS5 protein of the virulent West Nile virus NY99 strain is a potent antagonist of type I interferon-mediated JAK-STAT signaling. *Journal of virology* **84**:3503–15.
 94. **Leung DW, Amarasinghe GK.** 2012. Structural insights into RNA recognition and activation of RIG-I-like receptors. *Current opinion in structural biology* **22**:297–303.
 95. **Li X-F, Jiang T, Yu X-D, Deng Y-Q, Zhao H, Zhu Q-Y, Qin E-D, Qin C-F.** 2010. RNA elements within the 5' untranslated region of the West Nile virus genome are critical for RNA synthesis and virus replication. *The Journal of general virology* **91**:1218–23.
 96. **Lin R, Lacoste J, Nakhaei P, Sun Q, Yang L, Paz S, Wilkinson P, Julkunen I, Vitour D, Meurs E, Hiscott J.** 2006. Dissociation of a MAVS/IPS-1/VISA/Cardif-IKKepsilon molecular complex from the mitochondrial outer membrane by hepatitis C virus NS3-4A proteolytic cleavage. *Journal of virology* **80**:6072–83.
 97. **Lindenbach BD, Rice CM.** 1997. trans-Complementation of yellow fever virus NS1 reveals a role in early RNA replication. *Journal of virology* **71**:9608–17.
 98. **Lindenbach BD, Thiel H, Rice CM.** 2007. Flaviviridae: The viruses and their replication, p. . *In* Knipe, DM, Howley, PM (eds.), *Fields Virology*, 5th ed. Lippincott-Raven Publishers, Philadelphia.
 99. **Ling Z, Tran KC, Teng MN.** 2009. Human respiratory syncytial virus nonstructural protein NS2 antagonizes the activation of beta interferon transcription by interacting with RIG-I. *Journal of virology* **83**:3734–42.
 100. **Liu J, Henao-Mejia J, Liu H, Zhao Y, He JJ.** 2011. Translational regulation of HIV-1 replication by HIV-1 Rev cellular cofactors Sam68, eIF5A, hRIP, and DDX3. *Journal of neuroimmune pharmacology : the official journal of the Society on NeuroImmune Pharmacology* **6**:308–21.
 101. **Liu WJ, Chen HB, Khromykh AA.** 2003. Molecular and functional analyses of Kunjin virus infectious cDNA clones demonstrate the essential

roles for NS2A in virus assembly and for a nonconservative residue in NS3 in RNA replication. *Journal of virology* **77**:7804–13.

102. **Liu WJ, Chen HB, Wang XJ, Huang H, Khromykh AA.** 2004. Analysis of adaptive mutations in Kunjin virus replicon RNA reveals a novel role for the flavivirus nonstructural protein NS2A in inhibition of beta interferon promoter-driven transcription. *Journal of virology* **78**:12225–35.
103. **Lo MK, Tilgner M, Bernard KA, Shi P-Y.** 2003. Functional Analysis of Mosquito-Borne Flavivirus Conserved Sequence Elements within 3' Untranslated Region of West Nile Virus by Use of a Reporting Replicon That Differentiates between Viral Translation and RNA Replication. *Journal of Virology* **77**:10004–10014.
104. **Loo YM, Fornek J, Crochet N, Bajwa G, Perwitasari O, Martinez-Sobrido L, Akira S, Gill MA, Garcia-Sastre A, Katze MG, Gale Jr. M.** 2008. Distinct RIG-I and MDA5 signaling by RNA viruses in innate immunity. *J Virol*, 2007/10/19 ed. **82**:335–345.
105. **Lu C, Xu H, Ranjith-Kumar CT, Brooks MT, Hou TY, Hu F, Herr AB, Strong RK, Kao CC, Li P.** 2010. The structural basis of 5' triphosphate double-stranded RNA recognition by RIG-I C-terminal domain. *Structure (London, England : 1993)* **18**:1032–43.
106. **Luo D, Ding SC, Vela A, Kohlway A, Lindenbach BD, Pyle AM.** 2011. Structural insights into RNA recognition by RIG-I. *Cell* **147**:409–22.
107. **Mackenzie JM, Khromykh AA, Jones MK, Westaway EG.** 1998. Subcellular localization and some biochemical properties of the flavivirus Kunjin nonstructural proteins NS2A and NS4A. *Virology* **245**:203–15.
108. **Mackenzie JM, Kenney MT, Westaway EG.** 2007. West Nile virus strain Kunjin NS5 polymerase is a phosphoprotein localized at the cytoplasmic site of viral RNA synthesis. *The Journal of general virology* **88**:1163–8.
109. **Malathi K, Saito T, Crochet N, Barton DJ, Gale Jr. M, Silverman RH.** 2010. RNase L releases a small RNA from HCV RNA that refolds into a potent PAMP. *RNA*, 2010/09/14 ed. **16**:2108–2119.
110. **Manion M, Rodriguez B, Medvik K, Hardy G, Harding C V, Schooley RT, Pollard R, Asmuth D, Murphy R, Barker E, Brady KE, Landay A, Funderburg N, Sieg SF, Lederman MM.** 2012. Interferon-alpha administration enhances CD8+ T cell activation in HIV infection. *PloS one* **7**:e30306.

111. **Marfin AA, Petersen LR, Eidson M, Miller J, Hadler J, Farello C, Werner B, Campbell GL, Layton M, Smith P, Bresnitz E, Cartter M, Scaletta J, Obiri G, Bunning M, Craven RC, Roehrig JT, Julian KG, Hinten SR, Gubler DJ.** 2001. Widespread West Nile virus activity, eastern United States, 2000. *Emerg Infect Dis*, 2001/10/05 ed. **7**:730–735.
112. **Marques JT, Devosse T, Wang D, Zamanian-Daryoush M, Serbinowski P, Hartmann R, Fujita T, Behlke MA, Williams BRG.** 2006. A structural basis for discriminating between self and nonself double-stranded RNAs in mammalian cells. *Nature biotechnology* **24**:559–65.
113. **Masatani T, Ito N, Shimizu K, Ito Y, Nakagawa K, Sawaki Y, Koyama H, Sugiyama M.** 2010. Rabies virus nucleoprotein functions to evade activation of the RIG-I-mediated antiviral response. *Journal of virology* **84**:4002–12.
114. **Melian EB, Hinzman E, Nagasaki T, Firth AE, Wills NM, Nouwens AS, Blitvich BJ, Leung J, Funk A, Atkins JF, Hall R, Khromykh AA.** 2010. NS1' of flaviviruses in the Japanese encephalitis virus serogroup is a product of ribosomal frameshifting and plays a role in viral neuroinvasiveness. *Journal of virology* **84**:1641–7.
115. **Merino EJ, Wilkinson KA, Coughlan JL, Weeks KM.** 2005. RNA structure analysis at single nucleotide resolution by selective 2'-hydroxyl acylation and primer extension (SHAPE). *Journal of the American Chemical Society* **127**:4223–31.
116. **Meylan E, Curran J, Hofmann K, Moradpour D, Binder M, Bartenschlager R, Tschopp J.** 2005. Cardif is an adaptor protein in the RIG-I antiviral pathway and is targeted by hepatitis C virus. *Nature* **437**:1167–72.
117. **Mizushima S, Nagata S.** 1990. pEF-BOS, a powerful mammalian expression vector. *Nucleic acids research* **18**:5322.
118. **Mukhopadhyay S, Kuhn RJ, Rossmann MG.** 2005. A structural perspective of the flavivirus life cycle. *Nature reviews. Microbiology* **3**:13–22.
119. **Muñoz-Jordán JL, Laurent-Rolle M, Ashour J, Martínez-Sobrido L, Ashok M, Lipkin WI, García-Sastre A.** 2005. Inhibition of alpha/beta interferon signaling by the NS4B protein of flaviviruses. *Journal of virology* **79**:8004–13.
120. **Myong S, Cui S, Cornish PV, Kirchhofer A, Gack MU, Jung JU, Hopfner KP, Ha T.** 2009. Cytosolic viral sensor RIG-I is a 5'-triphosphate-

dependent translocase on double-stranded RNA. *Science*, 2009/01/03 ed. **323**:1070–1074.

121. **Nash D, et. al.** 2001. The Outbreak of West Nile Virus Infection in the New York City Area in 1999. *New England Journal of Medicine* **344**:1807–1814.
122. **Navarro-Sanchez E, Altmeyer R, Amara A, Schwartz O, Fieschi F, Virelizier J-L, Arenzana-Seisdedos F, Desprès P.** 2003. Dendritic-cell-specific ICAM3-grabbing non-integrin is essential for the productive infection of human dendritic cells by mosquito-cell-derived dengue viruses. *EMBO reports* **4**:723–8.
123. **Nekhai S, Jeang K-T.** 2006. Transcriptional and post-transcriptional regulation of HIV-1 gene expression: role of cellular factors for Tat and Rev. *Future microbiology* **1**:417–26.
124. **Netherton C, Moffat K, Brooks E, Wileman T.** 2007. A guide to viral inclusions, membrane rearrangements, factories, and viroplasm produced during virus replication. *Advances in virus research* **70**:101–82.
125. **Nishikura K.** 2010. Functions and regulation of RNA editing by ADAR deaminases. *Annual review of biochemistry* **79**:321–49.
126. **Nomaguchi M, Teramoto T, Yu L, Markoff L, Padmanabhan R.** 2004. Requirements for West Nile virus (-)- and (+)-strand subgenomic RNA synthesis in vitro by the viral RNA-dependent RNA polymerase expressed in *Escherichia coli*. *The Journal of biological chemistry* **279**:12141–51.
127. **Nybakken GE, Nelson CA, Chen BR, Diamond MS, Fremont DH.** 2006. Crystal structure of the West Nile virus envelope glycoprotein. *Journal of virology* **80**:11467–74.
128. **Oda S-I, Schröder M, Khan AR.** 2009. Structural basis for targeting of human RNA helicase DDX3 by poxvirus protein K7. *Structure (London, England : 1993)* **17**:1528–37.
129. **Oh W, Yang M-R, Lee E-W, Park K-M, Pyo S, Yang J-S, Lee H-W, Song J.** 2006. Jab1 mediates cytoplasmic localization and degradation of West Nile virus capsid protein. *The Journal of biological chemistry* **281**:30166–74.
130. **Orlinger KK, Hoenninger VM, Kofler RM, Mandl CW.** 2006. Construction and mutagenesis of an artificial bicistronic tick-borne encephalitis virus genome reveals an essential function of the second transmembrane region of protein e in flavivirus assembly. *Journal of virology* **80**:12197–208.

131. **Oshiumi H, Ikeda M, Matsumoto M, Watanabe A, Takeuchi O, Akira S, Kato N, Shimotohno K, Seya T.** 2010. Hepatitis C virus core protein abrogates the DDX3 function that enhances IPS-1-mediated IFN-beta induction. *PloS one* **5**:e14258.
132. **Oshiumi H, Sakai K, Matsumoto M, Seya T.** 2010. DEAD/H BOX 3 (DDX3) helicase binds the RIG-I adaptor IPS-1 to up-regulate IFN-beta-inducing potential. *European journal of immunology* **40**:940–8.
133. **Owsianka AM, Patel AH.** 1999. Hepatitis C virus core protein interacts with a human DEAD box protein DDX3. *Virology* **257**:330–40.
134. **Pachler K, Vlasak R.** 2011. Influenza C virus NS1 protein counteracts RIG-I-mediated IFN signalling. *Virology journal* **8**:48.
135. **Papon L, Oteiza A, Imaizumi T, Kato H, Brocchi E, Lawson TG, Akira S, Mechti N.** 2009. The viral RNA recognition sensor RIG-I is degraded during encephalomyocarditis virus (EMCV) infection. *Virology* **393**:311–8.
136. **Peisley A, Lin C, Wu B, Orme-Johnson M, Liu M, Walz T, Hur S.** 2011. Cooperative assembly and dynamic disassembly of MDA5 filaments for viral dsRNA recognition. *Proceedings of the National Academy of Sciences of the United States of America* **108**:21010–5.
137. **Petersen LR, Roehrig JT.** 2001. West Nile virus: a reemerging global pathogen. *Emerg Infect Dis*, 2001/10/05 ed. **7**:611–614.
138. **Peña J, Harris E.** 2011. Dengue virus modulates the unfolded protein response in a time-dependent manner. *The Journal of biological chemistry* **286**:14226–36.
139. **Pfaller CK, Li Z, George CX, Samuel CE.** 2011. Protein kinase PKR and RNA adenosine deaminase ADAR1: new roles for old players as modulators of the interferon response. *Current opinion in immunology* **23**:573–82.
140. **Pichlmair A, Schulz O, Tan CP, Naslund TI, Liljestrom P, Weber F, Reis e Sousa C.** 2006. RIG-I-mediated antiviral responses to single-stranded RNA bearing 5'-phosphates. *Science*, 2006/10/14 ed. **314**:997–1001.
141. **Pijlman GP, Funk A, Kondratieva N, Leung J, Torres S, van der Aa L, Liu WJ, Palmenberg AC, Shi PY, Hall RA, Khromykh AA.** 2008. A highly structured, nuclease-resistant, noncoding RNA produced by flaviviruses is required for pathogenicity. *Cell Host Microbe*, 2008/12/10 ed. **4**:579–591.

142. **Pijlman GP, Funk A, Kondratieva N, Leung J, Torres S, van der Aa L, Liu WJ, Palmenberg AC, Shi P-Y, Hall RA, Khromykh AA.** 2008. A highly structured, nuclease-resistant, noncoding RNA produced by flaviviruses is required for pathogenicity. *Cell host & microbe* **4**:579–91.
143. **Plumet S, Herschke F, Bourhis JM, Valentin H, Longhi S, Gerlier D.** 2007. Cytosolic 5'-triphosphate ended viral leader transcript of measles virus as activator of the RIG I-mediated interferon response. *PLoS One*, 2007/03/16 ed. **2**:e279.
144. **Ramesh A, DebRoy S, Goodson JR, Fox KA, Faz H, Garsin DA, Winkler WC.** 2012. The mechanism for RNA recognition by ANTAR regulators of gene expression. *PLoS genetics* **8**:e1002666.
145. **Rassa JC, Meyers JL, Zhang Y, Kudaravalli R, Ross SR.** 2002. Murine retroviruses activate B cells via interaction with toll-like receptor 4. *Proceedings of the National Academy of Sciences of the United States of America* **99**:2281–6.
146. **Rehwinkel J, Tan CP, Goubau D, Schulz O, Pichlmair A, Bier K, Robb N, Vreede F, Barclay W, Fodor E, Reis e Sousa C.** 2010. RIG-I detects viral genomic RNA during negative-strand RNA virus infection. *Cell*, 2010/02/11 ed. **140**:397–408.
147. **Roelofs KG, Wang J, Sintim HO, Lee VT.** 2011. Differential radial capillary action of ligand assay for high-throughput detection of protein-metabolite interactions. *Proceedings of the National Academy of Sciences of the United States of America* **108**:15528–33.
148. **Ron D, Walter P.** 2007. Signal integration in the endoplasmic reticulum unfolded protein response. *Nature reviews. Molecular cell biology* **8**:519–29.
149. **Roosendaal J, Westaway EG, Khromykh A, Mackenzie JM.** 2006. Regulated cleavages at the West Nile virus NS4A-2K-NS4B junctions play a major role in rearranging cytoplasmic membranes and Golgi trafficking of the NS4A protein. *Journal of virology* **80**:4623–32.
150. **Saito T, Gale Jr. M.** 2008. Differential recognition of double-stranded RNA by RIG-I-like receptors in antiviral immunity. *J Exp Med*, 2008/07/02 ed. **205**:1523–1527.
151. **Saito T, Hirai R, Loo YM, Owen D, Johnson CL, Sinha SC, Akira S, Fujita T, Gale M.** 2007. Regulation of innate antiviral defenses through a shared repressor domain in RIG-I and LGP2. *Proc Natl Acad Sci U S A* **104**:582–587.

152. **Saito T, Owen DM, Jiang F, Marcotrigiano J, Gale Jr. M.** 2008. Innate immunity induced by composition-dependent RIG-I recognition of hepatitis C virus RNA. *Nature*, 2008/06/13 ed. **454**:523–527.
153. **Samuel CE.** 2011. Adenosine deaminases acting on RNA (ADARs) are both antiviral and proviral. *Virology* **411**:180–93.
154. **Scadden ADJ.** 2005. The RISC subunit Tudor-SN binds to hyper-edited double-stranded RNA and promotes its cleavage. *Nature structural & molecular biology* **12**:489–96.
155. **Scadden ADJ, Connell MAO.** 2005. Cleavage of dsRNAs hyper-edited by ADARs occurs at preferred editing sites. *Reactions* **33**:5954–5964.
156. **Scherbik SV, Paranjape JM, Stockman BM, Silverman RH, Brinton MA.** 2006. RNase L plays a role in the antiviral response to West Nile virus. *J Virol*, 2006/02/28 ed. **80**:2987–2999.
157. **Schlee M, Roth A, Hornung V, Hagmann CA, Wimmenauer V, Barchet W, Coch C, Janke M, Mihailovic A, Wardle G, Juranek S, Kato H, Kawai T, Poeck H, Fitzgerald KA, Takeuchi O, Akira S, Tuschl T, Latz E, Ludwig J, Hartmann G.** 2009. Recognition of 5' triphosphate by RIG-I helicase requires short blunt double-stranded RNA as contained in panhandle of negative-strand virus. *Immunity*, 2009/07/07 ed. **31**:25–34.
158. **Schmidt A, Schwerdt T, Hamm W, Hellmuth JC, Cui S, Wenzel M, Hoffmann FS, Michallet MC, Besch R, Hopfner KP, Endres S, Rothenfusser S.** 2009. 5'-triphosphate RNA requires base-paired structures to activate antiviral signaling via RIG-I. *Proc Natl Acad Sci U S A*, 2009/07/04 ed. **106**:12067–12072.
159. **Schnettler E, Sterken MG, Leung JY, Metz SW, Geertsema C, Goldbach RW, Vlak JM, Kohl A, Khromykh AA, Pijlman GP.** 2012. Non-coding flavivirus RNA displays RNAi suppressor activity in insect and mammalian cells. *Journal of virology* JVI.01104–12–.
160. **Schoggins JW, Rice CM.** 2011. Interferon-stimulated genes and their antiviral effector functions. *Current opinion in virology* **1**:519–25.
161. **Schröder M.** 2010. Human DEAD-box protein 3 has multiple functions in gene regulation and cell cycle control and is a prime target for viral manipulation. *Biochemical pharmacology* **79**:297–306.
162. **Schröder M.** 2011. Viruses and the human DEAD-box helicase DDX3: inhibition or exploitation? *Biochemical Society transactions* **39**:679–83.

163. **Schröder M, Baran M, Bowie AG.** 2008. Viral targeting of DEAD box protein 3 reveals its role in TBK1/IKKepsilon-mediated IRF activation. *The EMBO journal* **27**:2147–57.
164. **Schuessler A, Funk A, Lazear H, Cooper DA, Torres S, Daffis S, Jha BK, Kumagai Y, Takeuchi O, Hertzog P, Silverman R, Akira S, Barton DJ, Diamond MS, Khromykh AA.** 2012. West Nile virus non-coding subgenomic RNA contributes to viral evasion of type I interferon-mediated antiviral response. *Journal of virology* JVI.00207–12–.
165. **Seth RB, Sun L, Ea C-K, Chen ZJ.** 2005. Identification and characterization of MAVS, a mitochondrial antiviral signaling protein that activates NF-kappaB and IRF 3. *Cell* **122**:669–82.
166. **Shi PY, Tilgner M, Lo MK, Kent KA, Bernard KA.** 2002. Infectious cDNA Clone of the Epidemic West Nile Virus from New York City. *Journal of Virology* **76**:5847–5856.
167. **Shih J-W, Wang W-T, Tsai T-Y, Kuo C-Y, Li H-K, Wu Lee Y-H.** 2012. Critical roles of RNA helicase DDX3 and its interactions with eIF4E/PABP1 in stress granule assembly and stress response. *The Biochemical journal* **441**:119–29.
168. **Shiryaev SA, Chernov A V, Aleshin AE, Shiryaeva TN, Strongin AY.** 2009. NS4A regulates the ATPase activity of the NS3 helicase: a novel cofactor role of the non-structural protein NS4A from West Nile virus. *The Journal of general virology* **90**:2081–5.
169. **Shiryaev SA, Ratnikov BI, Aleshin AE, Kozlov IA, Nelson NA, Lebl M, Smith JW, Liddington RC, Strongin AY.** 2007. Switching the substrate specificity of the two-component NS2B-NS3 flavivirus proteinase by structure-based mutagenesis. *Journal of virology* **81**:4501–9.
170. **Silva PA, Pereira CF, Dalebout TJ, Spaan WJ, Bredenbeek PJ.** An RNA pseudoknot is required for production of yellow fever virus subgenomic RNA by the host nuclease XRN1. *J Virol*, 2010/08/27 ed. **84**:11395–11406.
171. **Sirigulpanit W, Kinney RM, Leardkamolkarn V.** 2007. Substitution or deletion mutations between nt 54 and 70 in the 5' non-coding region of dengue type 2 virus produce variable effects on virus viability. *The Journal of general virology* **88**:1748–52.
172. **Song L, Gao S, Jiang W, Chen S, Liu Y, Zhou L, Huang W.** 2011. Silencing suppressors: viral weapons for countering host cell defenses. *Protein & cell* **2**:273–81.

173. **Stadler K, Allison S, Schlich J, Heinz F.** 1997. Proteolytic activation of tick-borne encephalitis virus by furin. *J. Virol.* **71**:8475–8481.
174. **Steele KE, Linn MJ, Schoepp RJ, Komar N, Geisbert TW, Manduca RM, Calle PP, Raphael BL, Clippinger TL, Larsen T, Smith J, Lanciotti RS, Panella NA, McNamara TS.** 2000. Pathology of fatal West Nile virus infections in native and exotic birds during the 1999 outbreak in New York City, New York. *Veterinary pathology* **37**:208–24.
175. **Stetson DB, Medzhitov R.** 2006. Antiviral defense: interferons and beyond. *J Exp Med*, 2006/08/02 ed. **203**:1837–1841.
176. **Strähle L, Marq J-B, Brini A, Hausmann S, Kolakofsky D, Garcin D.** 2007. Activation of the beta interferon promoter by unnatural Sendai virus infection requires RIG-I and is inhibited by viral C proteins. *Journal of virology* **81**:12227–37.
177. **Sumpter R, Loo YM, Foy E, Li K, Yoneyama M, Fujita T, Lemon SM, Gale M.** 2005. Regulating intracellular antiviral defense and permissiveness to hepatitis C virus RNA replication through a cellular RNA helicase, RIG-I. *J Virol* **79**:2689–2699.
178. **Suthar MS, Ramos HJ, Brassil MM, Netland J, Chappell CP, Blahnik G, McMillan A, Diamond MS, Clark EA, Bevan MJ, Gale M.** 2012. The RIG-I-like receptor LGP2 controls CD8(+) T cell survival and fitness. *Immunity* **37**:235–48.
179. **Szomolanyi-Tsuda E, Liang X, Welsh RM, Kurt-Jones EA, Finberg RW.** 2006. Role for TLR2 in NK cell-mediated control of murine cytomegalovirus in vivo. *Journal of virology* **80**:4286–91.
180. **Takahasi K, Yoneyama M, Nishihori T, Hirai R, Kumeta H, Narita R, Gale Jr. M, Inagaki F, Fujita T.** 2008. Nonself RNA-sensing mechanism of RIG-I helicase and activation of antiviral immune responses. *Mol Cell*, 2008/02/05 ed. **29**:428–440.
181. **Tanner NK, Linder P.** 2001. DExD/H box RNA helicases: from generic motors to specific dissociation functions. *Mol Cell*, 2001/09/08 ed. **8**:251–262.
182. **TenOever BR, Servant MJ, Grandvaux N, Lin R, Hiscott J.** 2002. Recognition of the measles virus nucleocapsid as a mechanism of IRF-3 activation. *J Virol*, 2002/03/22 ed. **76**:3659–3669.

183. **Tomecki R, Drazkowska K, Dziembowski A.** 2011. Mechanisms of RNA degradation by the eukaryotic exosome. *Chembiochem*, 2010/03/20 ed. **11**:938–945.
184. **Tomecki R, Dziembowski A.** 2010. Novel endoribonucleases as central players in various pathways of eukaryotic RNA metabolism. *RNA (New York, N.Y.)* **16**:1692–724.
185. **Town T, Bai F, Wang T, Kaplan AT, Qian F, Montgomery RR, Anderson JF, Flavell RA, Fikrig E.** 2009. Toll-like receptor 7 mitigates lethal West Nile encephalitis via interleukin 23-dependent immune cell infiltration and homing. *Immunity* **30**:242–53.
186. **Umbach JL, Cullen BR.** 2009. The role of RNAi and microRNAs in animal virus replication and antiviral immunity. *Genes & development* **23**:1151–64.
187. **Villordo SM, Gamarnik A V.** 2009. Genome cyclization as strategy for flavivirus RNA replication. *Virus research* **139**:230–9.
188. **Wang F, Gao X, Barrett JW, Shao Q, Bartee E, Mohamed MR, Rahman M, Werden S, Irvine T, Cao J, Dekaban GA, McFadden G.** 2008. RIG-I mediates the co-induction of tumor necrosis factor and type I interferon elicited by myxoma virus in primary human macrophages. *PLoS pathogens* **4**:e1000099.
189. **Wang R, Kushner S.** 1991. Construction of versatile low-copy-number vectors for cloning, sequencing and gene expression in *Escherichia coli*. *Gene* **100**:195–199.
190. **Wang T, Town T, Alexopoulou L, Anderson JF, Fikrig E, Flavell RA.** 2004. Toll-like receptor 3 mediates West Nile virus entry into the brain causing lethal encephalitis. *Nature medicine* **10**:1366–73.
191. **Wang Y, Lobigs M, Lee E, Mullbacher A.** 2003. CD8+ T Cells Mediate Recovery and Immunopathology in West Nile Virus Encephalitis. *Journal of Virology* **77**:13323–13334.
192. **Wang Y, Ludwig J, Schuberth C, Goldeck M, Schlee M, Li H, Juranek S, Sheng G, Micura R, Tuschl T, Hartmann G, Patel DJ.** 2010. Structural and functional insights into 5'-ppp RNA pattern recognition by the innate immune receptor RIG-I. *Nature structural & molecular biology* **17**:781–7.
193. **Ward S V, George CX, Welch MJ, Liou L-Y, Hahm B, Lewicki H, de la Torre JC, Samuel CE, Oldstone MB.** 2011. RNA editing enzyme adenosine deaminase is a restriction factor for controlling measles virus

replication that also is required for embryogenesis. *Proceedings of the National Academy of Sciences of the United States of America* **108**:331–6.

194. **Welte T, Reagan K, Fang H, Machain-Williams C, Zheng X, Mendell N, Chang G-JJ, Wu P, Blair CD, Wang T.** 2009. Toll-like receptor 7-induced immune response to cutaneous West Nile virus infection. *The Journal of general virology* **90**:2660–8.
195. **Welte T, Reagan K, Fang H, Machain-Williams C, Zheng X, Mendell N, Chang G-JJ, Wu P, Blair CD, Wang T.** 2009. Toll-like receptor 7-induced immune response to cutaneous West Nile virus infection. *The Journal of general virology* **90**:2660–8.
196. **Welte T, Xie G, Wicker JA, Whiteman MC, Li L, Rachamalla A, Barrett A, Wang T.** 2011. Immune responses to an attenuated West Nile virus NS4B-P38G mutant strain. *Vaccine* **29**:4853–61.
197. **Westaway EG, Khromykh AA, Mackenzie JM.** 1999. Nascent flavivirus RNA colocalized in situ with double-stranded RNA in stable replication complexes. *Virology* **258**:108–17.
198. **Westaway EG, Khromykh AA, Mackenzie JM.** 1999. Nascent flavivirus RNA colocalized in situ with double-stranded RNA in stable replication complexes. *Virology* **258**:108–17.
199. **Westaway EG, Mackenzie JM, Khromykh AA.** 2002. Replication and gene function in Kunjin virus. *Current topics in microbiology and immunology* **267**:323–51.
200. **Westaway E, Mackenzie J, Kenney M, Jones M, Khromykh A.** 1997. Ultrastructure of Kunjin virus-infected cells: colocalization of NS1 and NS3 with double-stranded RNA, and of NS2B with NS3, in virus- induced membrane structures. *J. Virol.* **71**:6650–6661.
201. **Wilkinson KA, Merino EJ, Weeks KM.** 2006. Selective 2'-hydroxyl acylation analyzed by primer extension (SHAPE): quantitative RNA structure analysis at single nucleotide resolution. *Nature protocols* **1**:1610–6.
202. **Wilkinson KA, Vasa SM, Deigan KE, Mortimer SA, Giddings MC, Weeks KM.** 2009. Influence of nucleotide identity on ribose 2'-hydroxyl reactivity in RNA. *RNA (New York, N.Y.)* **15**:1314–21.
203. **Wong TC, Ayata M, Hirano A, Yoshikawa Y, Tsuruoka H, Yamanouchi K.** 1989. Generalized and localized biased hypermutation affecting the

matrix gene of a measles virus strain that causes subacute sclerosing panencephalitis. *Journal of virology* **63**:5464–8.

- 204. **Xu L-G, Wang Y-Y, Han K-J, Li L-Y, Zhai Z, Shu H-B.** 2005. VISA is an adapter protein required for virus-triggered IFN-beta signaling. *Molecular cell* **19**:727–40.
- 205. **Ye C, Verchot J.** 2011. Role of unfolded protein response in plant virus infection. *Plant signaling & behavior* **6**:1212–5.
- 206. **Ye Ding CYC.** Sfold web server for statistical folding and rational design of nucleic acids.
- 207. **Yedavalli VSRK, Neuveut C, Chi Y-H, Kleiman L, Jeang K-T.** 2004. Requirement of DDX3 DEAD box RNA helicase for HIV-1 Rev-RRE export function. *Cell* **119**:381–92.
- 208. **Yoneyama M, Kikuchi M, Natsukawa T, Shinobu N, Imaizumi T, Miyagishi M, Taira K, Akira S, Fujita T.** 2004. The RNA helicase RIG-I has an essential function in double-stranded RNA-induced innate antiviral responses. *Nature immunology* **5**:730–7.
- 209. **Yonezawa A, Morita R, Takaori-Kondo A, Kadowaki N, Kitawaki T, Hori T, Uchiyama T.** 2003. Natural Alpha Interferon-Producing Cells Respond to Human Immunodeficiency Virus Type 1 with Alpha Interferon Production and Maturation into Dendritic Cells. *Journal of Virology* **77**:3777–3784.
- 210. **Youn S, Li T, McCune BT, Edeling MA, Fremont DH, Cristea IM, Diamond MS.** 2012. Evidence for a genetic and physical interaction between nonstructural proteins NS1 and NS4B that modulates replication of West Nile virus. *Journal of virology* **86**:7360–71.
- 211. **Zadeh JN, Steenberg CD, Bois JS, Wolfe BR, Pierce MB, Khan AR, Dirks RM, Pierce NA.** 2011. NUPACK: Analysis and design of nucleic acid systems. *Journal of computational chemistry* **32**:170–3.
- 212. **Zambrano JL, Ettayebi K, Maaty WS, Faunce NR, Bothner B, Hardy ME.** 2011. Rotavirus infection activates the UPR but modulates its activity. *Virology journal* **8**:359.
- 213. **Zhang B, Dong H, Stein DA, Iversen PL, Shi PY.** 2008. West Nile virus genome cyclization and RNA replication require two pairs of long-distance RNA interactions. *Virology*, 2008/02/09 ed. **373**:1–13.
- 214. **Zhang W, Chipman PR, Corver J, Johnson PR, Zhang Y, Mukhopadhyay S, Baker TS, Strauss JH, Rossmann MG, Kuhn RJ.**

2003. Visualization of membrane protein domains by cryo-electron microscopy of dengue virus. *Nature structural biology* **10**:907–12.
215. **Zhang Y, Kaufmann B, Chipman PR, Kuhn RJ, Rossmann MG.** 2007. Structure of immature West Nile virus. *Journal of virology* **81**:6141–5.
216. **Zuker M.** 2003. Mfold web server for nucleic acid folding and hybridization prediction. *Nucleic Acids Research* **31**:3406–3415.